Hydraulics Research
Wallingford

THE BEHAVIOUR OF ESTUARINE MUDS DURING TIDAL CYCLES

An experimental study and mathematical model

E A DELO, BSc, PhD, C Eng, MICE, MIWEM

Report No SR 138
February 1988

Registered Office: Hydraulics Research Limited,
Wallingford, Oxfordshire OX10 8BA.
Telephone: 0491 35381. Telex: 848552

This report describes work funded by the Department of the Environment under Research Contract PECD 7/6/57 for which the DoE nominated officer was Dr R P Thorogood. It is published on behalf of the Department of the Environment, but any opinions expressed in this report are not necessarily those of the funding Department. The work was carried out by Dr E A Delo assisted by Ms M C Ockenden and Mr A P Diserens in Mr T N Burt's section in the Tidal Engineering Department of Hydraulics Research, Wallingford, under the management of Mr M F C Thorn.

ABSTRACT

The erosion, transport, deposition and consolidation of cohesive sediment within estuarine or other water courses creates a wide range of design, maintenance and management problems in, for example, ports, harbours and docks. The overall movement of cohesive sediment within such facilities can have significant economical and ecological importance. Accumulation of cohesive sediments in navigation channels and berths reduces the water depths and often results in the need for dredging. Other schemes, such as the reclamation of intertidal mudflats or the construction of flood protection structures, or the laying of outfalls, require a sound engineering appraisal of the likely changes in the patterns of sediment movement which may result after the scheme is built. Many polluting chemical species are preferentially sorbed onto cohesive sediment and move with them in the water.

All of these problems highlight the need for good methods for predicting the movement of cohesive sediment. At present, numerical models do exist which predict the movement of cohesive sediment (see Hydraulics Research, 1985 and Hayter and Mehta, 1986). However, the physical processes are generally represented by simple empirical algorithms. Hence, there is a need to improve the modelling of cohesive sediment behaviour through a more rigorous mathematical representation of the mud bed processes and laboratory tests in the mud carousel flume.

The HR mud carousel flume was modified by the addition of a micro-computer for control, a densiometer for continuous measurement of the suspended solids concentration (linked to a chart recorder) and an ultrasonic transducer for non-destructive determination of the thickness of the mud bed. Laser doppler anemometry was employed to measure the vertical velocity profile at three sections across the width of the flume from which the bed shear stress was calculated. These developments enabled the carousel to be used for investigating the behaviour of a mud bed during simulated tidal cycles.

A mathematical model was formulated to simulate the three basic physical processes of mud, namely erosion, consolidation and deposition during repeated tidal cycles. The model extended the work done in another part of this contract (see Ginger, 1987) on the modelling of consolidating mud deposits.

New experimental procedures were developed to enable the erosion and consolidation properties of a mud to be determined. The new erosion tests were undertaken in the carousel and the procedure enabled the density of the eroding surface of the mud bed to be determined. The consolidation tests were performed in settling columns and involved the continuous deposition of material from suspension and the determination of important empirical relationships between voids ratio, effective stress and permeability.

Four carousel tidal cycle tests were conducted to investigate the behaviour of mud beds and to provide data for testing the mathematical model. The first test was used primarily to prove the carousel. The effect of progressively increasing the magnitude of the peak bed shear stress of repeated cycles was examined in the second test. The third test studied the

effect of progressively decreasing the peak bed shear stress while the fourth test was conducted to look at the effect of short periods of consolidation on the re-suspension of mud.

The mathematical model was used to simulate the behaviour of the experimental mud bed as tested during the second tidal cycles test. The results of the model showed reasonable agreement with experimental data in quantitative terms and good agreement in qualitative terms.

The mathematical model was used to simulate the behaviour of the mud bed at the entrance channel to Queen Alexandra Dock, Cardiff as part of a recent project study. The results for one position in the channel were presented and these clearly illustrated the importance of modelling the whole neap-spring-neap tidal processes with respect to the mud bed behaviour.

It is recommended that the laboratory and mathematical model simulation of tidal cycles be proved by detailed field measurement of the near-bed processes. This would provide invaluable data which would lead to a more informed assessment of the physical processes of mud in the field. The mud from the chosen field site would be tested in the laboratory to determine its basic physical properties which together with field data on the bed shear stress and near bed sediment concentrations would enable the mathematical model to be run to predict the changes in elevation and density structure of the bed.

CONTENTS

CONTENTS (CONT'D)

CONTENTS (CONT'D)

FIGURES (CONT'D)

CONTENTS (CONT'D)

FIGURES (CONT'D)

1 INTRODUCTION

1.1 The need for research

The erosion, transport, deposition and consolidation of cohesive sediment within estuarine or other water courses creates a wide range of design, maintenance and management problems in, for example, ports, harbours and docks. The overall movement of cohesive sediment within such facilities can have significant economical and ecological importance. Accumulation of cohesive sediments in navigation channels and berths reduces the water depths and often results in the need for dredging. Other schemes, such as the reclamation of intertidal mudflats or the construction of flood protection structures, or the laying of outfalls, require a sound engineering appraisal of the likely changes in the patterns of sediment movement which may result after the scheme is built. Many polluting chemical species are preferentially sorbed onto cohesive sediment and move with them in the water.

All of these problems highlight the need for good methods for predicting the movement of cohesive sediment. At present, numerical models do exist which predict the movement of cohesive sediment (see Hydraulics Research, 1985 and Hayter and Mehta, 1986). However, the physical processes are generally represented by simple empirical algorithms. Hence, there is a need to improve the modelling of cohesive sediment behaviour through a more rigorous mathematical representation of the mud bed processes and laboratory tests in the mud carousel flume.

1.2 Behaviour of cohesive sediment

The behaviour of cohesive sediment is complex (see Delo and Burt, 1986). It is governed by many

physiochemical and hydrodynamic parameters, for example, particle size, number of particles, mineralogy, ph, ionic strength, chemical composition and temperature of the suspending fluid and the velocity, turbulence, internal shear, bed shear stress and stress history of the fluid. Accordingly, as it is not yet possible to predict the behaviour of cohesive sediment from its physical and chemical properties alone studies of cohesive sediment have been conducted in the laboratory on an empirical and site specific basis.

Cohesive sediment can be considered to exist in four states. These four states are illustrated in Figure 1 and may be described as a mobile suspended sediment, a near bed stationary suspension of high concentration with a small cohesion which is sometimes referred to as fluid mud, a partially consolidated bed, and a settled bed.

The three processes of cohesive sediment of primary interest to the engineer are deposition, consolidation and erosion. Deposition involves the settling through the water column and on to the bed of flocculated sediment. Consolidation of a deposit is the gradual explusion of interstitial water by the self weight of the sediment accompanied by an increase in both the density of the bed and its strength with time. Erosion is the removal of sediment from the surface of the bed due to the stress of the moving water above the bed.

Even the laboratory studies to date, however, have had the drawback of mainly considering only one process in isolation, e.g. deposition or erosion, and even then usually at a constant rate of flow. In natural conditions the processes are often strongly cyclic with the deposition, partial consolidation and

re-erosion of cohesive sediment occurring repeatedly with the tides.

This report describes the laboratory investigation in the carousel flume and the numerical simulation of the physical processes of cohesive sediment during tidal cycles.

2 THE CAROUSEL

2.1 Description

The carousel (Fig 2) consists of an annular flume, with an outer diameter of 6m, a channel width of 0.4m and depth of 0.35m, and has a detachable roof 0.09m thick (see Burt and Game, 1985a). The flume stands approximately 1.1m off the ground, supported by 12 brick pillars. The channel and the roof are constructed of fibre-glass, with a 0.12m long perspex section in the channel for viewing. The roof fits into the channel, and floats on the fluid. Fluid motion in the carousel is induced and continued by the drag between the roof and the fluid surface as the roof rotates.

The driving mechanism for the roof consists of a DC Torque motor with a drive wheel, which turns a horizontal plate around the central spindle. It is to this plate that the drive arm is attached at one end (via the strain gauge) and to the roof at the other.

The strain gauge is used to measure the force applied to the roof of the carousel as it rotates. It consists of a spring and displacement transducer arrangement attached to the driving arm at the point of contact with the roof. The magnitude of the applied force is determined by the displacement transducer deflection, which is displayed on a chart

recorder. The strain gauge is calibrated by applying known forces via a pulley system.

The speed of the motor, and hence roof speed, is controlled by a micro computer. The motor speed can be set to an accuracy of 0.1% of the maximum speed. This produces a mean water velocity range in the flume from zero to approximately $0.7 ms^{-1}$.

In the carousel the sampling system consists of two port holes, one on each wall of the flume, 80mm above the floor. Through each of these port holes protrudes an 'L' shaped stainless steel sampling tube, which has an internal diameter of 2mm. The outer wall sampling tube has its entrance facing upstream and its elevation can be altered by rotating the outer portion of this tube across a scale corresponding to 0-100mm above the flume floor.

2.2 Instrumentation

2.2.1 Densiometer

Fluid is continuously extracted from the carousel by a peristaltic pump and passed through a constant temperature water bath and a densiometer before being returned to the carousel. The densiometer works on the principle of determining the frequency of a thin vibrating glass tube through which the fluid is pumped and comparing this to the frequency with clean water pumped through a second densiometer. The readings obtained are analysed and displayed on a chart recorder. Bottle samples of the fluid are taken from time to time and analysed gravimetrically to maintain an accurate calibration. In this manner it is possible to measure the suspended sediment concentration of the fluid in the carousel continuously to within a few percent. It has been

shown in previous measurements by Burt and Game (1985b) that the mean solids concentration of the fluid in the carousel is very close to the solids concentration at the centre of flow, certainly less than 5% difference.

2.2.2 Micro-computer Control

The speed of rotation of the roof of the carousel flume is controlled by a micro-computer. A 0-10V programmable signal from the micro-computer controls the DC Torque motor which drives the roof. This system enables the simulation of time varying bed shear stresses in the carousel. The required pattern of bed shear stress with time is first determined and then by working back through calibrations of average bed shear stress against mean flow velocity, speed of rotation against mean flow velocity, and voltage output from the micro-computer against speed of rotation, the necessary pattern of voltage output with time is derived and programmed into the micro-computer.

2.2.3 Ultrasonic Transducer

The thickness of the bed in the carousel is measured from beneath the flume at the perspex viewing section by an ultrasonic transducer. This instrument displays a peak in a signal which indicates the interface between the mud bed and the overlying fluid and enables the thickness of the bed to be determined to within 0.1mm. The transducer is calibrated through a fluid with a salinity similar to that in the mud bed. A movable mounting device holds the transducer in contact with the underside of the perspex section and is used to position the transducer at any point across the 0.4m width of the flume. In this way it is

possible to obtain profiles of the bed and determine the depth of erosion at any time during the test.

2.3 Bed shear stress measurement

Two methods were employed for measuring the average shear stress exerted by the fluid on the bed. The first method was simple and involved direct measurement of the energy input to the roof through the calibrated strain gauge for a number of different speeds of rotation of the roof.

The second and more complex way of determining the bed shear stresses was by measurement of the near bed velocity profiles in the flume using laser doppler anemometry. The measurements are very accurate ($\pm$ 1mms^{-1}) and can be made at any point in the cross-section of the flume, through the perspex section. These point velocities are used to obtain velocity profiles.

The equipment comprises three parts:

(a) Laser optical unit (Fig 3a). This consists of a 5 milliwatt helium-neon laser, a beam splitter, a Bragg cell and a lens.

(b) Photomultiplier optical unit (Fig 3b). This consists of a photomultiplier tube, an achromatic focus lens, a mirror and a viewing eye piece.

(c) Electronic units. These consist of power supplies for the laser and photomultiplier, Bragg cell driver(s) and electronic frequency shift, and circuitry to extract the relevant doppler frequency from the detector output signal.

The laser velocity meter operates by emitting two convergent beams in the same horizontal plane. These beams pass through the perspex window of the flume and intersect at some point in the flow. It is at this intersection point that the velocity component of the flow normal to the beam crossing is measured (see Fig 3c). The photomultiplier unit is focussed on the beams crossing point, and as a particle in the flow passes through the crossing point light is scattered from the two beams, doppler shifted in frequency by equal and opposite amounts. The difference is detected in a signal modulation, which is then converted by one of the electronic units into a voltage output which in turn is fed onto a chart recorder. From this the velocity can easily be calculated.

The friction velocity at the bed was determined from a log-linear plot of height above bed and tangential velocity. Velocities were determined at three sections across the width of the flume for different speeds of rotation of the roof. The bed shear stresses were then computed from the logarithmic portion of the velocity-depth profiles.

The average bed shear stress across the width of flume measured by the laser velocity is shown in Figure 4. Also given in Figure 4 is shear stress on the wetted perimeter as given by the energy input measured through the strain gauge. These two curves show reasonable agreement and indicate a steady increase in bed shear stress with increasing speed of rotation of the roof. For the purpose of estimating the bed shear stress during an erosion test the curve representing the average shear stress as calculated from the energy input was used. However, it must be appreciated that in an erosion test the fluid in the carousel may have

a high concentration of suspended solids and accordingly will behave slightly differently from the clear water in which the calibrations were undertaken.

3 FORMULATION OF MODEL

3.1 Introduction

A mathematical model was developed to simulate the behaviour of a consolidating mud bed subject to the cyclic process of erosion and deposition. In the closed system of the carousel, conservation of mass implies that at any time the mean concentration of solids in the overlying suspension will be directly proportional to the mass of material eroded per unit area. Furthermore, if it is assumed that the solids in suspension are well mixed throughout the carousel flow (that is, vertically, radially and circumferentially) then the concentration, c, is given by

$$\frac{\partial (dc)}{\partial t} = \frac{dm}{dt} \qquad (1)$$

where

d = water depth (m)

t = time (s)

$\frac{dm}{dt}$ = erosion from or deposition on the bed ($kg/m^2/s$)

The structure of the bed at any instant in time, t, may be represented by the rate of change of mass in suspension with depth of erosion,

$$\rho_h = \frac{dm}{dh} \frac{1}{A} \qquad (2)$$

where

ρ_h = dry density of bed at an erosion depth h (kg/m^3)
m = mass of solids in suspension (kg/m^2)
A = surface area of mud (m^2)

The purpose of the mathematical model was to predict the concentration of suspended solids in the carousel for a prescribed pattern of shear stress with time and given physical properties of the mud. This in effect required the erosion, deposition and consolidation properties of the mud to be described by equations and the parameters in the equations determined individually by experiment.

3.2 Erosion

Intuitively, one would expect erosion to start when the stress exerted by the flow exceeded the shear strength of the exposed bed and the erosion rate to depend on the excess shear. If the erosive power of the stream is low not much erosion would be expected to take place. There will be times when a burst of turbulence slightly higher than average hits a slightly weaker part of the bed causing untypical erosion, but for practical purposes this can be ignored and it may be assumed that there is a cut off for erosion. The most common representation of erosion is

$$\frac{dm}{dt} = m_e (\tau - \tau_e) \qquad (3)$$

where

$\frac{dm}{dt}$ = unit erosion rate ($kg/m^2/s$)
m_e = erosion constant ($kg/N/s$)
τ = applied shear stress (N/m^2)
τ_e = erosion shear strength (N/m^2)

This means that erosion is gradual which is not necessarily the case for certain types of newly formed slack water deposits. Although there is no physical reason for assuming erosion rate to be directly proportional to the excess shear, Delo and Burt (1986) showed that this is a better variable for describing mud erosion than others. In any event it is not too important in tidal conditions to know the erosion rate precisely because the erosion process is self correcting in the sense that if the erosion constant is too high then too much erosion occurs in the early stages, but this exposes stronger bed material and erosion slows down accordingly. The opposite happens if m_e is under-valued. The ultimate result in any case would be erosion down to the bed level, where the strength of the exposed material corresponds to the maximum bed stress of the tidal cycle or of the spring-neap cycle, if longer periods are being considered.

3.3 Deposition

Net deposition from a dilute suspension is usually assumed to occur when the bed stress falls below a critical value τ_d and the deposition rate for stresses lower than this is usually represented as

$$\frac{dm}{dt} = -cw_{50}(\tau_d - \tau)/\tau_d \qquad (4)$$

where

$\frac{dm}{dt}$ = unit deposition rate ($kg/m^2/s$)
c = near bed concentration (kg/m^3)
$w_{50}(c)$ = medium settling velocity (m/s)
τ_d = critical deposition stress (N/m^2)
τ = applied shear stress (N/m^2)

This can be thought of as a deposition proportional to τ_d and a vertical diffusive flux proportional to τ.

When $\tau = \tau_d$, the rate of settling is balanced by the vertical diffusive flux due to turbulence and there is no deposition. As the current slows down, its associated bed stress and turbulent intensity reduce, thereby weakening the vertical diffusive flux, resulting in a net deposition. This is a simplification of what, in nature, is a very complicated process. For example, there will not be an abrupt cut off τ_d for deposition but rather a gradual change over from a non-depositional to a fully depositional state. In between, there is likely to be some interchange of suspended particles with bed particles. However, for the purpose of making engineering judgements it is sufficient to represent the deposition in the above manner, and accordingly, to simulate depositions, values are required for $w_s(c)$ and τ_d.

The value of $w_s(c)$ is normally found by measurement in the field of the settling velocity of the flocs using an Owen tube. The settling velocity is correlated with the suspended solids concentration.

For the purpose of simulating the deposition of mud in the carousel the settling behaviour of the mud was determined from the rate of decrease of suspended solids concentration of a fluid in the carousel in quiescent conditions (see Section 4.3). The ratio of the near bed suspended solids concentration to depth-averaged concentration was taken to be constant during a tidal cycle.

3.4 Consolidation

The representation of the bed as a number of discrete layers in the present model was based on the work recently undertaken by Ginger (1987) on the modelling of consolidating mud deposits. The details of the

model do not need to be repeated but the three principal assumptions are:

1. that there is a unique relationship between the voids ratio (volume of water/volume of solids) and the permeability for a particular soil, whatever its history,

2. that there is a similar unique relationship between the voids ratio and the effective stress,

3. that the bed of a consolidating soil can be considered to be made up of layers, each with a certain voids ratio (and therefore unique values of permeability, effective stress and density) and pore water pressure.

The model was substantially modified, however, to enable mud to be eroded from, or deposited on, the surface of the bed. Furthermore, the empirical relationships between the voids ratio and the permeability and effective stress respectively were derived from the results of laboratory settling column tests on the same mud as that used in the tidal cycle tests in the carousel. This method was preferable to that of adopting general empirical equations derived by other researchers.

4 PHYSICAL PROPERTIES TESTS

4.1 Introduction

The mathematical model presented in the preceding section requires certain parameters, which describe the basic physical behaviour of the mud, to be determined. These parameters are:

m_e = erosion constant

$\tau_e(\rho)$ = erosion shear strength (as a function of density)

$w_{50}(c)$ = median settling velocity (as a function of suspended solids concentration)

τ_d = critical shear stress for deposition

K_{13} = ratio of near-bed to depth-averaged suspended solids concentrations (when $\tau<\tau_d$)

$k(e)$ = permeability (as a function of voids ratio)

$\sigma'_v(e)$ = effective stress (as a function of voids ratio)

ρ_o = initial density of a new deposit

Of these eight parameters only τ_d was not determined experimentally for the Kelang mud. The next three Sections describe the tests undertaken to quantify the other seven parameters. A summary of the results is presented in Section 4.5.

4.2 Erosion

4.2.1 Bed preparation

The filling and emptying processes involved with the carousel are shown schematically in Figure 5. Before a suspension is put into the carousel, it is first mixed homogeneously. This is achieved by putting the mud and water into the mixing tank and pumping the fluid through the recirculatory system.

The suspension is then pumped into the flume from the tank until the required depth of suspension in the flume is reached. The roof is lowered onto the suspension surface and the mud in suspension is allowed to deposit and consolidate. The period of consolidation is usually in the range of 2-10 days and the resulting bed has a thickness of between 15-25mm.

The depth of fluid above the bed is adjusted to be close to 100mm which corresponds to the depth of flow for which the bed shear stress measurements were made.

4.2.2 Test procedure

An erosion test in the carousel comprises a number of discrete runs during which the speed of rotation of the roof (and hence the bed shear stress) is held constant. In a test there may be between 2-5 runs each lasting 60-200 minutes. The speed of the carousel is systematically increased for each successive run.

A run commences when the concentration of suspended solids is constant in the previous run. The speed of rotation of the flume is increased relatively quickly to its new value. The concentration of suspended solids as measured continuously by the densiometer will at first increase rapidly (indicating strong erosion), then more smoothly (modest erosion) and finally the concentration will remain nearly constant (no erosion). This pattern is reflected by the readings from the ultrasonic transducer which is mounted on the underside of the flume mid-way across its width. The readings are directly proportional to the depth of erosion.

At the end of a run when erosion has stopped the actual depth of erosion at a 20mm interval across the width of the flume is determined using the ultrasonic transducer. The typical depth of erosion which is normally attained at the end of the test is about 5mm. If more mud is eroded then the high concentrations of suspended sediment begin to prevent the densiometer and ultrasonic depth transducer from functioning correctly. Furthermore, at the higher speeds of

rotation the effects of secondary currents are greater and the differential depth of erosion across the flume becomes more pronounced.

4.2.3 Analysis

The basic data obtained from a test are the suspended solids concentration with time, the depth of erosion at the mid-section of the flume with time and the depths of erosion across the flume at the equilibrium point in each run. The objectives of the analysis are to calculate the relationship between the shear strength of the mud with density and the rate of erosion with applied shear stress.

The shear strength with density relationship is described by the discrete values at the equilibrium point in each run of the speed of rotation of the roof, the suspended solids concentration of the fluid and the average depth of erosion across the flume. Using the results presented in Figure 4 the average bed shear stress is then estimated for the prescribed speed of rotation of each run. At equilibrium in each run, the shear strength of the exposed surface of the bed is equal to the applied shear stress. Accordingly, the shear strength depth profile of the eroded portion of the bed can be described by these points. This gives an expression

$$\tau_e = K_1 + K_2 h^{K_3} \qquad (5)$$

where

τ_e = erosion shear strength of bed (N/m^2)
h = average depth of erosion below original surface (m)
K_1, K_2, K_3 = constants

It is also necessary to calculate the variation in density of the mud bed with depth. The density may be expressed as

$$\rho_h = \frac{dm}{dh}\frac{1}{A} \qquad (6)$$

where

ρ_h = dry density of bed at an erosion depth h (kg/m^3)
m = mass of solids in suspension (kg)
A = area of erosion (m^2)

Expressing the mass of solids in terms of the concentration of suspended solids, equation (6) can be rewritten as:

$$\rho_h = \frac{dc}{dh}\frac{V}{A} \qquad (7)$$

where

c = concentration of suspended solids (kg/m^3)
V = volume of suspension (m^3)

The ratio of V/A in equation (7) will be nearly constant during a test and is the depth of flow, d. By plotting the concentration of suspended solids against the average depth of erosion a quadratic relationship may be approximated of the form

$$c = K_4 + K_5 h + K_6 h^2 \qquad (8)$$

where

K_4, K_5, K_6 = constants

Differentiating equation (8) and substituting into equation (7) leads to the relationship

$$\rho_h = K_7 + K_8 h \tag{9}$$

Combining equations (5) and (9) leads to an expression which relates the erosion shear strength to the density of the exposed mud, and which can be approximated to the form

$$\tau_e = K_9 \rho_h^{K_{10}} \tag{10}$$

A useful analysis of the erosion constant can be made by assuming that the shear strength of the bed during any discharge run is proportional to the eroded mass (Miles, 1985). The constant of proportionality for a run is given by

$$\alpha = \frac{\tau_b - \tau_o}{c_e - c_o} \tag{11}$$

where

τ_b = applied bed stress for the run
τ_o = shear strength of bed at start = equilibrium from previous run
c_e = equilibrium concentration at the end of run
c_o = initial concentration = equilibrium concentration at end of previous run

This does not assume that there is a linear relationship between strength of bed and overlying weight for the complete bed. This overall structure is fixed by the equilibrium conditions at the end of each run. We have merely assumed a linear variation from one equilibrium state to the next and α can vary for each run.

If we further assume that the erosion rate for exposed mud surface area is given by equation (3) we obtain, using (11) and replacing m by cV

$$\frac{dc}{dt} = Am_e \alpha(c_e - c_o)/V \qquad (12)$$

Where V is the volume of fluid in the flume and A is the area of erosion. This can be integrated as

$$(c_e - c) = (c_e - c_o) \exp(-Am_e \alpha t/V) \qquad (13)$$

This solution exhibits the expected behaviour of concentrations, tending to equilibrium values for large times. Based on the analytic form of this theoretical solution, the carousel erosion flume results for a test can be normalised and plotted using linear (αt) and logarithmic $[(c_e - c_o)/(c_e - c)]$ axes to give a representative erosion constant for the test.

4.2.4 Results

The description of the beds which were tested in the three erosion tests is given in Table 1. The consolidation periods for Tests 1, 2 and 3 were 4 days, 6 days and 17 days respectively. The resulting mean densities of the beds were 163, 165 and 193kg/m^3 respectively which indicated the effect of consolidation on the beds.

The details of the runs in each test are presented in Table 2. Four runs were conducted in Test 1; two runs in Test 2; and three runs in Test 3. Tests 2 and 3 were designed to extend the range of mud densities investigated compared to the runs in Test 1. Accordingly, the first run in these two tests was at a speed of rotation equal to the last run in Test 1.

The results of each test are shown in a group of five figures: Test 1 - Figures 6-10, Test 2 - Figures 11-15, and Test 3 - Figures 16-20 and are summarised in Table 3. The format of the presentation is similar for each test. The first figure shows the variation in speed of rotation, suspended solids concentration and average depth of erosion with time. An indication of the profile of the eroded bed at the end of each run is shown in the second figure of each group (i.e. Figures 7, 12 and 17). Some differential erosion occurred in all tests with the depth of erosion being greater on the outside of the flume where the circumferential velocity is higher.

The relationships between suspended solids concentration, dry density of mud and erosion shear strength each against the depth of erosion are shown for each test in Figures 8, 13 and 18 respectively. Figures 9, 14 and 19 depict the variation in erosion shear strength with dry density on a log-log plot. In Figures 10, 15 and 20 the plots of normalised suspended solids concentration against normalised time are presented with straight line curve fits illustrating the values of the erosion rate constant, m_e.

The most appropriate way of interpreting the data of the three tests with respect to erosion strength and density is to combine all three sets of data into one graph. This is shown in Figure 21 which depicts the erosional shear strength (N/m^2) against dry density (kg/m^3). A straight line fit through all the error bars of the data points indicated that the power-law relationship was given by:

$$\tau_e = 0.00050\ \rho_h^{1.4} \qquad (14)$$

The value of the erosion constant, m_e was found to

vary from run to run and from test to test. In Test 1 (Fig 10) the erosion constant was calculated to be around 0.0009kg/N/s for Runs 1 and 4 and 0.0005kg/N/s for runs 2 and 3. In the second test (Fig 15) the two runs each gave a similar value for the erosion constant of approximately 0.0005kg/N/s. Test 3 (Fig 20) yielded an erosion constant of only 0.0002kg/N/s for Run 1, whereas, for Runs 2 and 3 the constant was double that value at approximately 0.0004kg/N/s. Overall, a typical value for the erosion constant was,

$$m_e = 0.0005 \text{kg/N/s} \tag{15}$$

4.3 Deposition

4.3.1 Test procedure

A series of experiments in the carousel was conducted to determine the value of the coefficients in the equation used to represent the median settling velocity of the flocs w_{50} (c) as a function of suspended solids concentration c,

that is,

$$w_{50}(c) = K_{11}\, c^{K_{12}} \tag{16}$$

and the constant in the relationship between the near bed suspended solids concentration c_{nb}, and the depth averaged concentration $\bar{c}$, that is,

$$c_{nb} = K_{13}\, \bar{c} \tag{17}$$

The tests were conducted in quiescent conditions and involved recording the concentration of suspended solids at mid-depth in a settling suspension which had been initially well mixed. The starting suspended

solids concentration was varied in the tests and the range of values used was chosen to reflect the likely range of solids concentration in the carousel tidal cycle tests. Accordingly, tests were carried out in which the initial solids concentration was approximately 3.2, 1.7, 1.2 and 0.5kg/m^3 respectively. The depth of suspensions in all the tests was 0.1m.

A simple mathematical model was formulated to simulate the settling of suspended solids through a fluid in which the local settling velocity of the flocs was given by equation (16). For given values of K_{11}, K_{12} and K_{13} the model yielded the depth averaged suspended solids concentration with time. By comparing the data of a test with that of the model at mid-depth it was possible to adjust the values of the coefficients to give the closest agreement.

4.3.2 Results

The measured concentrations of suspended solids at mid-depth in the tests are shown in Figures 22 and 23. Simulation of this mid-depth concentration was undertaken using the mathematical model and the results are also shown in Figures 22 and 23. The best fit coefficients for equation (17) were found to be K_{11} = 0.00002 and K_{12} = 0.8. The ratio of near bed to mean suspended solids concentration was estimated to be K_{13} = 1.6.

4.3.3 Critical shear stress

The shear stress, τ_d, at which deposition of cohesive sediment is assumed to occur from flowing water has been studied in the laboratory by a number of researchers (see Delo and Burt, 1986 for a review). Different muds have been tested over the years by various workers and the value of the critical shear

stress has been found to be about 0.06 N/m^2. As no laboratory tests to determine τ_d were conducted on the Kelang mud used in the tidal cycles tests, this typical value for the critical shear stress (i.e. τ_d = 0.06 N/m^2) was adopted.

4.4 Consolidation tests

4.4.1 Description of apparatus

The tests were carried out in a settling column of 2 metres height and 92mm internal diameter constructed of perspex sections (see Fig 24). The column was graduated in millimetres for the first half metre section and marked at 1 metre intervals throughout its length.

Density profiles were obtained for each bed in the settling column by measuring the transmission of emissions from a ^{133} Ba source over 30 seconds at 2mm or 5mm intervals throughout the depth of the bed. The density probe was calibrated by measuring the count rate in saline solutions of known density. This indicated a linear relationship over the density range applicable in the tests of the form,

$$\rho = K_{14} r + K_{15} \qquad (18)$$

where

ρ = bulk density (kg/m^3)
r = count rate per minute
K_{14}, K_{15} = constants

Because the total quantity of sediment in the initial suspension was known, integration of the density profiles should indicate (i) the distribution of mass

through the column, and (ii) the total mass in the column.

A sample of silt from Port Kelang was used throughout the experimental investigation. The mud was sieved through a 200μm sieve to remove shells, sand and large organic particles. A stock suspension was made up of around 7kg/m^3 of mud at 33kg/m^3 NaCl. This suspension was well mixed.

The stock suspension was held in a container above the column and was constantly mixed by re-circulating pumping to prevent settlement of coarser silt particles. The column was filled to the height of the outlet port with 33kg/m^3 saline solution. The silt suspension was introduced into the column through a port at a height of 500mm from the stock suspension container. The excess water was drained through an outlet at the top of the column and discarded. The rate of input to the column was regulated using a variable speed peristaltic pump. A constant rate of input over a set period of time was chosen for each test. Bed thickness and density profiles were recorded at intervals during deposition and consolidation.

4.4.2 Analysis

The two fundamental assumptions made in the modelling of the consolidation process are that there are unique variations of effective stress with voids ratio and permeability with voids ratio relationships. The rate of consolidation is principally governed by the variation of permeability with voids ratio relationships and the profile when consolidation is virtually complete is determined by the variation of effective stress with voids ratio relationship. These

two relationships have to be determined experimentally in the laboratory.

When consolidation is nearly complete the effective stress (σ') may be equated to the total stress (σ) as the pore pressure is almost zero. A plot of total stress against voids ratio through the depth of the bed will therefore give the voids ratio against effective stress relationship. The total stress at a depth below the surface can be found by measuring the submerged weight of the layers above, that is

$$\sigma_z = \Sigma_0^z \ \rho_d \ K_{16} \ \Delta h \qquad (19)$$

$$K_{16} = g(\rho_s - \rho_w)/\rho_s$$

where

σ_z = total stress at depth z (N/m^2)
ρ_d = dry density (kg/m^3)
ρ_s = particle density (kg/m^3)
ρ_w = water density (kg/m^3)
g = acceleration due to gravity (m/s^2)
Δh = change in depth (m)

The voids ratio e can be calculated from the density at a particular point by

$$e = \frac{\rho_s}{\rho_d} - 1 \qquad (20)$$

The relationship between effective stress and voids ratio can be expressed in the form

$$\sigma' = \frac{K_{17}}{e^{K_{18}}} - K_{19} \qquad (21)$$

where

K_{17}, K_{18}, K_{19} = constants

Also it is evident that this equation gives a unique density against depth profile for the completely consolidated bed, hence the density profile of a bed approaching complete consolidation can be used directly to determine the effective stress and voids ratio relationship.

Since, effective stress is a function of cumulative mass from the surface (Equ 19) and voids ratio is a function of density (Equ 20), the relationship between these parameters (Equ 21) may also be expressed in these terms. Differentiating this relationship between cumulative mass and density and re-arranging, gives:

$$z = \left(\frac{\rho_s}{\rho_d}\right)^{K_{18}-1} \frac{\rho_s}{\rho_d^2} \frac{1}{K_{16}} + K_{20} \qquad (22)$$

where

K_{20} = function (K_{16}, K_{17}, K_{18} and K_{19})

The permeability against voids ratio can be determined using experimental data collected as the bed is being deposited. An assumption is made that the pore water pressure equals the total stress and hence the effective stress is zero.

From Darcy's law

$$q = A\ k\ i \qquad (23)$$

where

q = volume of water per unit time (m^3/s)
A = area (m^2)
k = permeability constant (m/s)
i = hydraulic gradient

The excess hydraulic gradient at a point in the bed can be calculated from the relationship

$$i = (\rho_d - \rho_w)/\rho_w \qquad (24)$$

The volume of water per unit time is equivalent to the velocity of the sediment particles so permeability becomes

$$k = \frac{v_s \rho_w}{(\rho_d - \rho_w)} \qquad (25)$$

where
v_s = velocity of sediment particles (m/s)

The position of the point in the bed is determined using the cumulative mass against depth relationship. The values of permeability, k for each layer are plotted against voids ratio, e from which a best fit curve is determined of the type

$$k = K_{21}\, e^{K_{22}} \qquad (26)$$

where

K_{21}, K_{22} = constants.

4.4.3 Results

The results of Test 1 (Table 4) are plotted as bed thickness against time and density against time in

Figure 25. The bed thickness increased linearly as the silt was deposited to a maximum of 75mm after 4 hours when deposition ceased. The bed thickness then decreased exponentially to a minimum of approximately 30mm. The mean dry density increased from 25kg/m^3 at the time when the bed thickness was at a maximum to 120kg/m^3 after 6 days. The density profiles at 24 hourly intervals are shown together in Figure 26. Each successive profile indicated an increase in density throughout the bed, the first density profile (after 4 hours) showed little vertical variation in density, the density being around 25kg/m^3 throughout the bed. The final density profile (4 days) showed a much larger increase in bulk density vertically - ranging from 25 to 120kg/m^3.

The results for Test 2 (Table 5) are plotted as bed thickness against time and mean bulk density against time in Figure 27. The bed thickness increased linearly to a maximum of approximately 63mm after 6$\frac{1}{2}$ hours and thereafter decreased exponentially to near 30mm after 7 days as the bed consolidated. The mean dry density increased to 120kg/m^3 after 4 days. The density profiles at successive times are shown together in Figure 28. The mean density increased throughout the test and the density gradient in the bed increased with time.

The results for Test 3 (Table 6) are plotted as bed thickness against time and mean bulk density against time in Figure 29. The bed thickness increased linearly to a maximum of approximately 96mm after 5 hours and thereafter decreased exponentially to near 50mm after 4 days as the bed consolidated. The mean dry density increased to 82kg/m^3 after 4 days. The density profiles at successive times are shown together in Figure 30. The mean density increased

throughout the test and the density gradient in the bed decreased with time.

The final density profile for each test was plotted as density against depth from surface (see Fig 31) and a best fit line arrived at from which the voids ratio against effective stress relationship for each test was derived (see Fig 32). Test 3 gave slightly lower densities for a given depth than either Tests 1 or 2 and hence the constants are slightly larger, see Table 7. The effective stress varied from $0N/m^2$ at the surface of the bed (voids ratio = ∞) to $10N/m^2$ at a voids ratio of 10.

The permeability against voids ratio figures were calculated and plotted together (Fig 32) and the best fit line for all the results was calculated. Test 3 gave insufficient data for calculation of permeability. The permeability ranged from $10^{-3}m/s$ at a voids ratio of 200 to 10^{-6} at a voids ratio of 5.

4.5 Summary of results

The following mean values of the parameters of the Kelang mud were determined:

$$m_e = 0.0005 kg/N/s$$

$$\tau_e = 0.00050\ \rho_h^{1.4}\ (N/m^2)$$

$$w_{50} = 0.00002\ C^{0.8}\ (m/s)$$

$$\tau_d = 0.06 N/m^2$$

$$K_{13} = 1.6$$

$$k = 10^{-7.5} e^2\ (m/s)$$

$$\sigma'_v = 5000/e^2 \quad (N/m^2)$$

$$\rho_o = 25 kg/m^3$$

5 CAROUSEL TIDAL CYCLE TESTS

5.1 Introduction

Four carousel tidal cycle tests were conducted with the objectives of assessing the general performance of the system, investigating the behaviour of mud beds during different types of tidal cycles and providing data with which to test the mathematical model.

The first test was designed primarily to prove the performance of the system. The second and third tests were structured to study the effect of progressively increasing or decreasing respectively the magnitude of the peak applied bed shear stress. This is somewhat akin to the process which takes place during the neap-spring and spring-neap tidal cycles respectively as the tidal range, peak flow velocity and peak bed shear stress increase towards the spring tide and subsequently decrease towards the neap tide. The last tidal cycle test was conducted to examine the influence of the time of consolidation between the periods of erosion of the bed.

The carousel calibrations of voltage against speed of rotation of roof and speed of rotation against average bed shear stress are shown in Figure 33. The required pattern of bed shear stress with time for each test is first determined and then by working back through these calibrations the necessary pattern of voltage output with time can be derived and input into the micro-computer.

5.2 Test A

5.2.1 Description of cycles

The first tidal cycles test in the carousel was undertaken principally to ensure that the control and recording systems of the carousel functioned properly. Nevertheless, the test was structured so that some insight into the behaviour of an estuarine mud bed could be obtained during the series of simulated tidal cycles.

The applied average bed shear stress against time for Test A is shown in Figure 34. The length of time at the peak shear stress was varied from cycle to cycle starting at zero for the first cycle and progressively increasing at every other cycle. The rising limb, falling limb and the time at zero rotation were the same in all nine cycles which comprised the test. At the start of a cycle the voltage setting increased linearly to obtain the maximum value of 4.0V (i.e. 2.9rpm, $\tau_b = 0.31 N/m^2$) after 1.33 hours. After a period of time at this maximum (i.e. zero for cycles 1 and 2, 1 hr for cycles 3 and 4, 2 hrs for cycles 5 and 6, 3 hrs for cycles 7 and 8, and 4 hrs for cycle 9) the voltage decreased to zero over the following 1.33 hrs, after which it remained at zero for 3.33 hrs. Accordingly, the overall length of the nine tidal cycles were 6,6,7,7,8,8,9,9 and 10 hours respectively.

5.2.2 Results

For this proving test the concentration of suspended solids at mid-depth was continuously recorded during the nine cycles. The results of the time-varying concentration of suspended solids with time are seen in Figure 34. The overall pattern is one in which

the concentration of solids increases sharply during the rising limb of the flow cycle, then continues to increase but at a reduced rate during the constant rate of flow period (cycles 3 to 9 only). After this the concentration decreases a little during the falling limb of the cycle and then reduces quickly to virtually zero during the no flow period. The peak concentration of suspended solids in each cycle followed a consistent trend in that it was similar for cycles with identical flow history but overall the peak value increased from one pair of cycles to the next up to a value of about 2.7kg/m^3, which was not exceeded during the ninth cycle.

The magnitude of the concentration of suspended solids may be considered to reflect the average depth of erosion of material from the bed. In this proving test no direct measurement of the bed level was made using the ultrasonic transducer. Therefore, the results may be interpreted to indicate that by the ninth cycle the peak shear stress had been applied to the bed for a sufficiently long enough period to erode down to a surface of mud which had a shear strength equivalent to the applied stress. During the first six cycles the concentration of suspended solids was still increasing at the time when the applied shear stress was reduced. This implies that the bed was still eroding at this time.

It is interesting to consider the rate of increase of the concentration of suspended solids and particularly to compare this for successive cycles. The results of the first three cycles have been plotted relative to the time after the start of each cycle in Figure 35. The increase in suspended solids concentration during the first cycle occurred later relative to the second cycle up until the maximum applied shear stress at which time the two curves became coincident. This

clearly indicates the difference between the first time erosion of the bed which had consolidated for almost 6 days and the erosion or re-suspension of the material deposited during the first cycle which had consolidated for only 2 hours or so. Not surprisingly, the younger deposit was more easily removed.

Because the deposition and consolidation phases of each cycle were identical, the structure of the bed may be assumed to have been the same at the beginning of cycles 2 and 3. Accordingly, the increase in suspended solids concentration up to the time of peak bed shear stress in both cycles 2 and 3 was identical (see Fig 35). Beyond this time the bed in cycle 3 continued to be eroded as the peak shear stress was maintained for a period of 1 hour.

The results of cycles 3, 4 and 5 are presented relative to the time from the beginning of each cycle on a common time axis in Figure 36. The slight difference in cycles 3 and 4 between the times of approximately one to two hours after the start of each cycle is the result of the difference in consolidation time of that portion of the bed which is being eroded during that period. In cycle 3, the material which gave rise to concentrations of suspended solids greater than about 1.8kg/m^3 (i.e. the maximum concentration in cycle 2) may be considered to have been eroded for the first time. However, in cycle 4, this same material is being resuspended after having consolidated for the relatively short period of only three hours or so. Cycle 5, which had a similar bed structure to cycle 4 at the start, may be seen from Figure 36 to have produced identical concentrations of suspended solids up until the time when the applied shear stress began to reduce in cycle 4.

One further point of interest in the graphs of suspended solids concentration is the time after the start of a cycle at which the increase in the concentration is first recorded. This time was virtually the same for all the cycles around 30 minutes after the start except the first in which it was 5-10 minutes later. The shear stress at these points indicate the critical shear strength of the surface of the deposits. Understandably, the surface of the bed at the start of cycle 1 would have had a somewhat higher shear strength due to its longer period of consolidation.

5.3 Test B

5.3.1 Description of cycles

The second tidal cycles test was conducted to investigate the behaviour of a deposited mud bed subject to a series of cycles in which the peak applied shear stress progressively increased. The applied bed shear stress against time for Test B is shown in Figure 37. Each of the four cycles was six hours in duration and all had a similar rate of increase in the voltage setting during the rising limb of the cycle. The time during which the voltage setting was reduced from its peak value to zero was 30 minutes in all cycles. The cycles had peak voltage settings of cycle 1 - 4.0V (ie 2.9rpm, $\tau_b = 0.31 N/m^2$); cycle 2 - 4.66V (ie 3.3rpm, $\tau_b 0.40 N/m^2$); cycle 3 - 5.33v (ie 3.8rpm, $\tau_b = 4.48 N/m^2$); cycle 4 - 6.0V (ie 4.2rpm, $\tau_b = 0.57 N/m^2$). The time for which the voltage was zero accordingly differed from cycle to cycle. For cycle 1 it was 250 minutes, cycle 2 it was 237 minutes, cycle 3 it was 223 minutes and for cycle 4 it was 210 minutes.

5.3.2 Results

The time varying applied bed shear stress, suspended solids concentration and depth of erosion of Test B are shown in Figure 37. Overall, the pattern of the variation with time of suspended solids concentrations was a steep increase in concentration which began part way through the rising limb of the applied shear stress and ended coincident with the peak in shear stress, followed by a small decrease during the falling limb of the shear stress cycle and a sharp reduction which progressively reduced during the period when the fluid was still. Looking in more detail at cycles 2, 3 and 4, it may be observed from Figure 37 that a temporary reduction in the rate of increase in the concentration of suspended solids occurred part way through each cycle. This corresponds with the maximum concentration attained in the previous cycle and may be considered to mark the division in each cycle between the re-suspended material and the first-time eroded material. The fact that this was characterised by a reduction in effectively the rate of erosion indicates that the re-suspended material had a somewhat lower shear strength than the original material. This would further imply that this was the result of lower densities in the re-suspended material due to the considerably shorter consolidation time - three hours against 20 days. Hence, the discontinuity in density of the bed at the start of cycles 2, 3 and 4 may reasonably be assumed to have been present at the interface of the re-suspended material and the original bed.

The depth of erosion (also shown in Figure 37) was measured using the ultrasonic transducer during cycles 1, 2 and 3. The readings were taken only during the erosion part of the cycles and in particular to the first-time erosion of the bed material.

The time during each cycle at which the suspended solids concentration first shows an increase may be used to estimate the critical shear strength of the surface of the bed. In cycle 1 an increase in concentration was first recorded at 0.8 hours after the start of the cycle. The applied bed shear stress at this stage was $0.15N/m^2$. For cycles 2, 3 and 4 the onset of erosion of the surface layers characterised by the increase in suspended solids concentration occurred somewhat earlier in the cycle at approximately 0.5 hours after the start. This indicated a lower surface shear strength of around $0.06N/m^2$. This was understandable as the consolidation period of the recently deposited layers was only about four hours.

5.4 Test C

5.4.1 Description of cycles

The tidal cycles in the third test were similar to those in Test B except that the peak applied bed shear stress progressively decreased during the three cycles. The sawtooth profile of shear stress against time is presented in Figure 38. The experiment began by eroding the bed down to an average depth which was capable of resisting an applied shear stress of approximately $0.19N/m^2$. After quickly reducing the fluid velocity to zero the sediment in suspension was allowed to deposit and consolidate for a period of 3.5 hours. The voltage setting was then increased at a constant rate to 3.0V ($\tau_b = 0.19N/m^2$) and then reduced over the following half an hour to zero. The peak voltage of cycle 2 was 2.5V ($\tau_b = 0.14N/m^2$) and for cycle 3 it was 2.0V ($\tau_b = 0.09N/m^2$). Each cycle lasted six hours.

5.4.2 Results

The applied bed shear stress, suspended solids concentration and depth of erosion with time are shown for Test C in Figure 38. The concentration of suspended solids exhibited a pattern similar to the applied stress. Peak concentration coincided with the peak shear stress and the magnitude of the peak concentration consistently decreased in the three cycles.

During the first cycle, although the upper part of the bed had been eroded and re-deposited only three hours before erosion re-commenced, the bed had gained sufficient strength not to be immediately eroded back down to that previous depth. In fact, the surface of the bed resisted a shear of about $0.06 N/m^2$ before erosion occurred which was about equal to the erosional shear strength of the surface of the original bed.

In the subsequent cycles, the peak shear stress was lower which had the effect of eroding less material in each cycle. The onset of erosion in cycle 2 and cycle 3 occurred at a shear stress equal to that in cycle 1.

5.5 Test D

5.5.1 Description of cycles

The purpose of the tidal cycles run in Test D was to investigate the importance of the time of consolidation on the erosion of the bed. Only relatively short times of consolidation were investigated, namely between 2 and 9 hours, as this was considered to be representative of slack water periods during the semi-diurnal tidal cycle.

The time profile of average applied bed shear stress is shown for Test D in Figure 39. The rising part of each cycle was identical and took the voltage setting from zero to 4.0V (2.9rpm, τ_b= 0.31N/m^2) in 0.5 hours. The time at peak bed shear stress was dependent on the period of consolidation preceding the cycle and was between 1 and 2 hours. The exact time at the peak bed shear stress was not important as the function of this part of the cycle was to erode down to the previously exposed level in the mud bed. This ensured that the initial conditions for the deposition and consolidation phases were the same for each cycle.

The four cycles had times of consolidation of 2 hours (cycle 1), 4 hours (cycle 2), 9 hours (cycle 3) and 2 hours (cycle 4). Cycle 4 was the same as cycle 1 and was conducted to give an indication of the repeatability of the system.

5.5.2 Results

The time varying applied bed shear stress and concentration of suspended solids are shown in Figure 39. Inspection of the concentration curves of the four cycles indicates broadly similar peak values but slightly different rates of increase towards the peak value. This is more clearly illustrated in Figure 40 in which the concentration of suspended solids is shown for cycle 1 (2 hours consolidation) and cycle 3 (9 hours consolidation).

Although the peaks are different, somewhat higher for cycle 3, the most interesting feature is the relative shape of the curves in the first half an hour of each cycle. During this time the bed in cycle 3 erodes at a slower rate than in cycle 1 which indicates a more resistant bed. This is consistent with the knowledge that the greater time of consolidation in cycle 3

(i.e. 9 hours) would have generated a more dense bed, and hence more resistance to erosion, in comparison with the bed in cycle 1 (2 hours of consolidation).

In cycle 4, the shape of the profile in the earlier stages is very similar to that in cycle 1 which was an identical cycle. However, the increase in the peak concentration in cycle 4 over cycle 1 is probably attributed to the fact that equilibrium was not attained at the very beginning of the test before cycle 1. Nevertheless, overall the results were consistent and showed clearly the effect of consolidation on the re-suspension of mud deposits.

6 MODEL SIMULATION

6.1 Carousel tidal cycles

The model described in Section 3 was developed to simulate the behaviour of mud beds during tidal cycles. The performance of the model was assessed by comparing the model results and laboratory data of Test B. The basis for the comparison was the concentration of suspended solids with time.

The model required as input the parameters which described the basic behaviour of the mud in respect to its erosion, deposition and consolidation properties (see Section 4). In addition, it was necessary to define the initial density structure of the bed, and the average applied bed shear stress with time.

The initial density structure of the bed in the carousel could not easily be determined. Accordingly, reference was made to the mud bed in erosion Test 3 which had been deposited from the same concentration

of suspended solids and which had consolidated for a similar period time. This was shown to have a density structure in the top 0.002m given by:

$$\rho_h = 69 + 57200h \qquad (27)$$

where

ρ_h = dry density (kg/m^3)
h = depth below original surface (m)

The results of the model simulation of Test B are shown in Figure 41. It is clear that in qualitative terms there is good agreement between the model simulation and the laboratory experimental results. This is illustrated by the occurrence in both sets of results of periods of a low rate of increase in concentration of suspended solids part way through each cycle. This, as previously discussed in Section 5.3.2, represents the transition between the erosion of recently deposited material (i.e. from the last cycle) and the erosion of the original bed.

In quantitative terms the agreement between the model simulation and the laboratory results is reasonable. The first cycle is matched well by the model although the onset of erosion is a little later in the model than in the carousel test. In cycles 2 and 3 the model gave consistently higher values of suspended solids concentration during the erosion phase. During the deposition phase the model tended to slightly over-estimate the rate of settling which resulted in generally lower concentrations of suspended solids. Cycle 4 gave the closest correlation between the model and the carousel test during the majority of the erosion phase, although the peak concentration was under-predicted by the model.

Overall, the results of the model are encouraging in that it shows that the algorithms used to describe the different phases of behaviour of the mud can be successfully combined to predict the behaviour of a mud bed during tidal cycles. The laboratory data from the carousel has enabled the model to be proved in addition to providing useful information on the basic behaviour of muds during tidal cycles.

6.2 Cardiff Docks entrance channel

The model has also been used to simulate the behaviour of the mud in the entrance channel to Queen Alexandra Dock, Cardiff (see Hydraulics Research, 1987). The procedure for implementing the model was similar to that used for the carousel tidal cycles. A sample of mud taken from Cardiff Bay was tested in the laboratory to determine its erosion and consolidation properties. The floc settling velocity had been determined in the field during a previous study (Hydraulics Research, 1984) and the critical shear stress for deposition was estimated on past experience. The applied bed shear stress during the diurnal tidal cycle and the spring-neap cycle were determined from measurements of velocity and water elevation in a laboratory physical scale model.

Unlike the closed system of the carousel in which the total mass in the bed and in suspension is constant it is necessary in the field situation to prescribe the near-bed concentration of suspended solids. This was done from field measurements taken at a number of positions within and offshore of Cardiff Bay.

The results of the physical properties tests may be summarised in the following relationships:

$m_e = 0.0008 kg/N/s$

$\tau_e = 0.00022 \rho_h^{1.5}$ (N/m^2)

$\tau_d = 0.08 N/m^2$

$k = 10^{-9} e^2$ (m/s)

$\sigma'_v = 300/e^2 - 4.5$ (N/m^2)

$\rho_o = 80 kg/m^3$

The applied bed shear stress and the near-bed concentration of suspended solids at one position in the entrance channel are shown in Figures 42 and 43 respectively. Values of both parameters were linearly interpolated from the spring and neap curves for other stages during the spring-neap cycle.

The results of the model run are shown in Figures 44, 45 and 46. The quantity of mud eroded and deposited during each tidal cycle (Fig 44) indicates that both of these quantities reach a peak at the maximum spring tide. The mass of mud deposited is in proportion to the tidal range and has a minimum value at the minimum neap tide. However, the mass of mud eroded does not reach a significant value until cycle 9 after which it follows in proportion to the tidal range until cycle 21. Thereafter, the mass of mud eroded is insignificant. In broad terms, some deposition occurs in each the tidal cycle, whereas, erosion is limited to the thirteen spring tides.

The net quantity of mud either deposited or eroded during each cycle is shown together with the cumulative quantity in Figure 45. Depositional and erosional processes are small around neap tides and the net effect is only slight deposition. Also for the ten largest spring tides these processes are almost in balance and the net effect varies between slight deposition and slight erosion. However, during the two periods of mid-tides at cycles 4 to 10 and

21 to 25 inclusive the net effect is clearly deposition. Accordingly, the cumulative mass of mud added to the original bed increases sharply during these mid-tide periods but remains reasonably constant during the principal neap and most of the spring tides.

The density profiles through the new deposit after 7, 14, 21 and 28 cycles are shown in Figure 46. Because the model represents the bed as a series of discrete layers each with a certain depth and mass (and hence density) the profiles are shown in a series of steps. Nevertheless, the increase in the density of the layers and the increase in the number of layers with time is clearly shown. For example, the bottom layer of the new deposit had a dry density of 114kg/m^3 at cycle 7 which then increased by consolidation to 143kg/m^3 at cycle 14, 153kg/m^3 at cycle 21 and 173kg/m^3 at cycle 28.

This example of the application of the model illustrates the importance of modelling the entire neap-spring-neap cycle and the consolidation process of the bed. By this approach it is considered that a better understanding of the mud regime at locations within harbours, ports, navigation channels and estuaries generally will be attained, and predictions of erosion and deposition will be improved.

7 CONCLUSIONS AND RECOMMENDATIONS

7.1 Conclusions

1. The HR mud carousel flume was modified by the addition of a micro-computer for control, a densiometer for continuous measurement of the suspended solids concentration (linked to a chart recorder) and an ultrasonic transducer for

non-destructive determination of the thickness of the mud bed. Laser doppler anemometry was employed to measure the vertical velocity profile at three sections across the width of the flume from which the bed shear stress was calculated. These developments enabled the carousel to be used for investigating the behaviour of a mud bed during simulated tidal cycles.

2. A mathematical model was formulated to simulate the three basic physical processes of mud, namely erosion, consolidation and deposition during repeated tidal cycles. The model extended the work done in another part of this contract (see Ginger, 1987) on the modelling of consolidating mud deposits.

3. New experimental procedures were developed to enable the erosion and consolidation properties of a mud to be determined. The new erosion tests were undertaken in the carousel and the procedure enabled the density of the eroding surface of the bed to be determined. The consolidation tests were performed in settling columns and involved the continuous deposition of material from suspension and the determination of important empirical relationships between voids ratio, effective stress and permeability.

4. A mud from Kelang was selected for the tidal cycle experiments. The physical properties of the mud were investigated by erosion, consolidation and deposition tests and the following mean values of the empirical relationships were determined:

$m_e = 0.0005 kg/N/s$

$$\tau_e = 0.00050\ \rho_h^{1.4}\ (N/m^2)$$

$$w_{50} = 0.00002\ C^{0.8}\ (m/s)$$

$$\tau_d = 0.06 N/m^2$$

$$K_{13} = 1.6$$

$$k = 10^{-7.5} e^2\ (m/s)$$

$$\sigma'_v = 5000/e^2\ (N/m^2)$$

$$\rho_o = 25 kg/m^3$$

5. Four carousel tidal cycle tests were conducted to investigate the behaviour of mud beds and to provide data for testing the mathematical model. The first test was used primarily to prove the carousel. The effect of progressively increasing the magnitude of the peak bed shear stress of repeated cycles was examined in the second test. The third test studied the effect of progressively decreasing the peak bed shear stress while the fourth test was conducted to look at the effect of short periods of consolidation on the re-suspension of mud.

6. The results of the first tidal cycles tests showed that the carousel performed satisfactorily. Increasing the peak bed shear stress progressively on alternate tidal cycles revealed differences in the erosion of re-deposited material and the underlying original bed material. This was characterised by an assumed discontinuity in the density profile of the bed at the end of a tidal cycle. The effect of a consolidation period of 9 hours compared to

2 hours was to produce a bed with higher densities and have more resistance to re-erosion.

7. The mathematical model was used to simulate the behaviour of the experimental mud bed as tested during the second tidal cycles test. The results of the model showed reasonable agreement with experimental data in quantitative terms and good agreement in qualitative terms.

8. The mathematical model was used to simulate the behaviour of the mud bed at the entrance channel to Queen Alexandra Dock, Cardiff as part of a recent project study. The results for one position in the channel were presented and these clearly illustrated the importance of modelling the whole neap-spring-neap tidal processes with respect to the mud bed behaviour.

7.2 Recommendations

1. It is recommended that the laboratory and mathematical model simulation of tidal cycles be proved by detailed field measurement of the near-bed processes. This would provide invaluable data which would lead to a more informed assessment of the physical processes of mud in the field. The mud from the chosen field site would be tested in the laboratory to determine its basic physical properties which together with field data on the bed shear stress and near bed sediment concentrations would enable the mathematical model to be run to predict the changes in elevation and density structure of the bed.

8 REFERENCES

1. Burt, T N and Game, A C. "The Carousel: commissioning of a circular flume for sediment transport research", Hydraulics Research, Wallingford, England, Report No SR 33, January 1985a.

2. Burt, T N and Game, A C. "Deposition of fine sediment from flowing water: An investigation of dependence on concentration", Hydraulics Research, Wallingford, England. Report No SR 27, February 1985b.

3. Delo, E A and Burt, T N. "The hydraulic engineering characteristics of estuarine muds." Hydraulics Research, Wallingford, England, Report No SR 77, December 1986.

4. Ginger, C M. "Simulation and experimental determination of a consolidating mud deposit". Hydraulics Research, Wallingford, England, Report No SR 95, July 1987.

5. Hayter, E J and Mehta, A J. "Modelling cohesive sediment transportation in estuarial waters". Applied Mathematical Modelling, Vol 10, August 1986.

6. Hydraulics Research. "Teddington Flow Proposal. The effect on turbidity and siltation in the tidal Thames." Report No EX 1350, October 1985.

7. Hydraulics Research. "Cardiff Bay Feasibility Study, Part A: Tidal Studies, Vol II, Physical Model". Report No EX 1629, 1987.

8. Miles, G V. "Numerical simulations of the erosion of marine mud". Hydraulics Research, Wallingford, England, Report No SR 31, February 1985.

TABLES.

TABLE 1: Description of beds in erosion tests

TEST NO	DEPTH OF SUSPENSION (m)	CONCENTRATION OF SUSPENSION (kg/m^3)	SALINITY (kg/m^3)	CONSOLIDATION PERIOD (days)	BED THICKNESS (m)	MEAN DENSITY (kg/m^3)
1	0.100	28.26	30.2	4	0.0175	163
2	0.100	28.26	30.2	6	0.0171	165
3	0.100	28.26	30.2	17	0.0146	193

TABLE 2: Details of runs in erosion tests

TEST NO	NUMBER OF RUNS	SPEED OF ROTATION OF RUNS (RPM)				TEMPERATURE
		1	2	3	4	°C
1	4	1.60	2.17	2.52	2.86	12.0 - 12.2
2	2	2.86	3.52			12.6 - 13.0
3	3	2.86	3.84	4.15		15.8 - 16.0

TABLE 3: Summary of erosion test results

TEST NO	MAXIMUM EROSION DEPTH (m)	DENSITY - DEPTH CONSTANTS		EROSION SHEAR STRENGTH AGAINST DENSITY CONSTANTS		EROSION CONSTANT m_e (kg/N/s)
		K_7	K_8	K_9	K_{10}	range
1	0.0022	35	34300	0.000057	1.9	0.0005 - 0.0009
2	0.0037	27	27100	*	*	0.0005*
3	0.0018	69	57200	0.0032	1.0	0.0002 - 0.0004
ALL	-	-	-	0.00050	1.4	

Notes

Density ρ_h against depth h relationship has the form $\rho_h = K_7 + K_8 h$ $(h \leq h_{max})$

Erosion shear strength τ_e against density ρ_h relationship has the form $\tau_e = K_9 \rho_h^{K_{10}}$

The values of the constants K_7 to K_{10} are in SI units where applicable. The erosion constant is defined in the equation describing the rate of erosion, $\frac{dm}{dt} = m_e (\tau - \tau_e)$

* Insufficient data.

TABLE 4: Consolidation Test 1 results

DURATION OF DEPOSITION : 4.0hours
CONCENTRATION : 5.00kg/m^3
RATE OF INPUT TO COLUMN : 2.3 $10^{-7}m^3/s$
RATE OF DEPOSITION : 1.7 $10^{-4}kg/m^2/s$

TIME (hours)	BED THICKNESS (mm)	CUMULATIVE MASS (kg/m^2)	DENSITY (kg/m^3)
0.00	0	0.0	1
1.00	10	0.4	40
1.25	15	0.1	7
1.50	21	0.7	33
2.00	30	0.9	30
3.00	55	0.9	16
3.50	65	1.7	26
4.00	75	1.9	25
5.00	69	2.2	32
5.50	65	2.3	35
6.25	61	3.0	49
22.50	39	3.6	92
101.00	31	3.4	110
119.25	30	3.6	120

TABLE 5: Consolidation Test 2 results

DURATION OF DEPOSITION : 6.50hours
CONCENTRATION : 5.00kg/m^3
RATE OF INPUT TO COLUMN : 2.5 $10^{-7}m^3/s$
RATE OF DEPOSITION : 1.9 $10^{-4}kg/m^2/s$

TIME (hours)	BED THICKNESS (mm)	CUMULATIVE MASS (kg/m^2)	DENSITY (kg/m^3)
0.00	0	0.0	1
2.00	20	1.0	51
4.00	40	2.2	55
5.00	50	2.7	55
6.25	63	2.9	46
77.00	32	3.5	108
96.00	31	3.4	109
168.00	29	3.5	121

TABLE 6: Consolidation Test 3 results

DURATION OF DEPOSITION : 6.50hours
CONCENTRATION : 5.00kg/m^3
RATE OF INPUT TO COLUMN : 3.0 10^{-7}kg/m^3/s
RATE OF DEPOSITION : 2.3 10^{-4}kg/m^2/s

TIME (hours)	BED THICKNESS (mm)	CUMULATIVE MASS (kg/m^2)	DENSITY (kg/m^3)
0.00	0	0.0	1
3.30	65	1.7	26
4.00	96	1.4	15
28.50	71	3.9	55
168.00	50	4.0	80
300.00	49	4.0	82

TABLE 7: Effective stress against voids ratio constants

TEST NO	EFFECTIVE STRESS CONSTANTS		
	K_{17}	K_{18}	K_{19}
1	450	550	250
2	2.0	2.0	2.0
3	0.081	0.058	0.180

FIGURES.

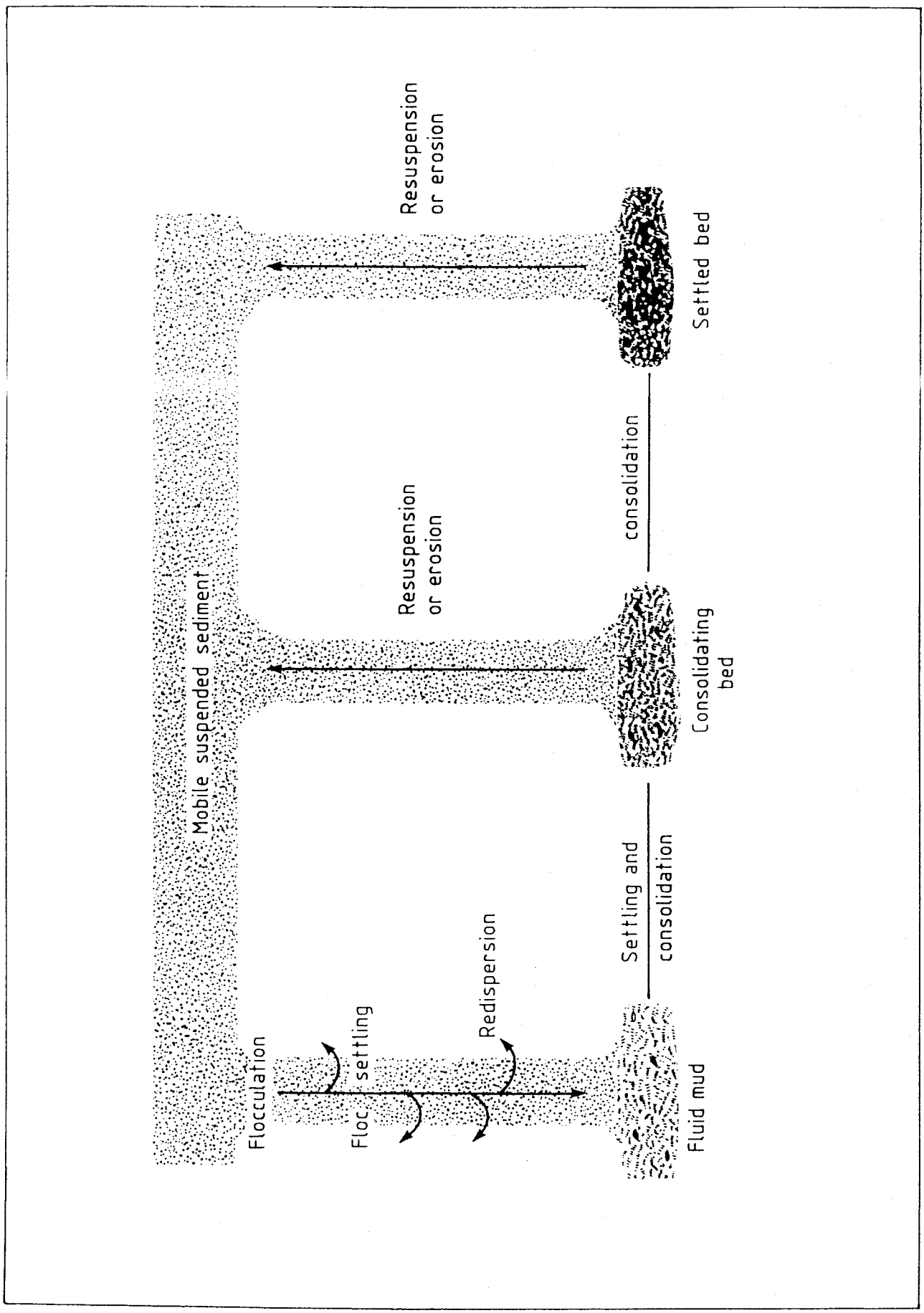

Fig 1 States of cohesive sediments

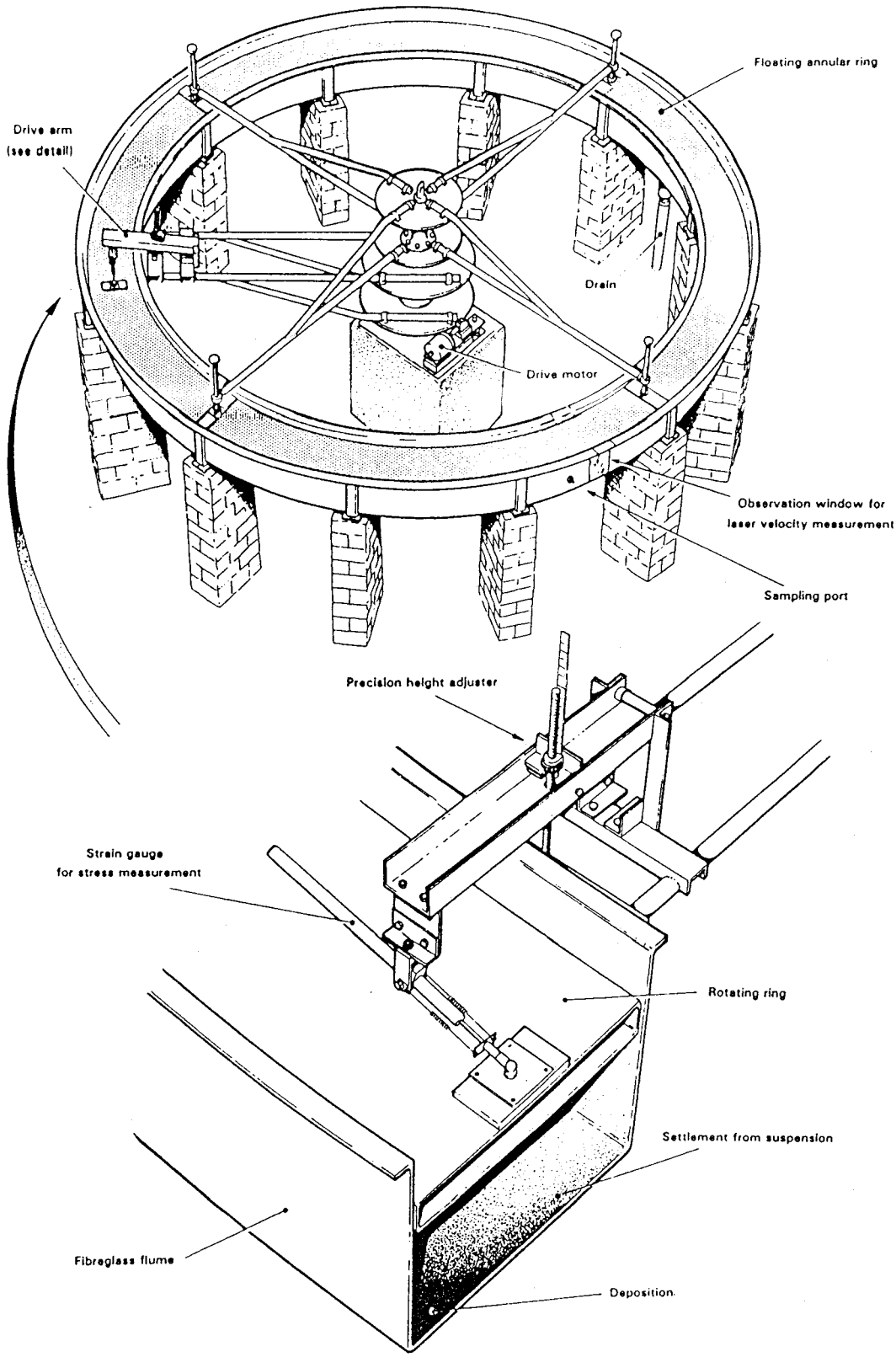

Fig 2 The Carousel

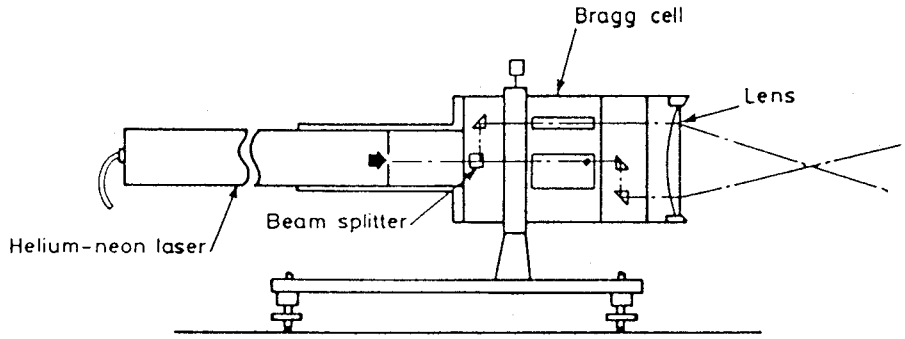

(a) Laser optical unit

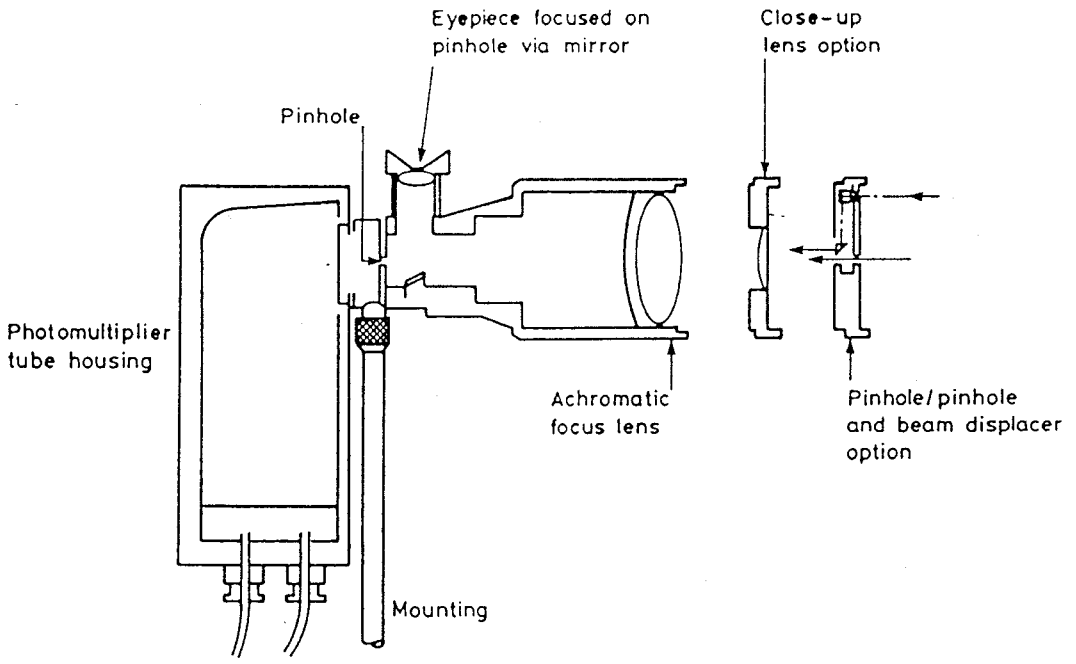

(b) Photomultiplier optical unit

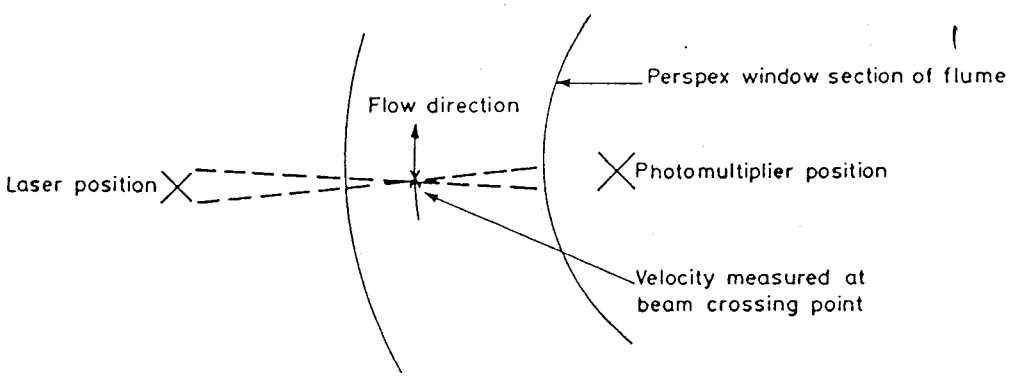

(c) Velocity measuring position

Fig 3 The laser velocity meter

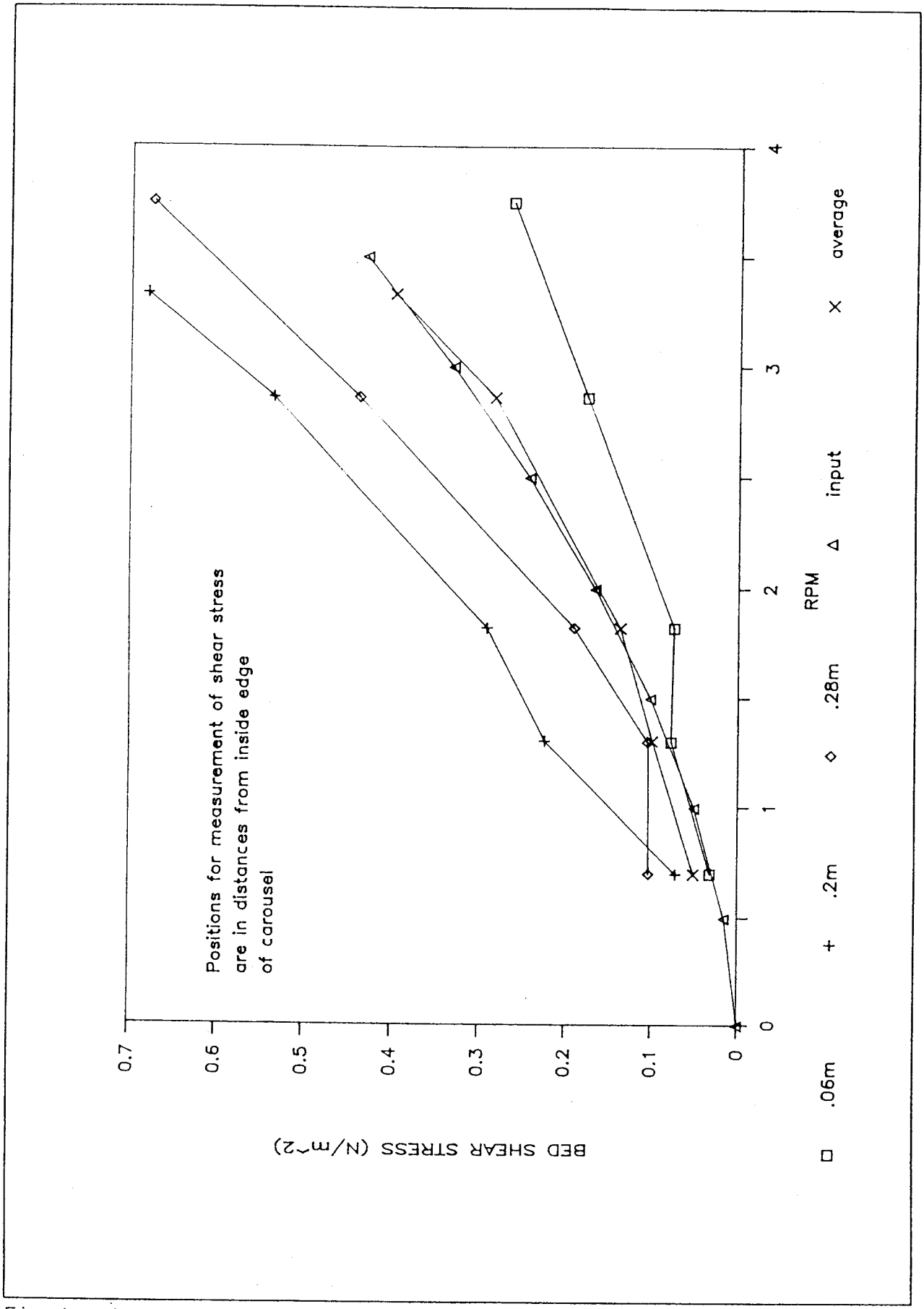

Fig 4 Average bed shear stress in carousel Flume

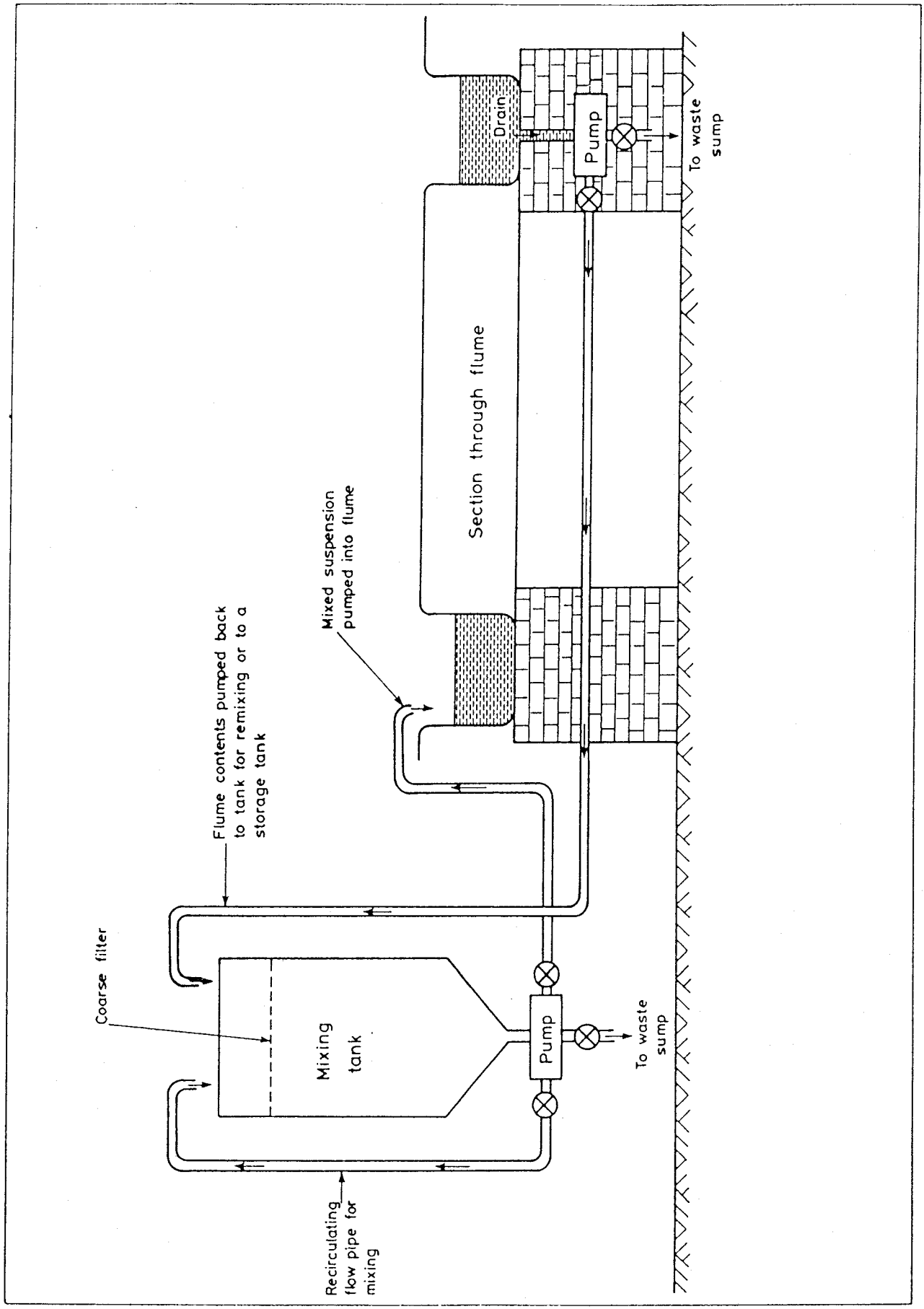

Fig 5 Filling and emptying system

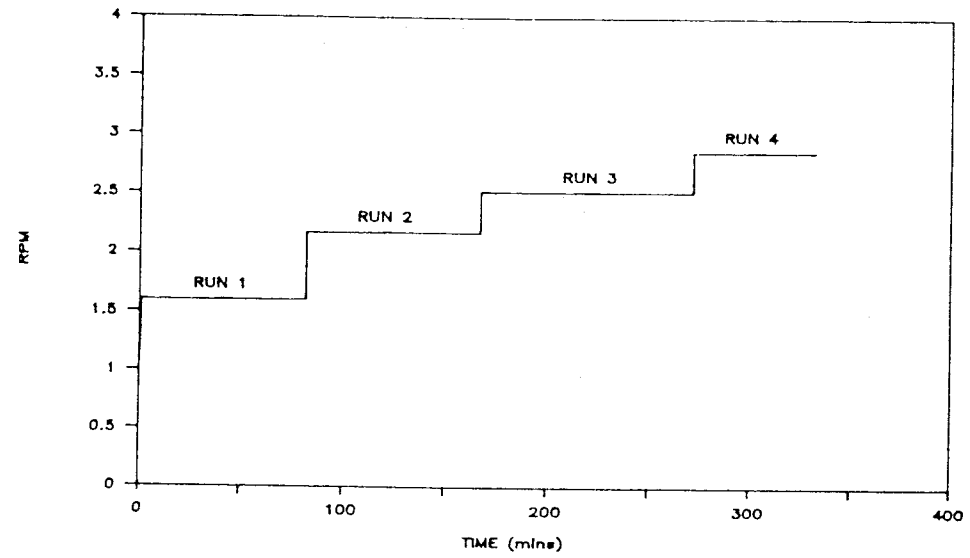

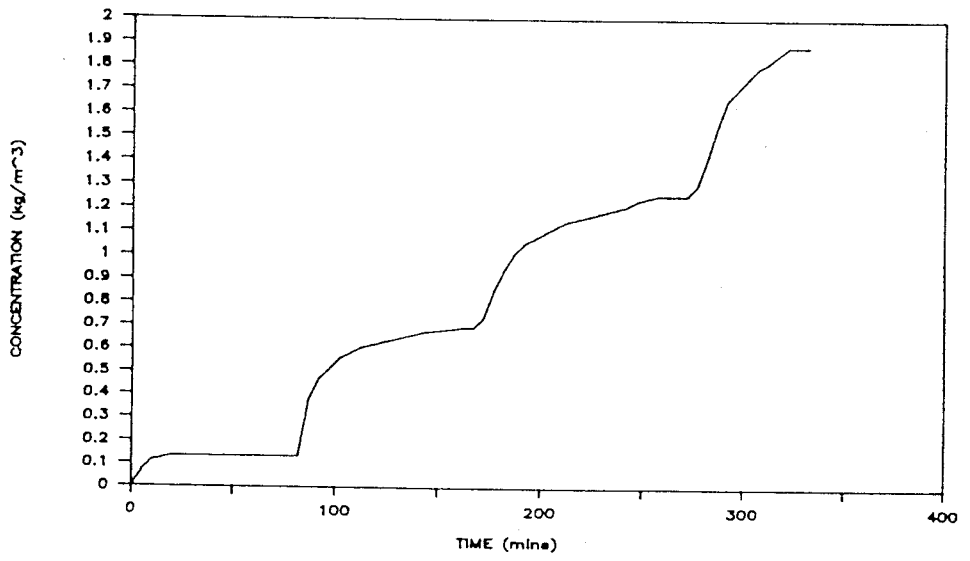

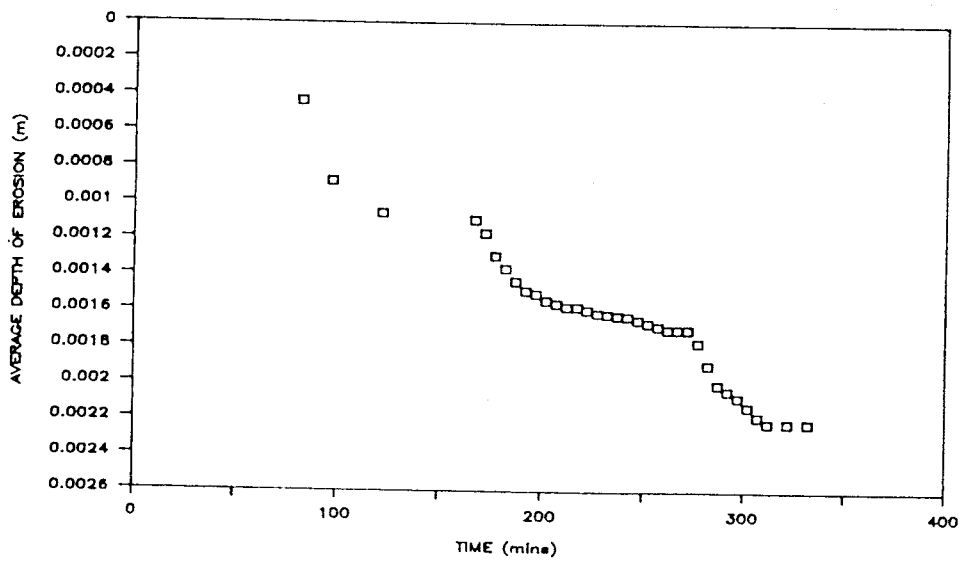

Fig 6 Erosion Test 1 Roof speed, suspended solids concentration and depth of erosion

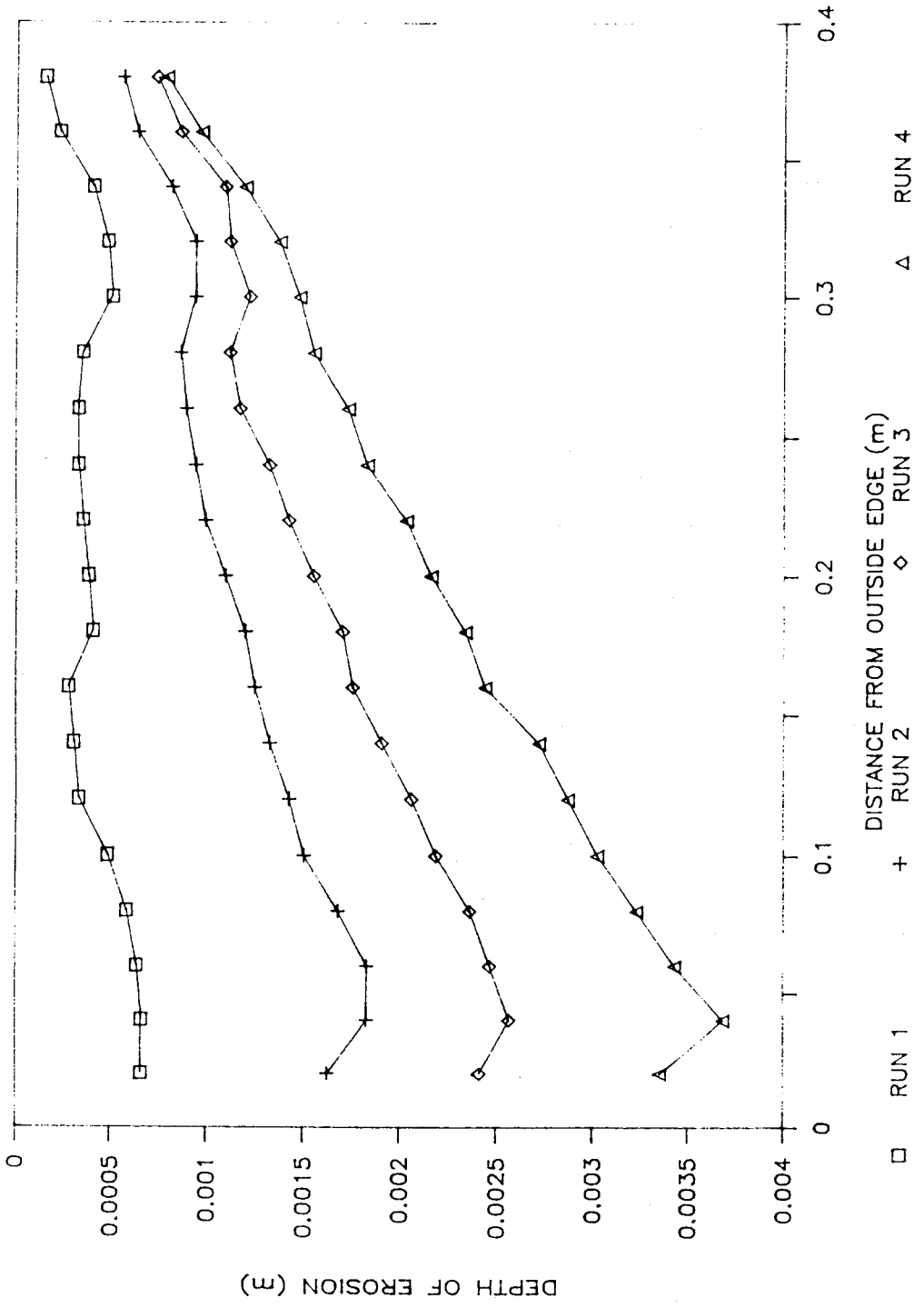

Fig 7 Erosion Test 1 Depth of erosion across the width of the flume

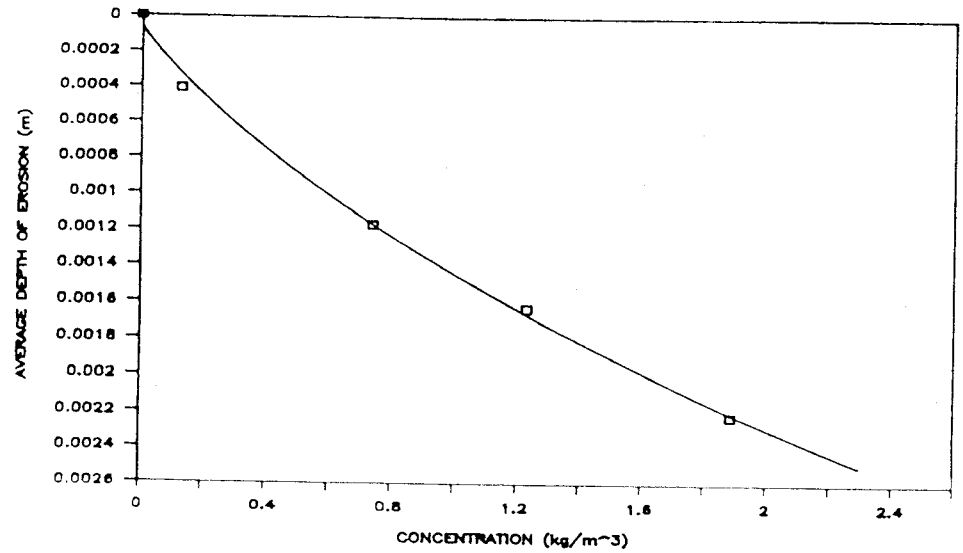

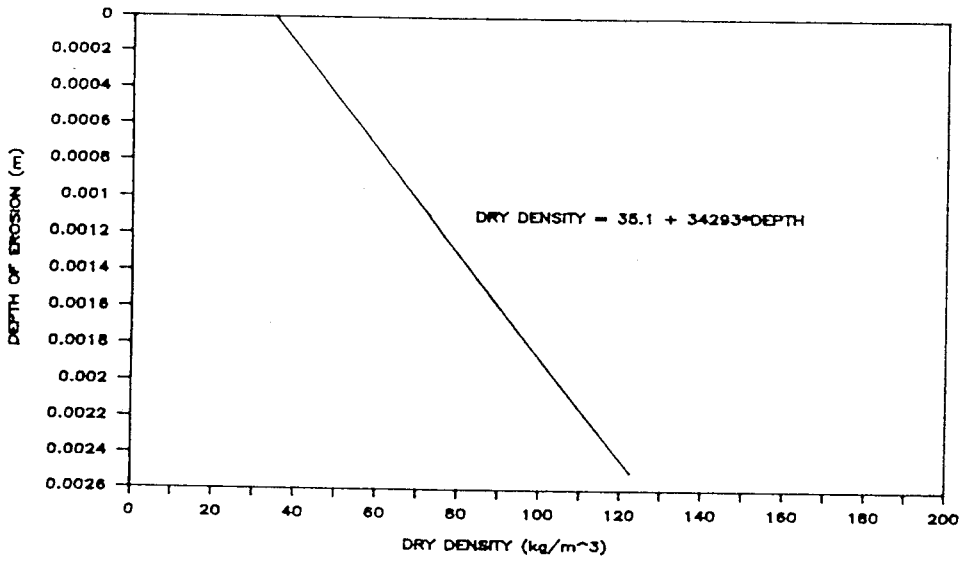

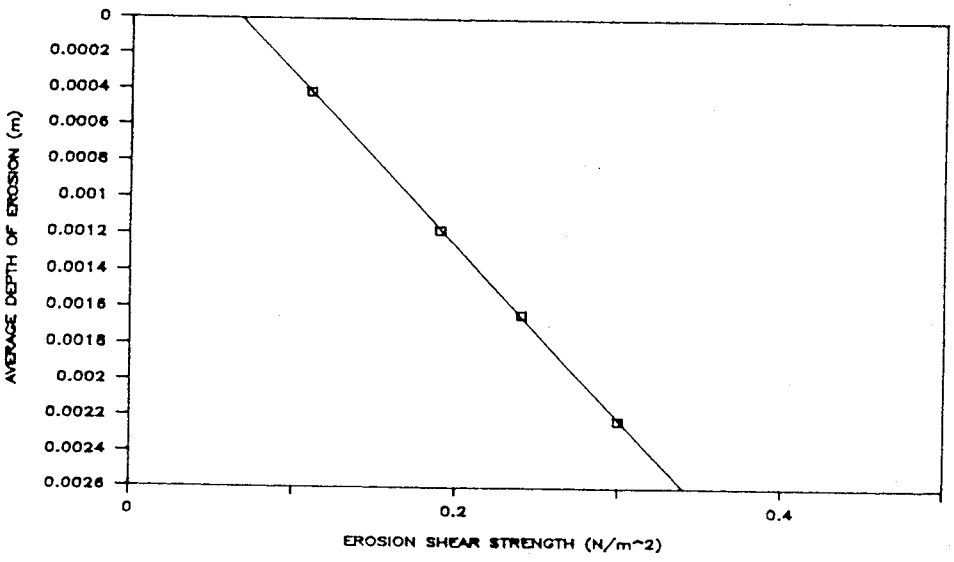

Fig 8 Erosion Test 1 Shear strength, suspended solids concentration and density against depth of erosion

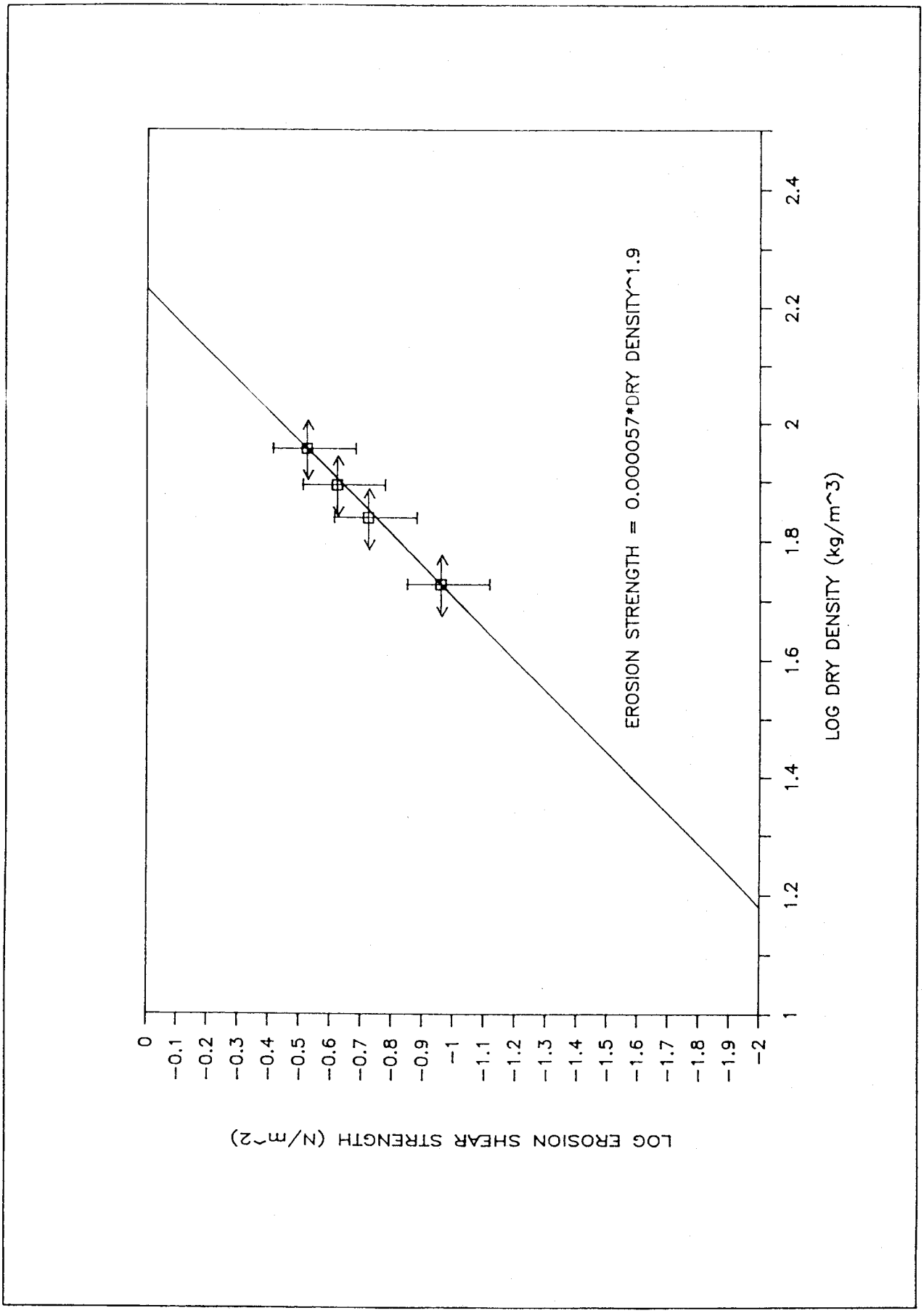

Fig 9 Erosion Test 1 Shear strength against density

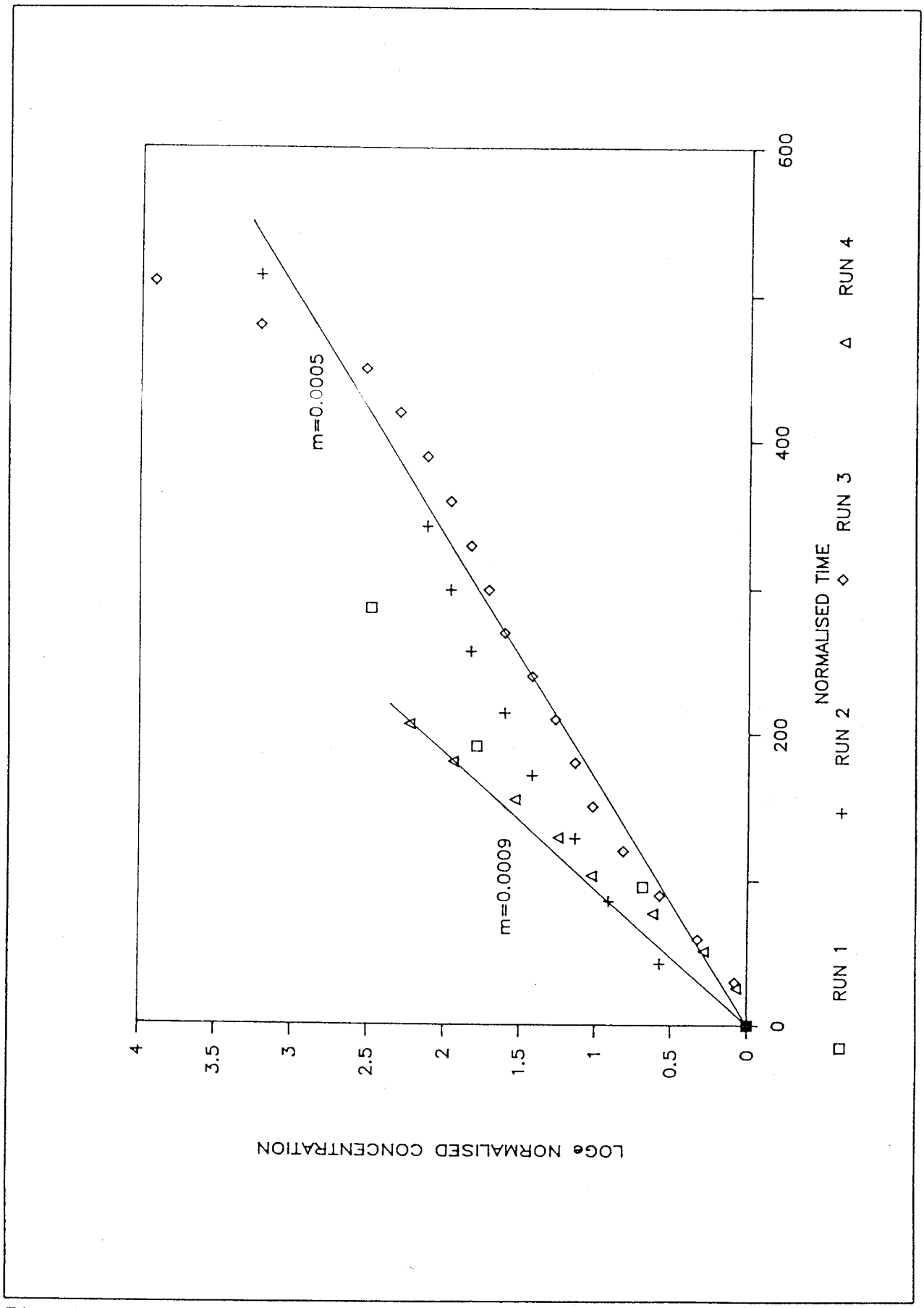

Fig 10 Erosion Test 1 Normalised results of erosion rate

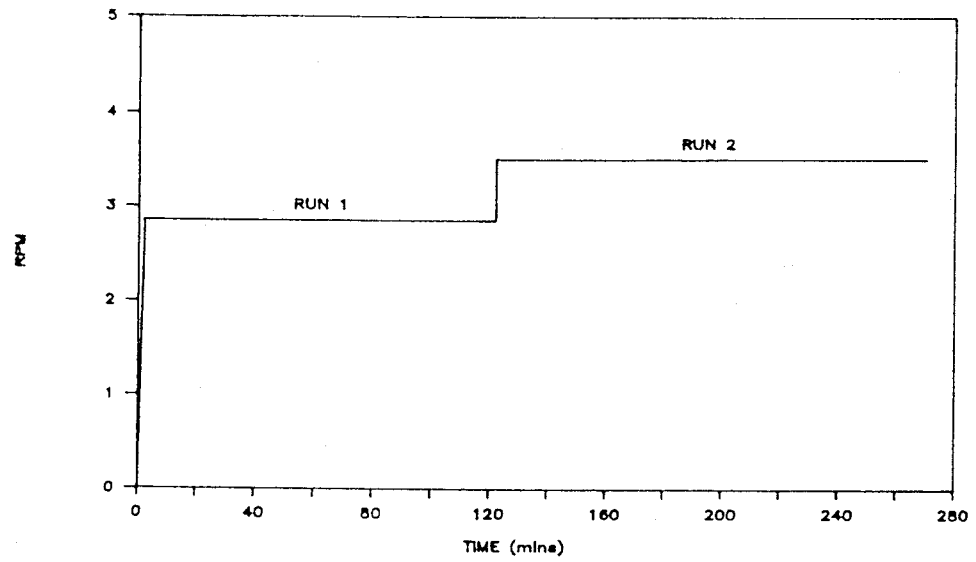

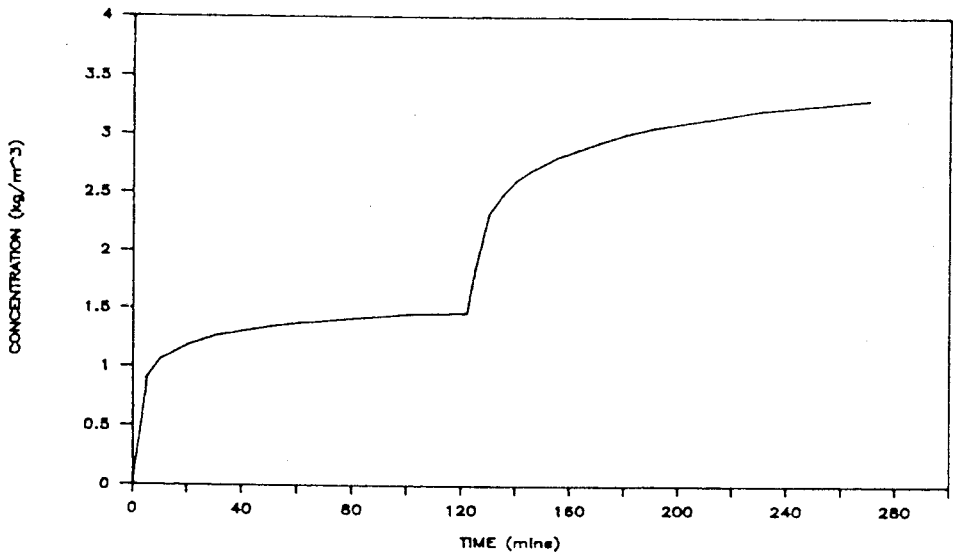

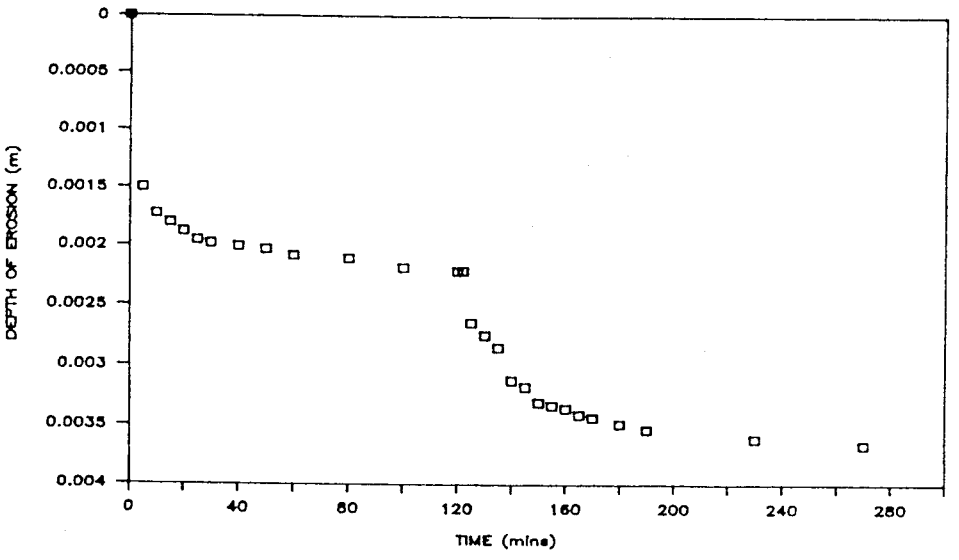

Fig 11 Erosion Test 2 Roof speed, suspended solids concentration and depth of erosion

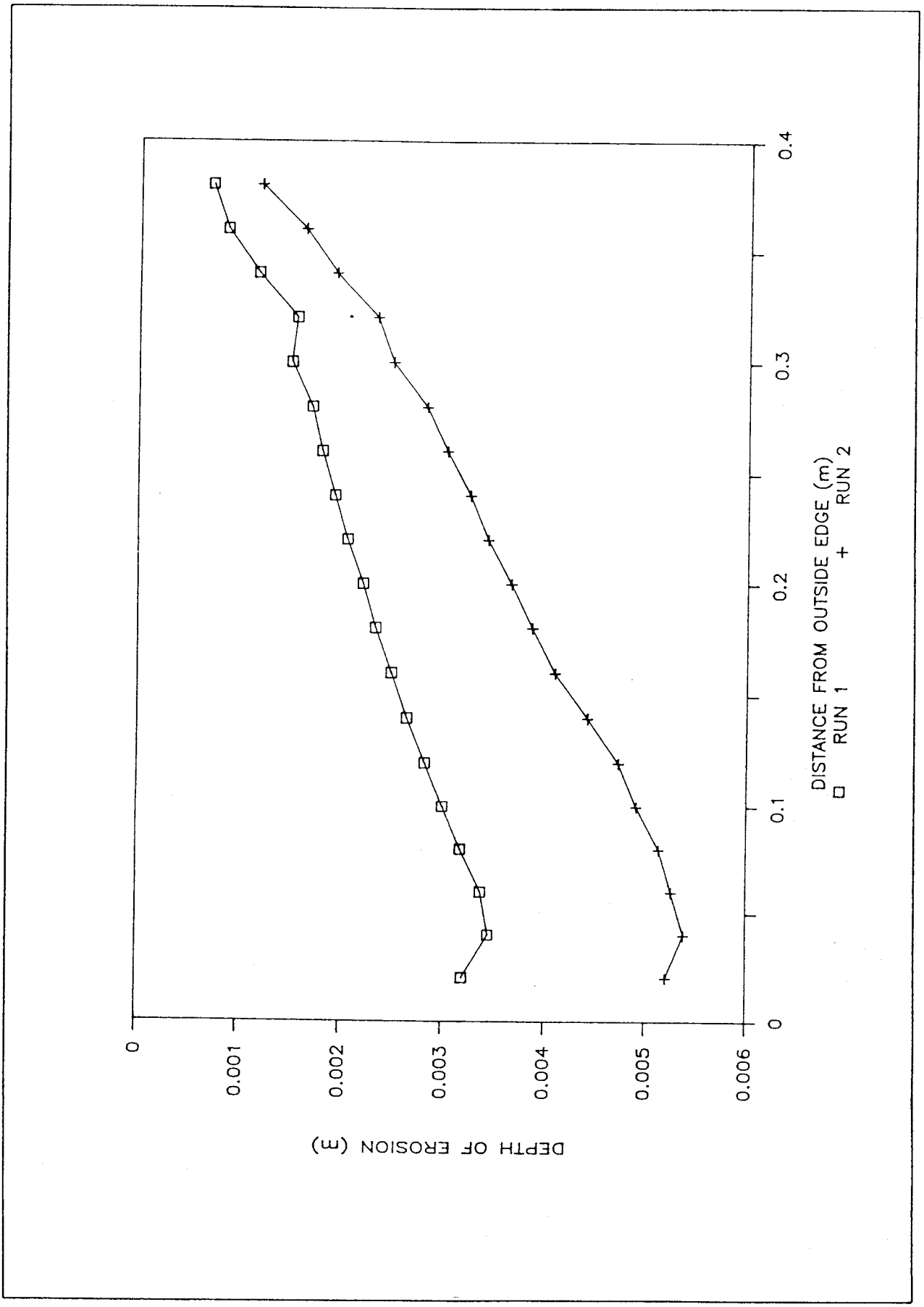

Fig 12 Erosion Test 2 Depth of erosion across the width of the flume

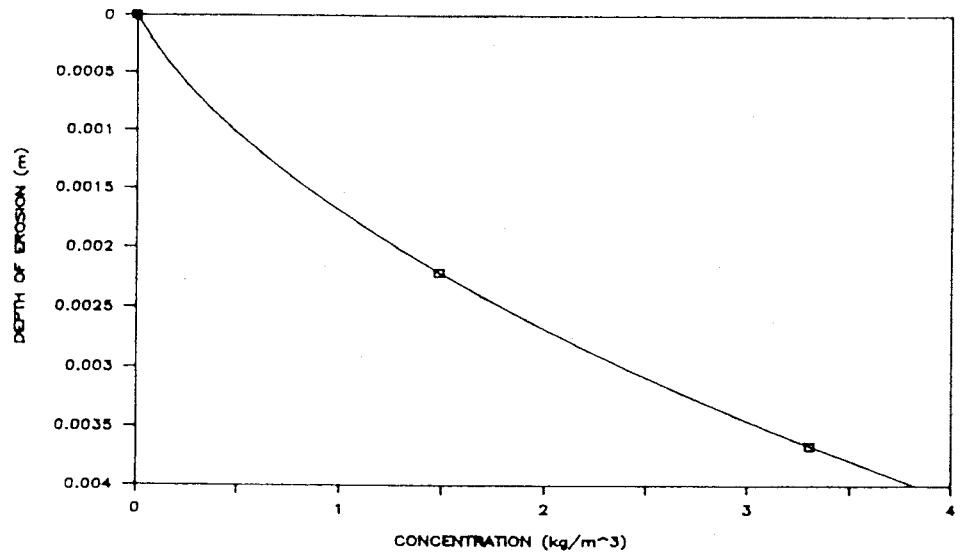

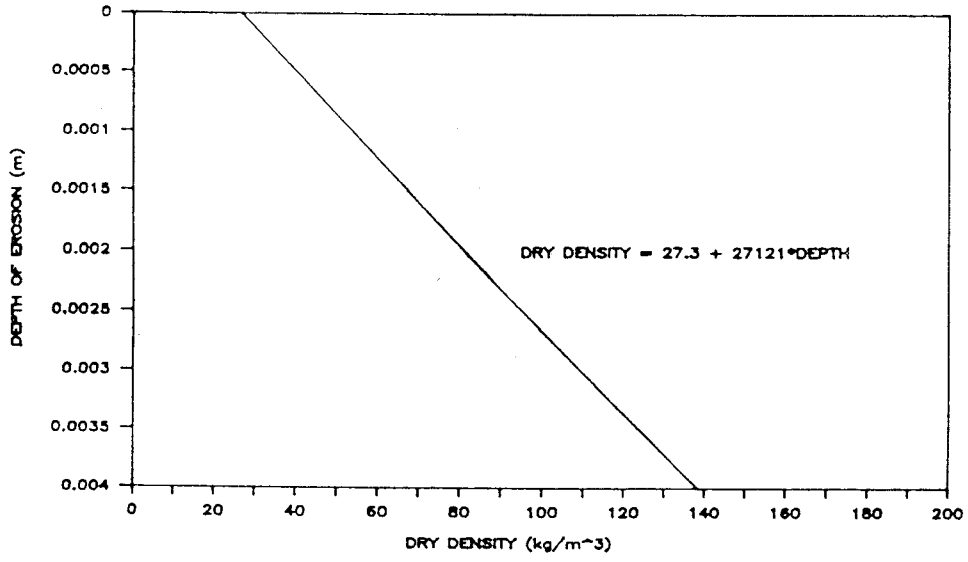

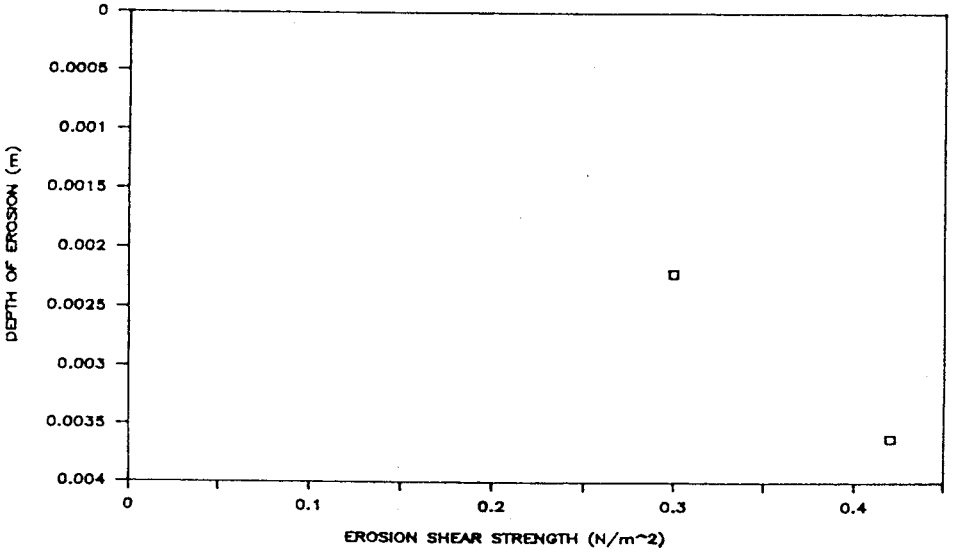

Fig 13 Erosion Test 2 Shear strength, suspended solids concentration and density against depth of erosion

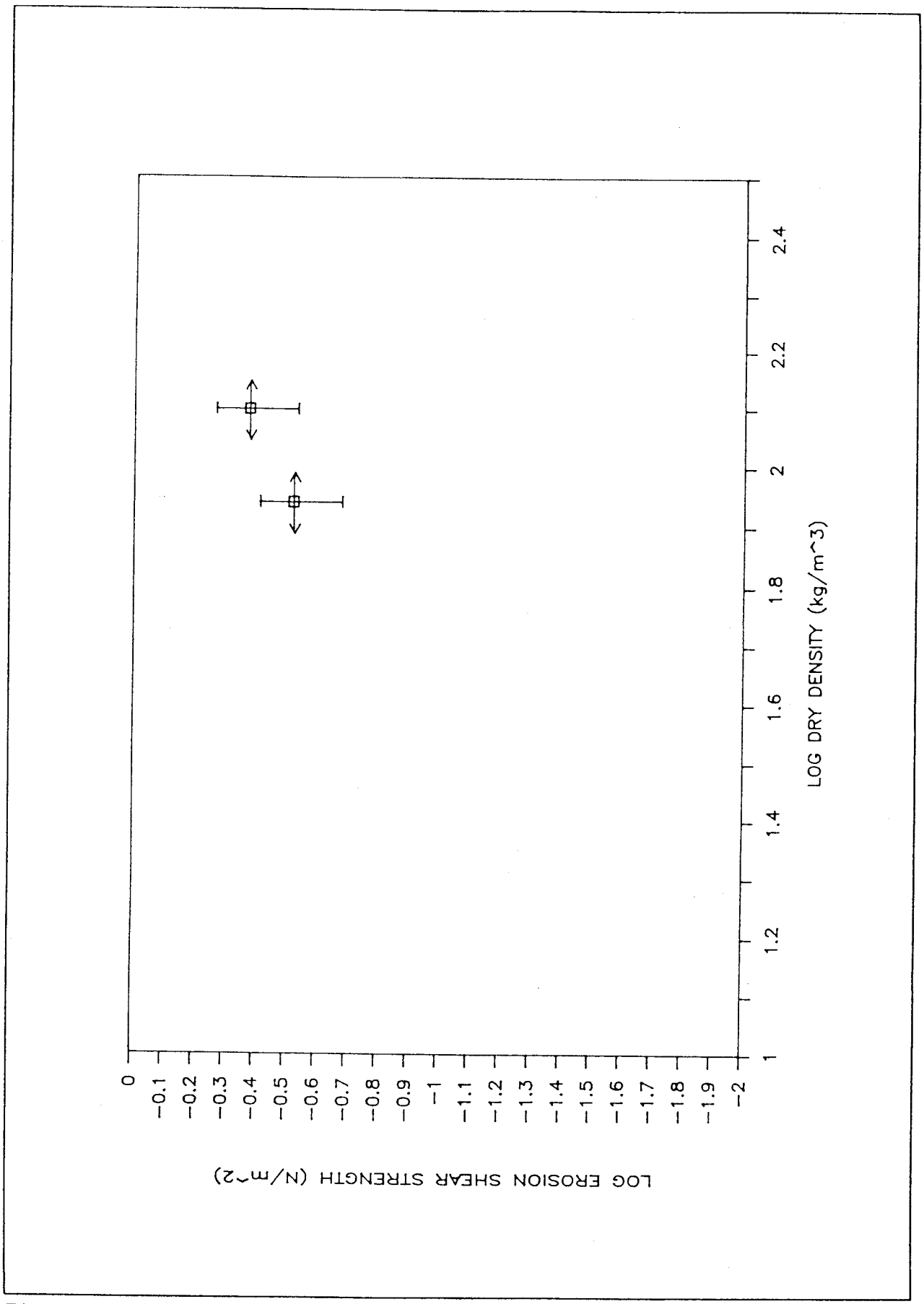

Fig 14 Erosion Test 2 Shear strength against density

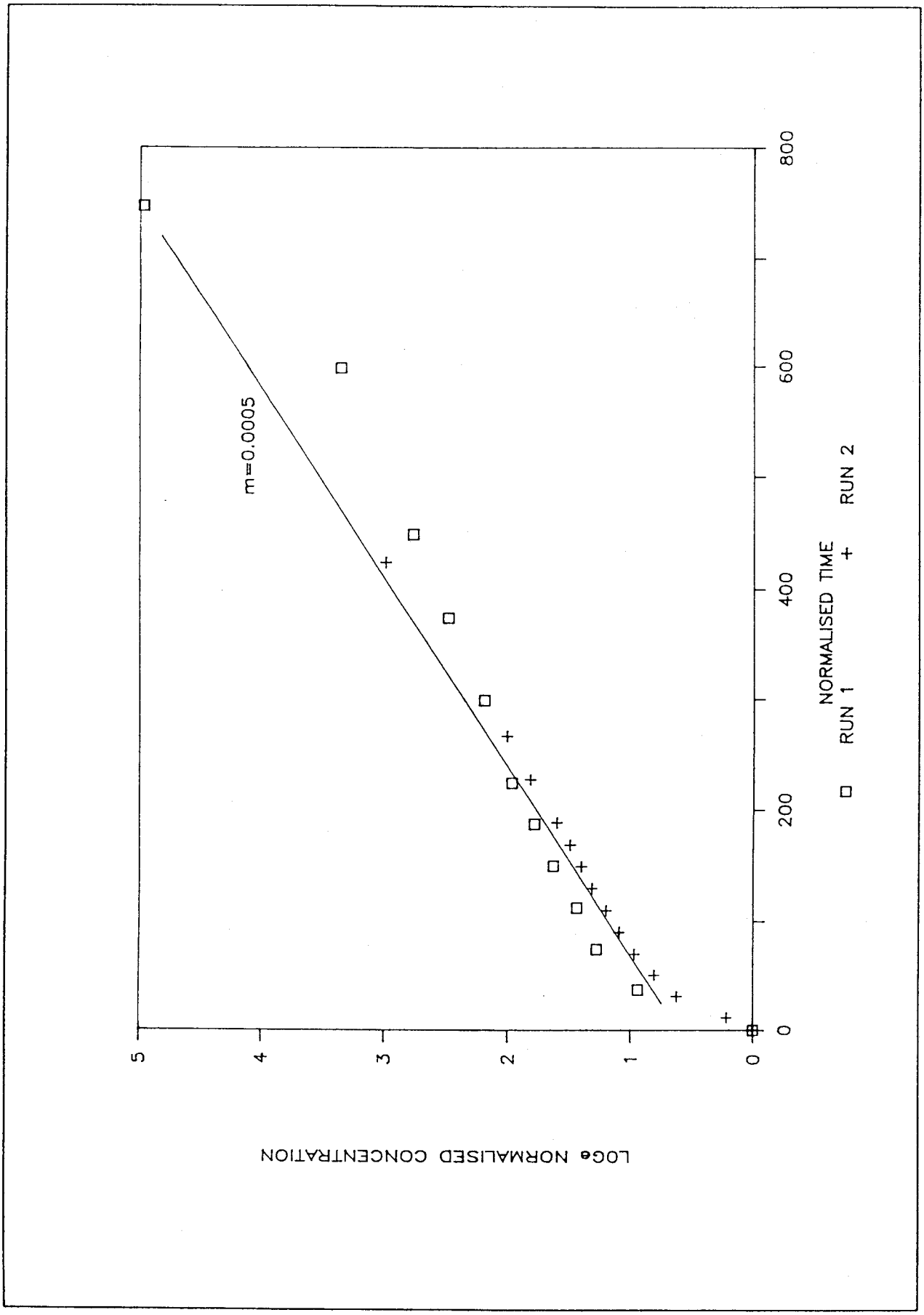

Fig 15 Erosion Test 2 Normalised results of erosion rate

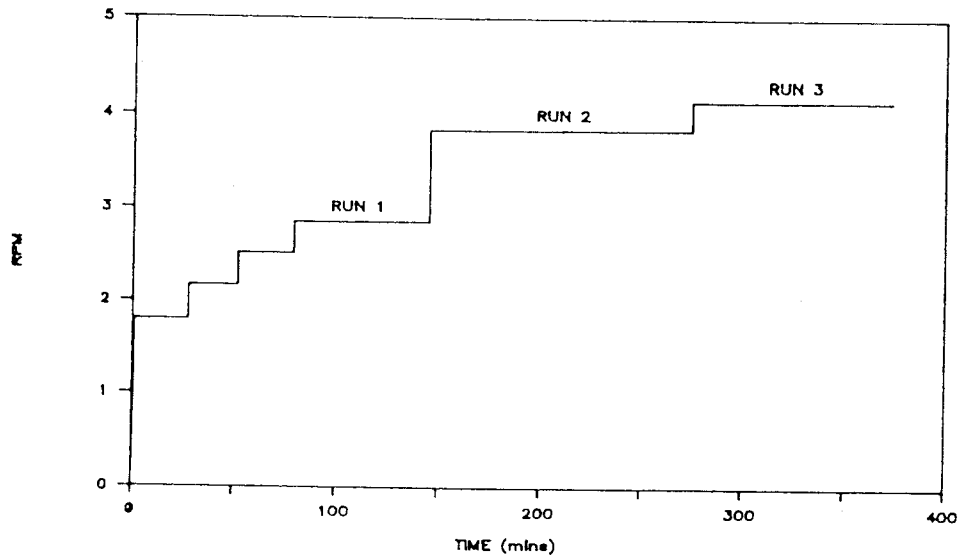

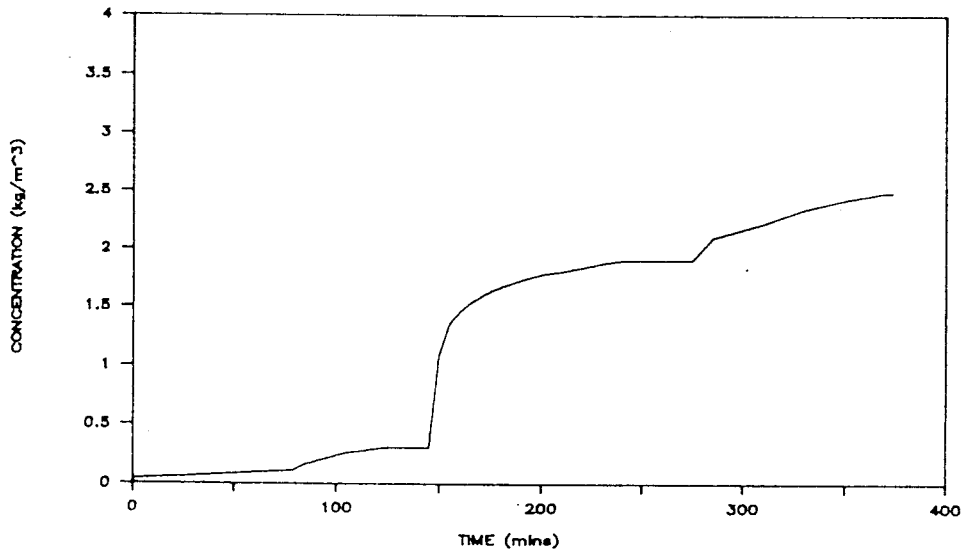

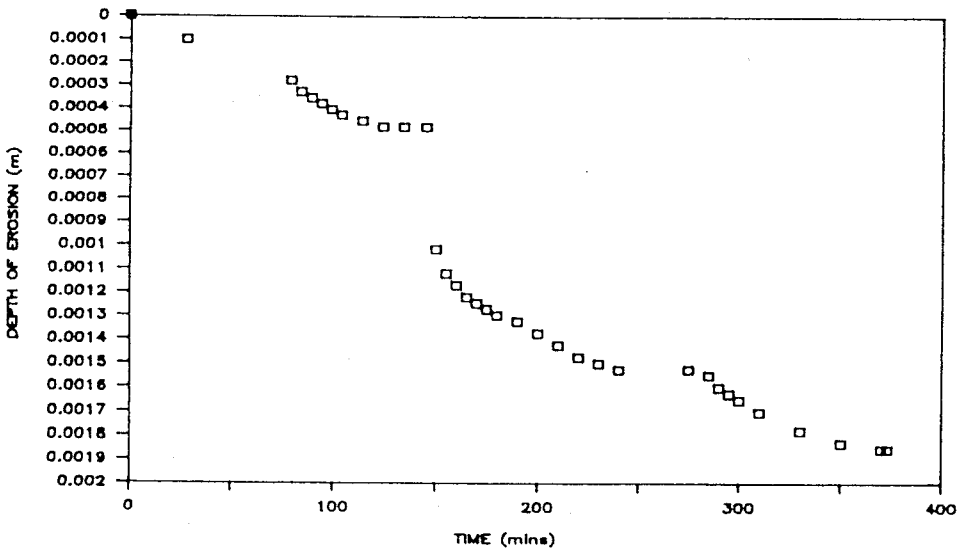

Fig 16 Erosion Test 3 Roof speed, suspended solids concentration and depth of erosion

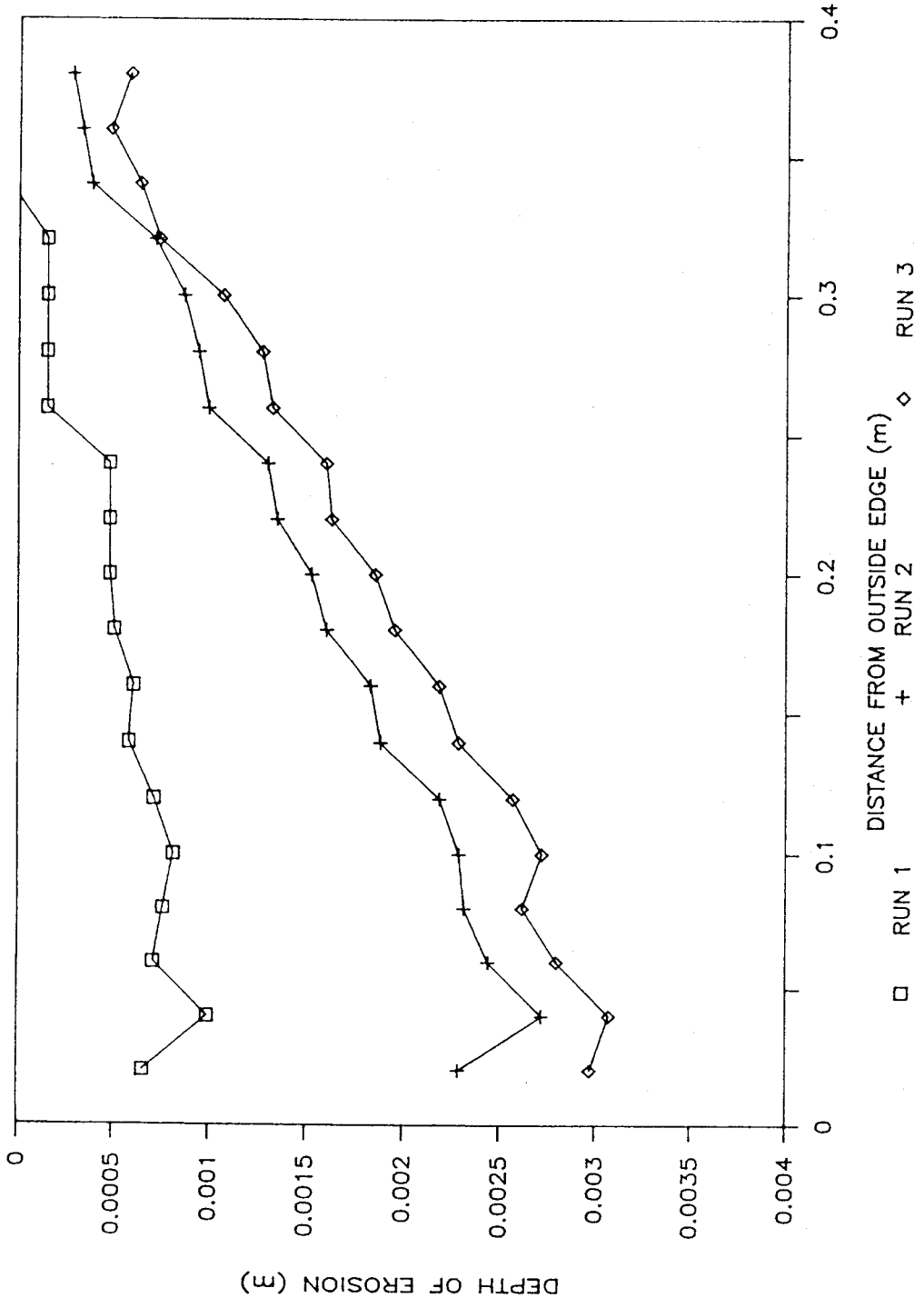

Fig 17 Erosion Test 3 Depth of erosion across the width of the flume

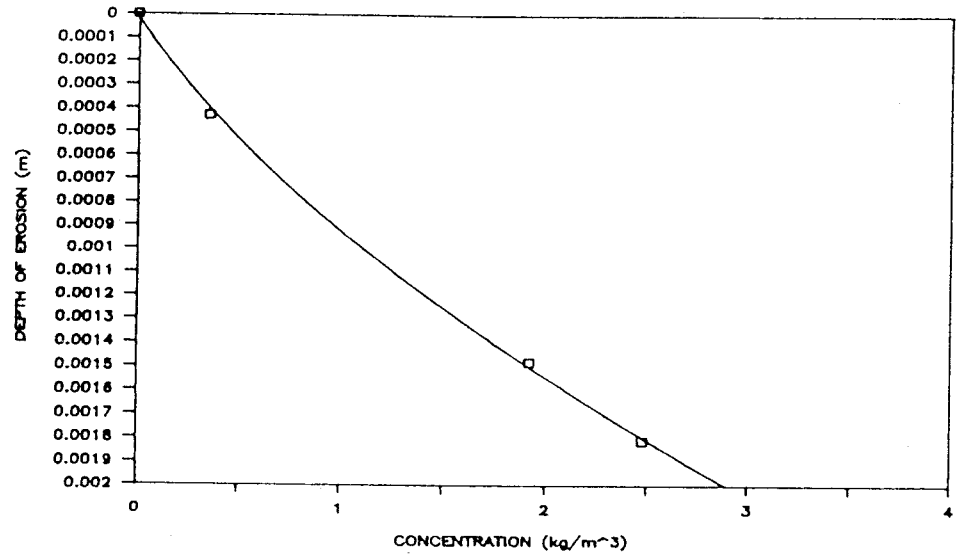

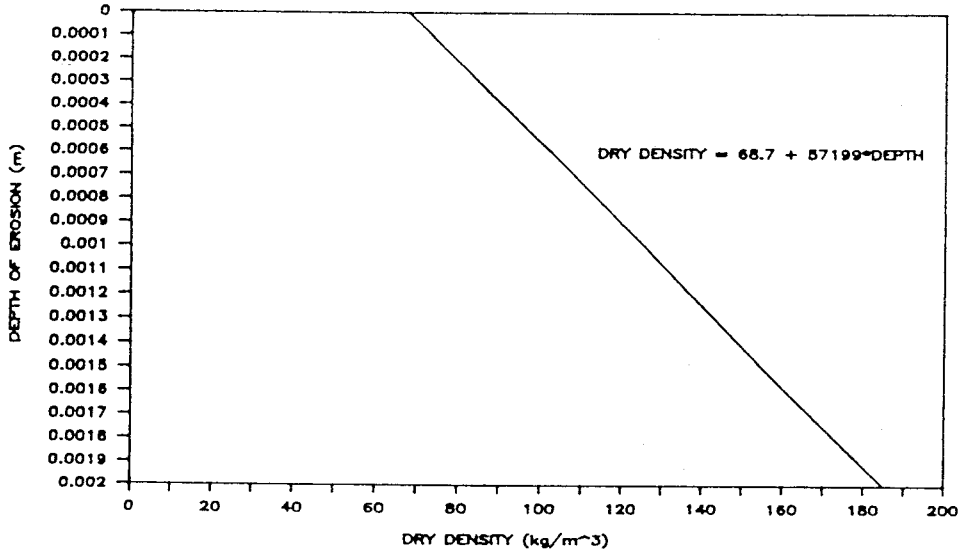

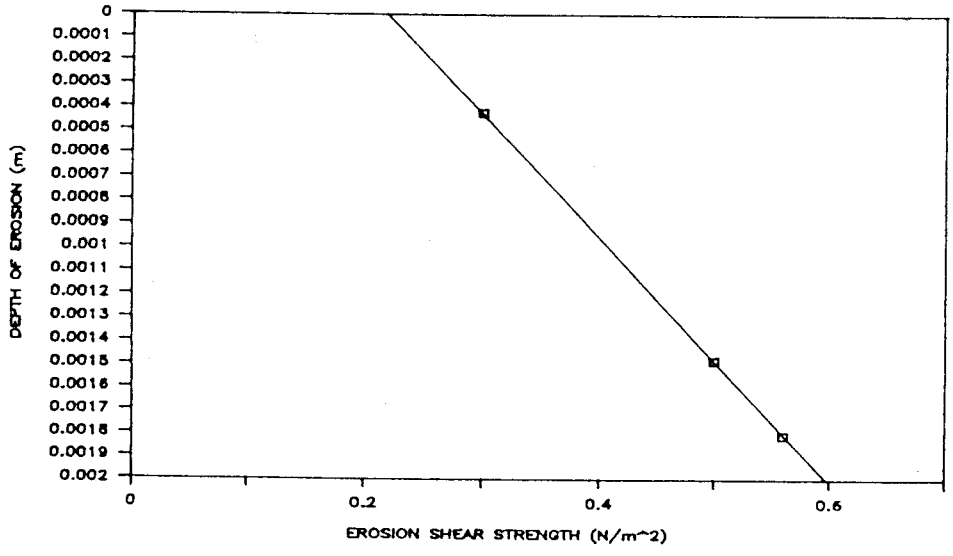

Fig 18 Erosion Test 3 Shear strength, suspended solids concentration and density against depth of erosion

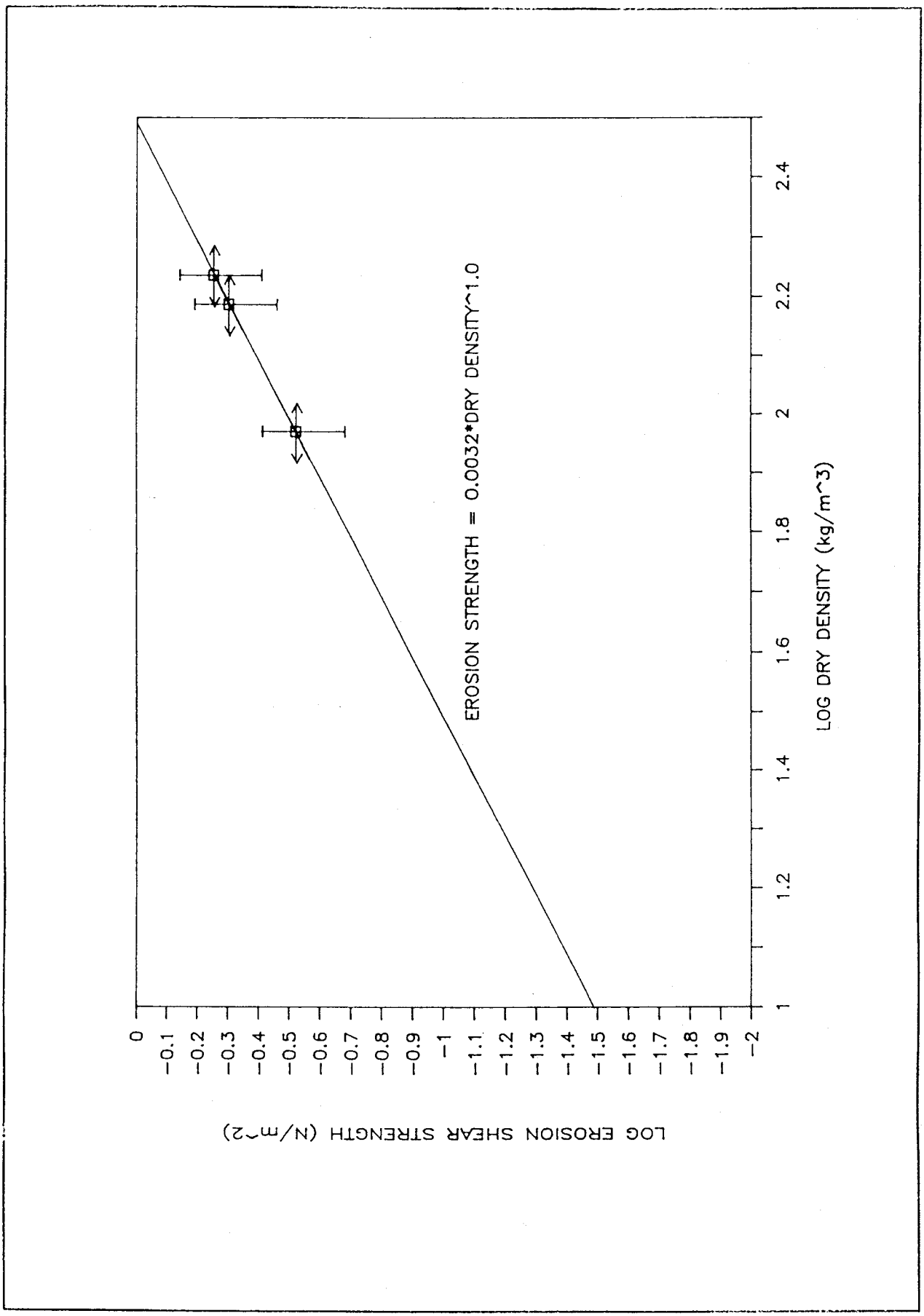

Fig 19 Erosion Test 3 Shear strength against density

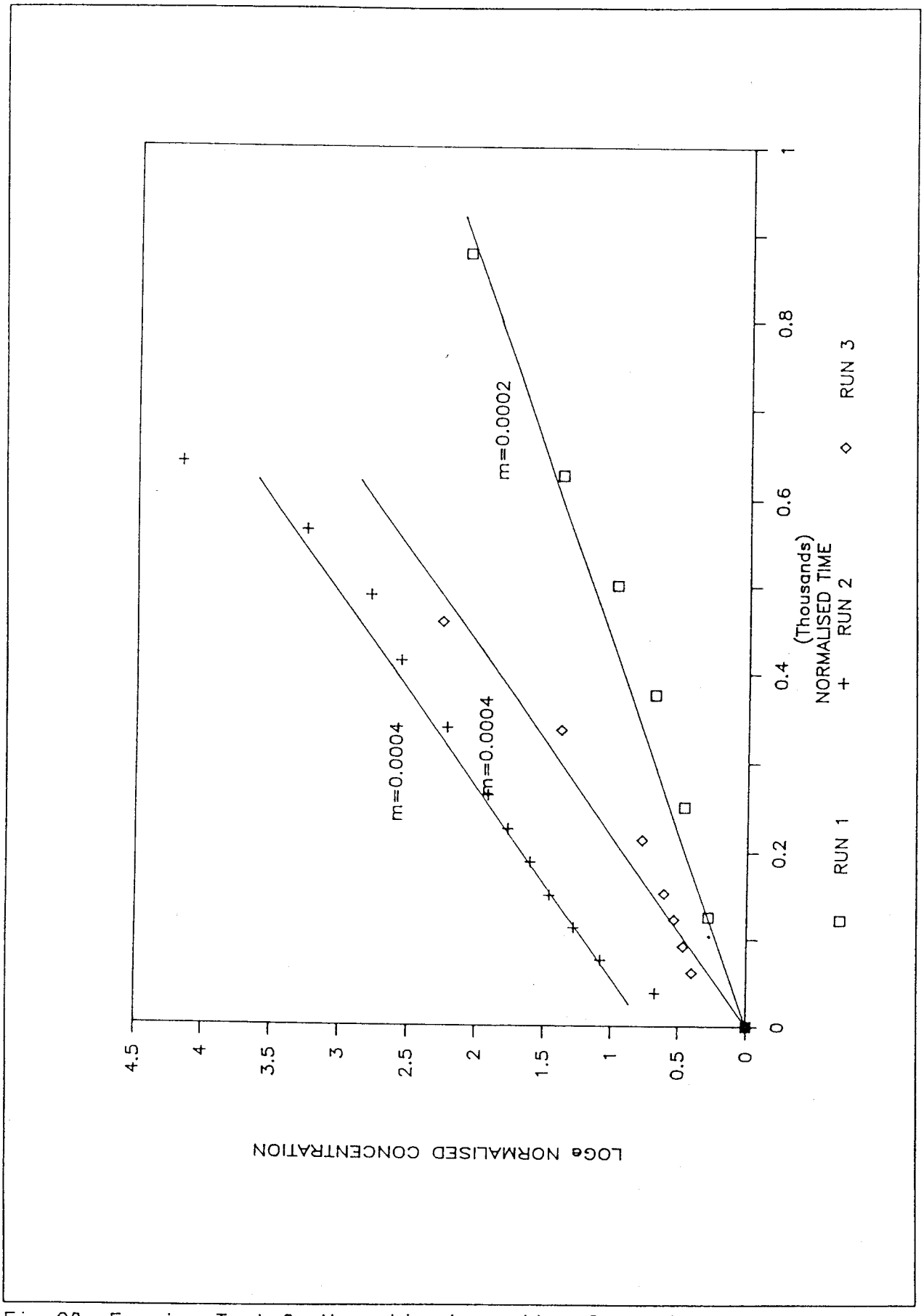

Fig 20 Erosion Test 3 Normalised results of erosion rate

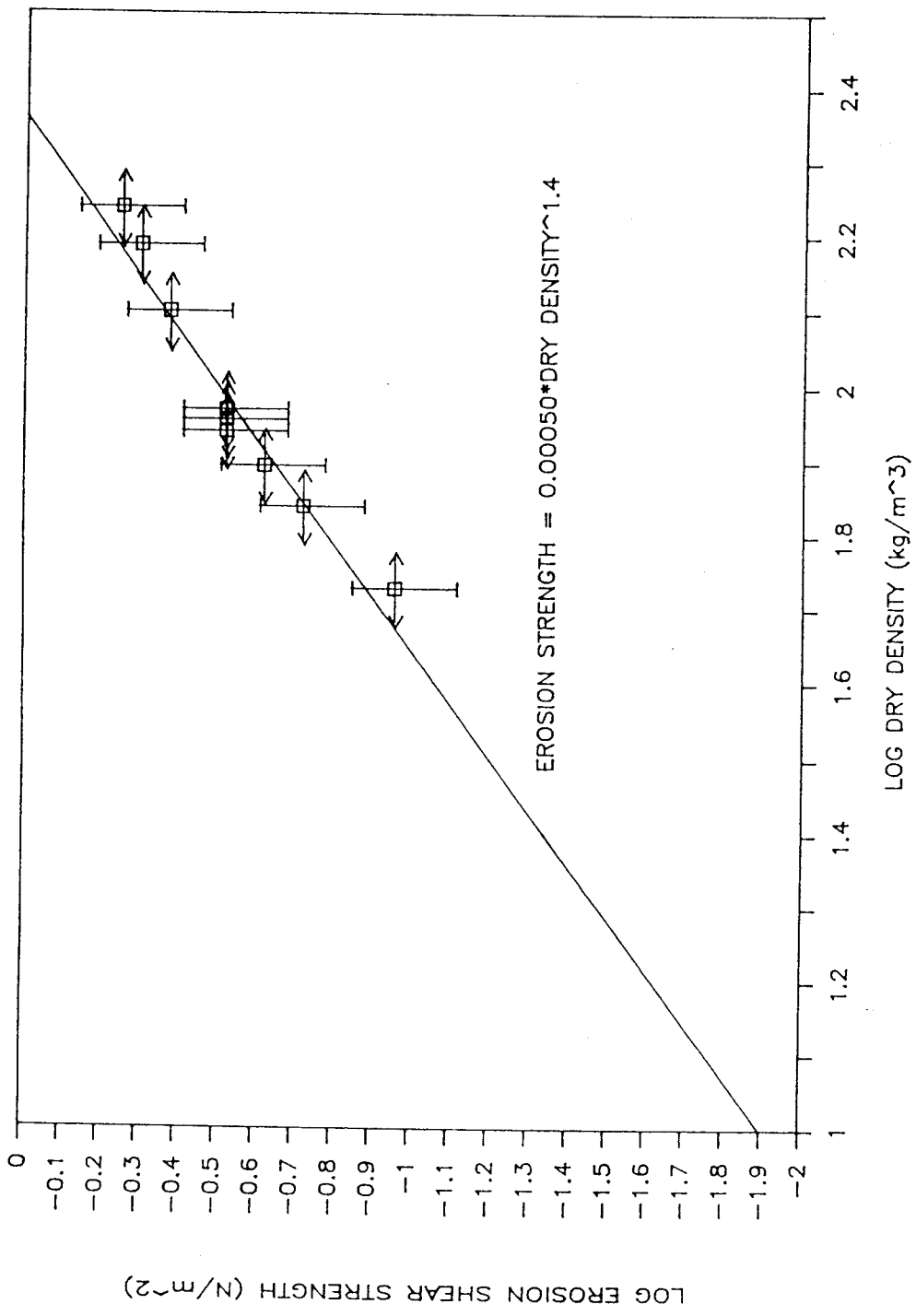

Fig 21 Erosion Tests 1, 2 and 3 Shear strength against density

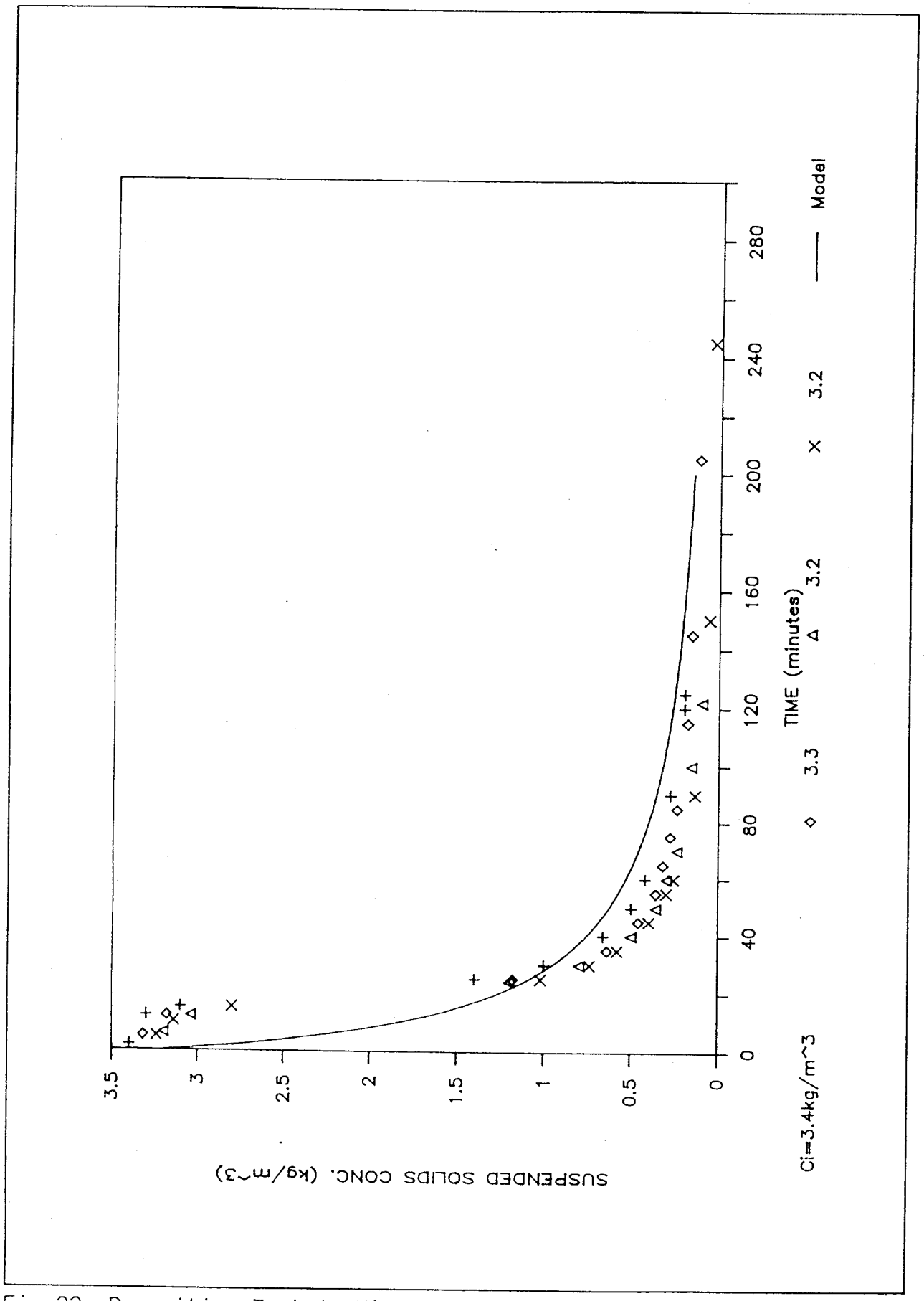

Fig 22 Deposition Test 1 Mid-depth suspended solids concentration against time

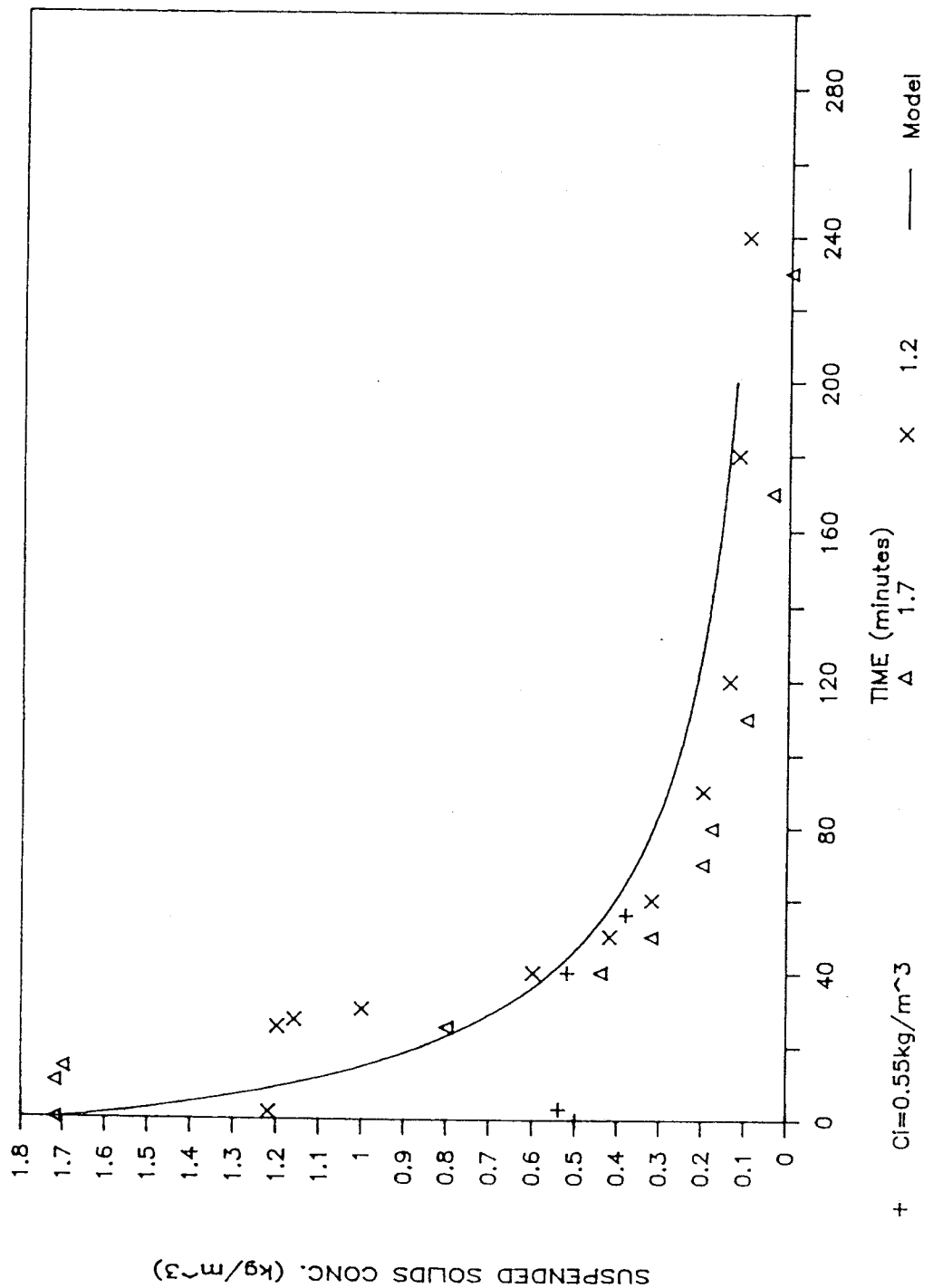

Fig 23 Deposition Tests 2, 3 and 4 Mid-depth suspended solids concentration against time

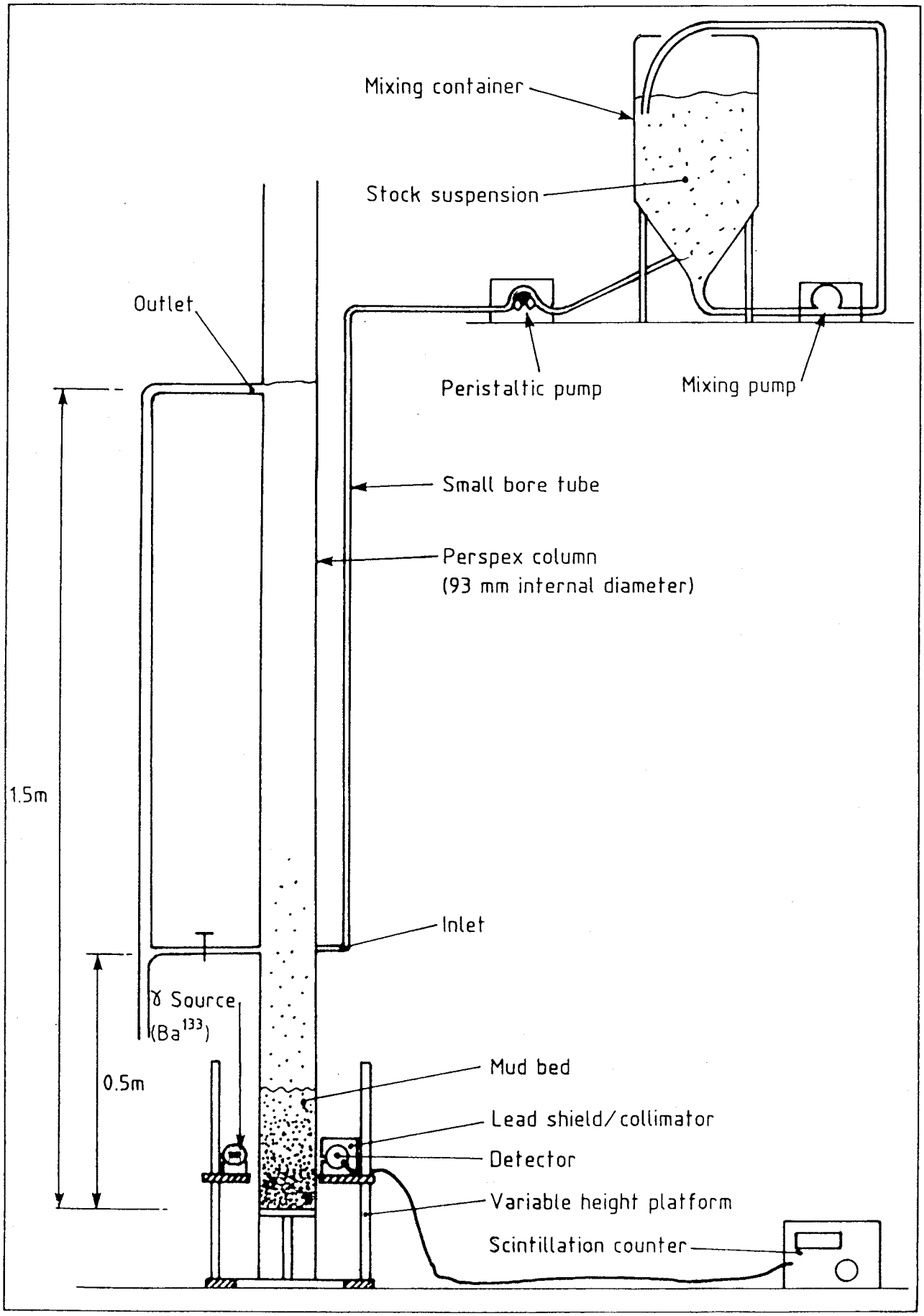

Fig 24 Settling column apparatus.

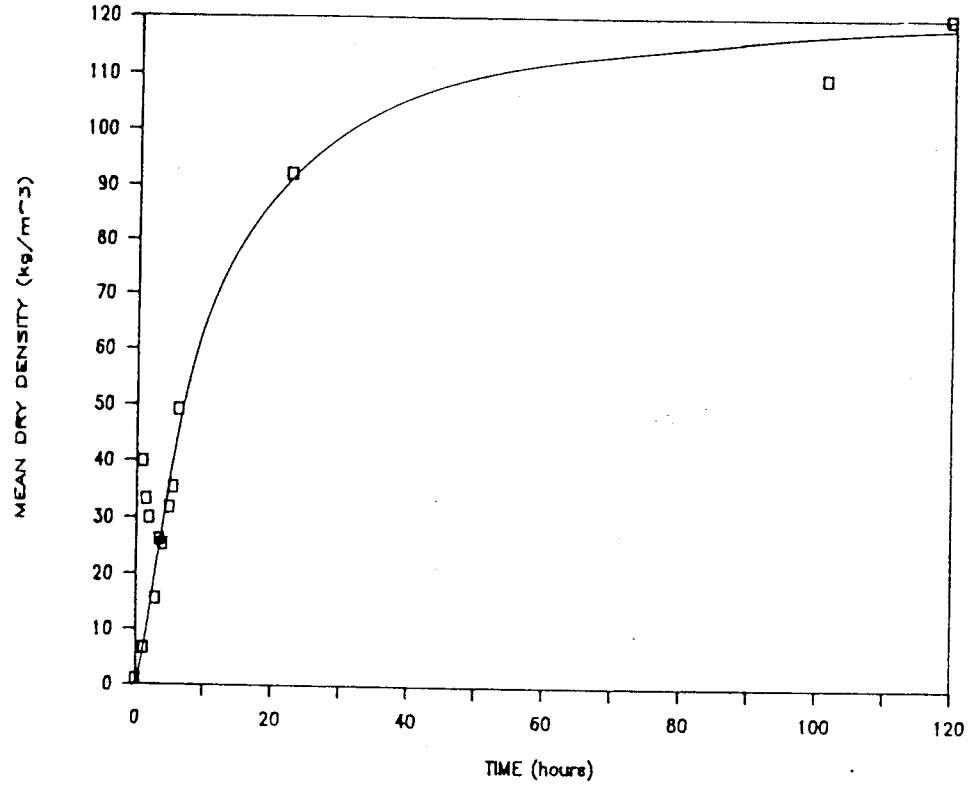

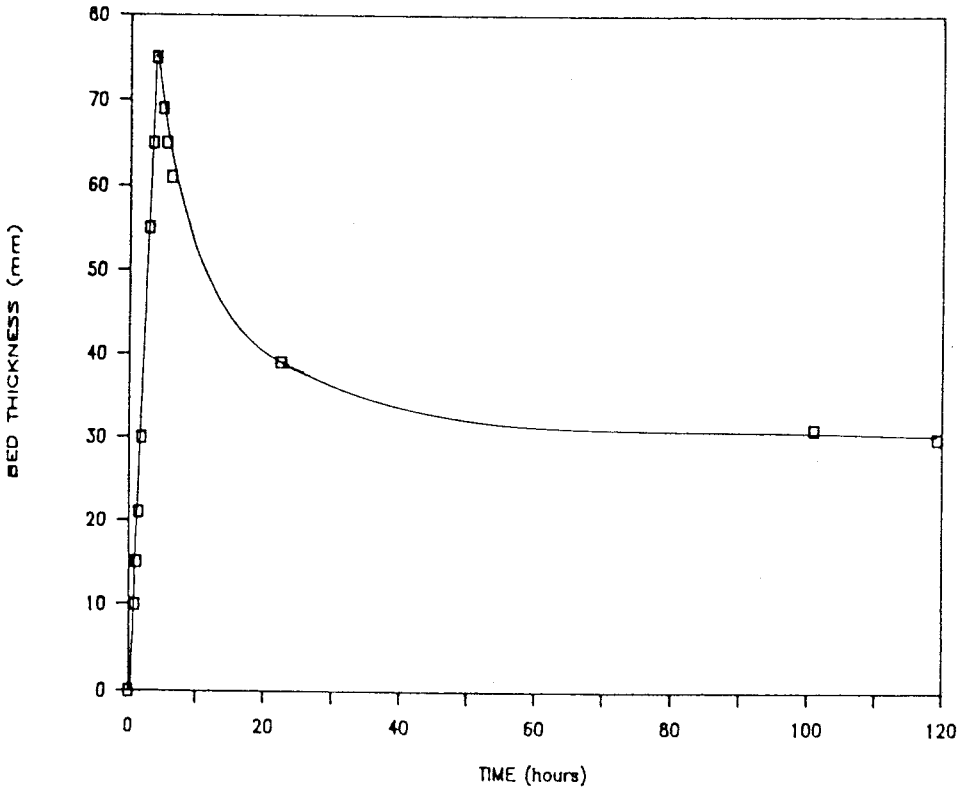

Fig 25 Consolidation Test 1 Variation of bed thickness and mean density against time

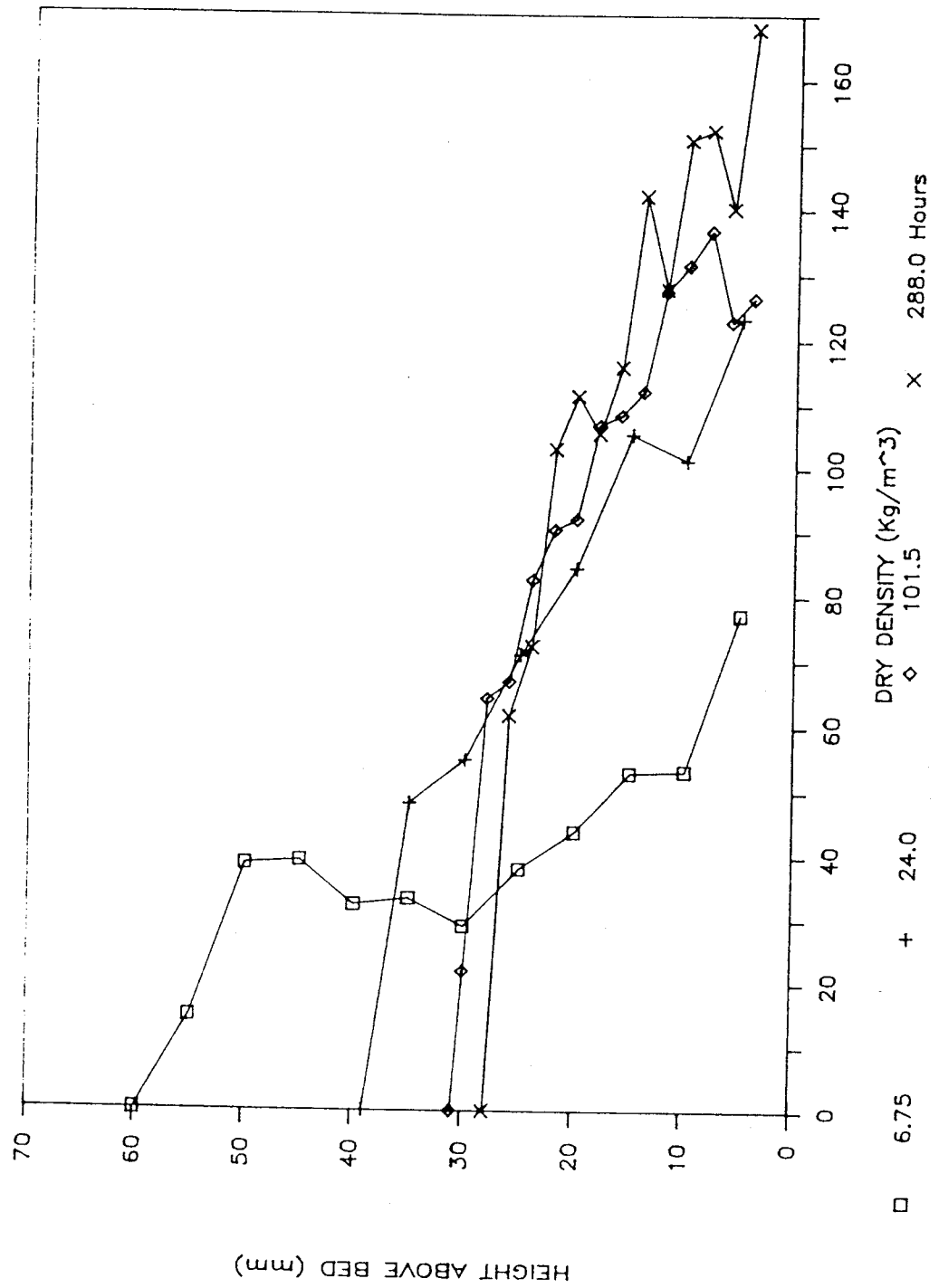

Fig 26 Consolidation Test 1 Density profiles with time

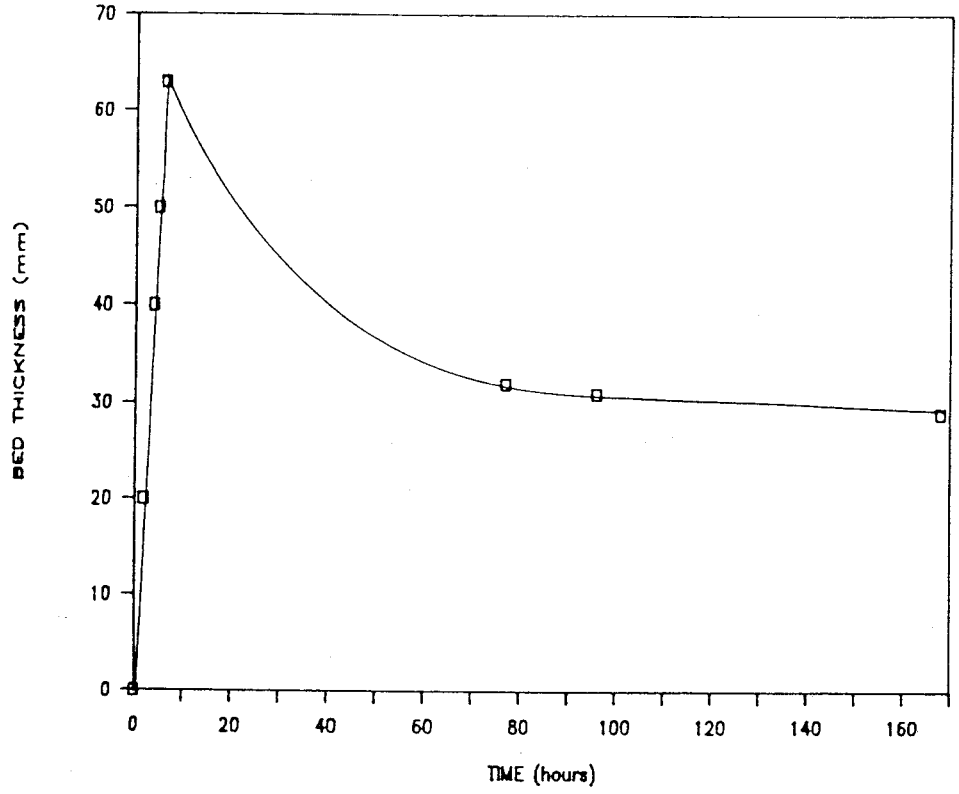

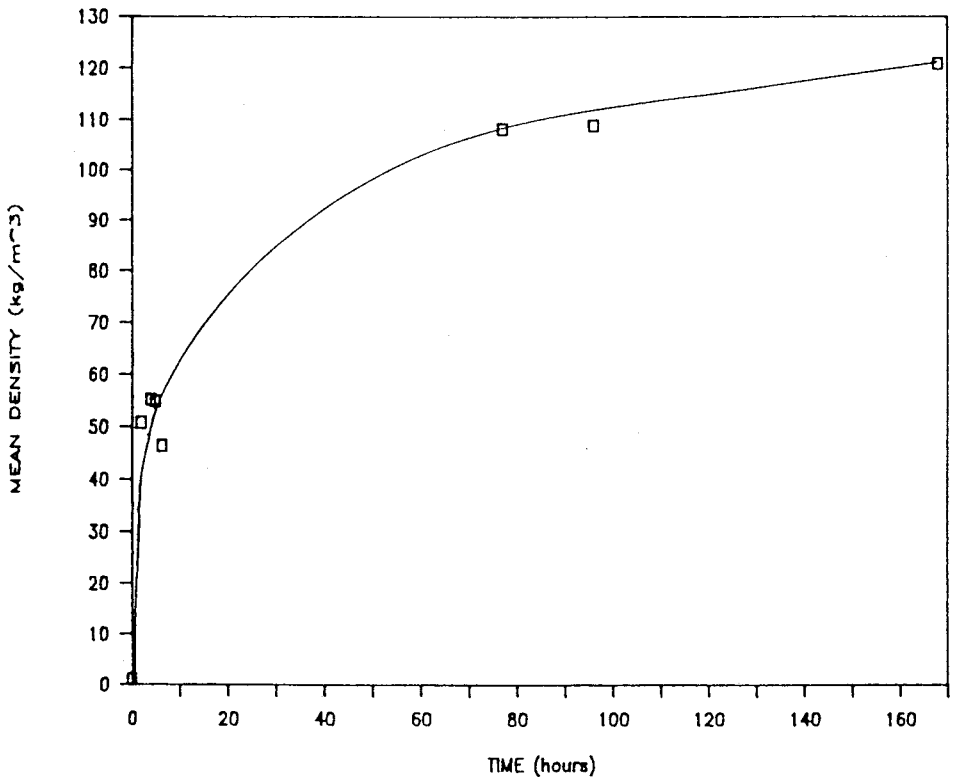

Fig 27 Consolidation Test 2 Variation of bed thickness and mean density against time

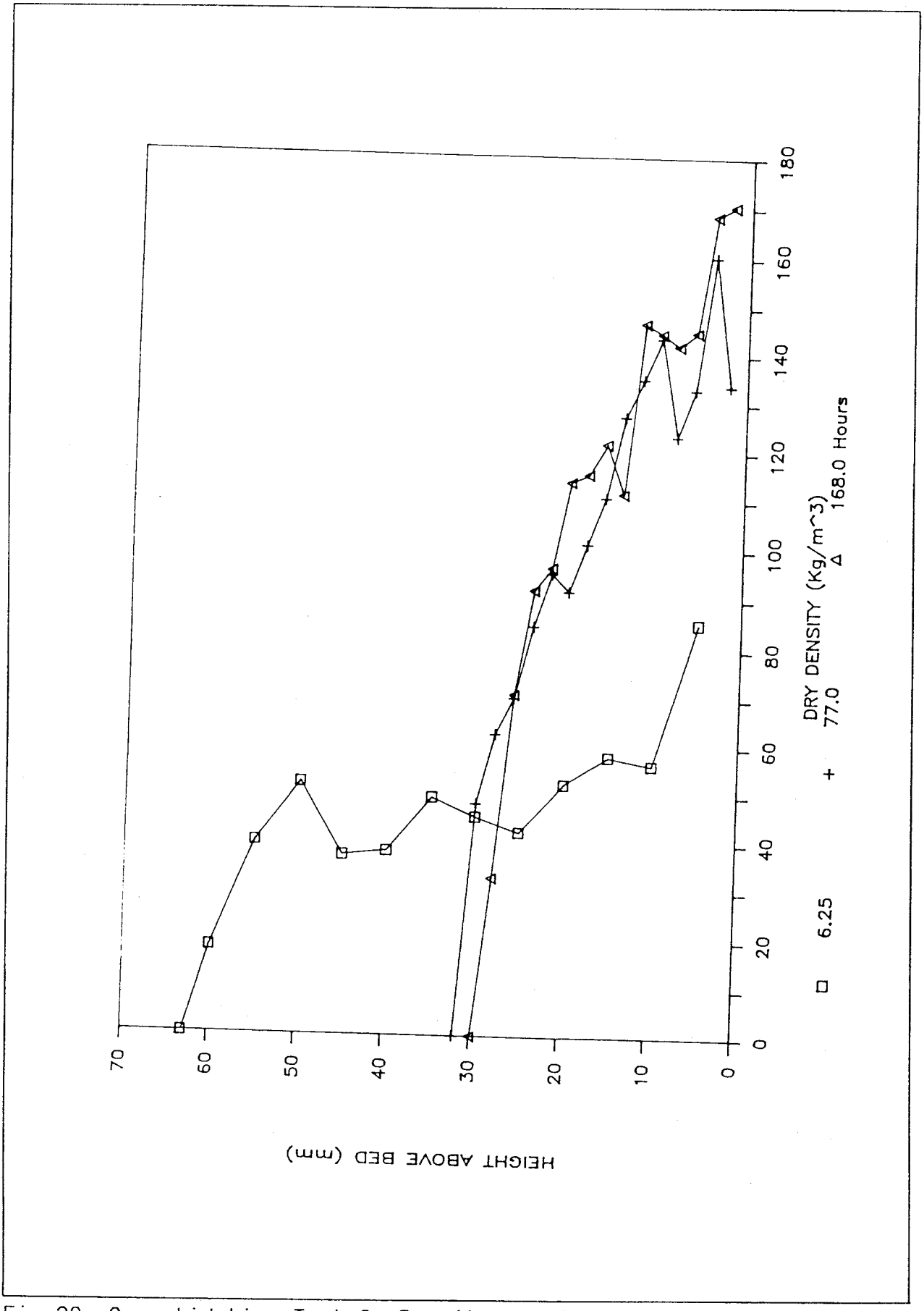

Fig 28 Consolidation Test 2 Density profiles with time

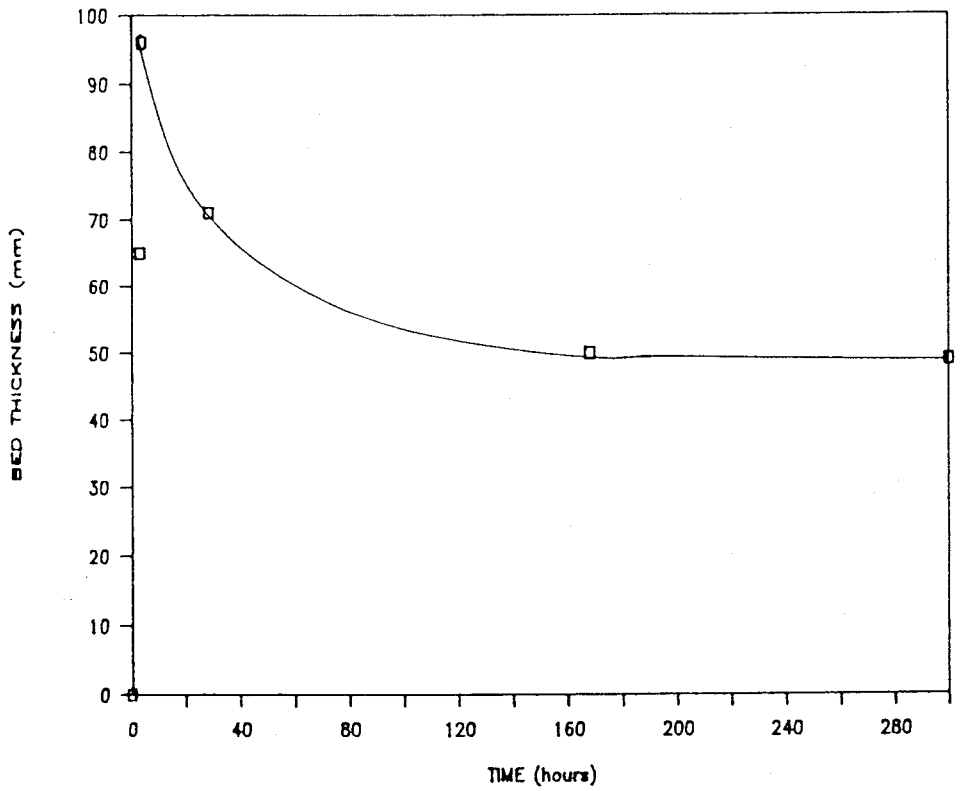

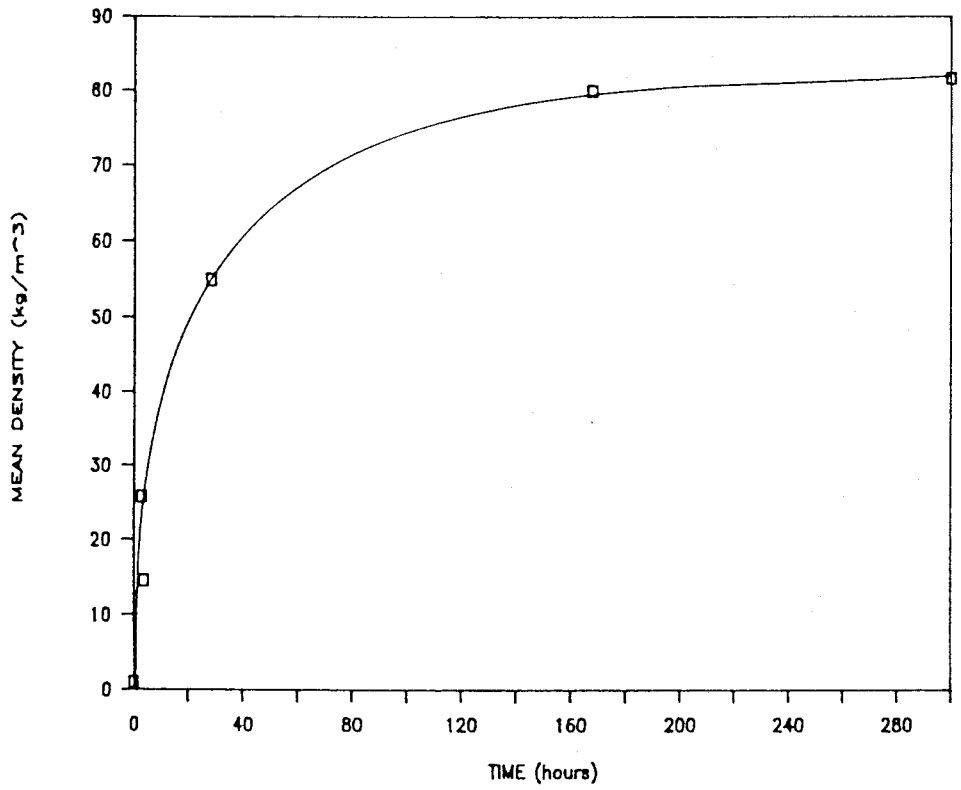

Fig 29 Consolidation Test 3 Variation of bed thickness and mean density against time

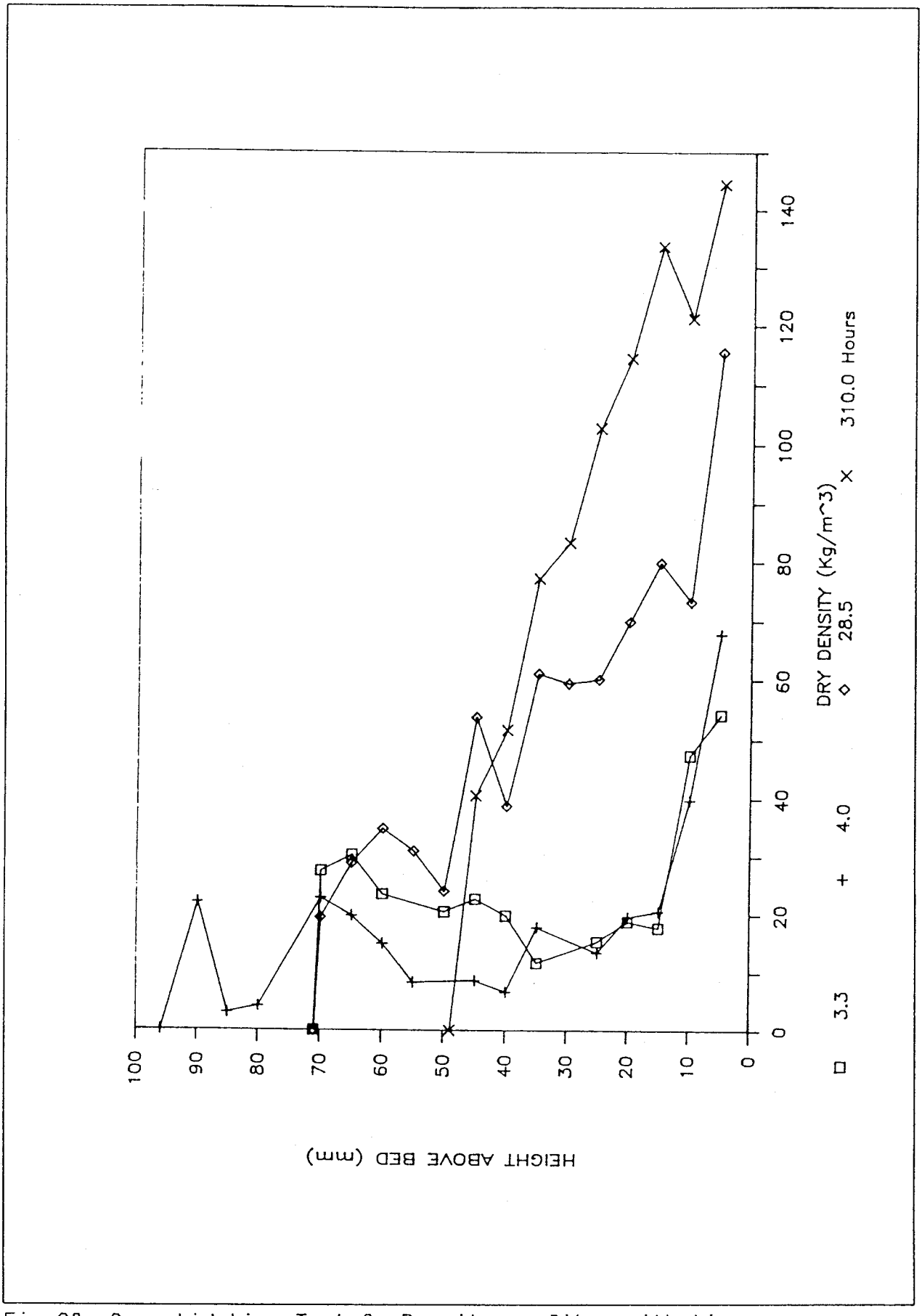

Fig 30 Consolidation Test 3 Density profiles with time

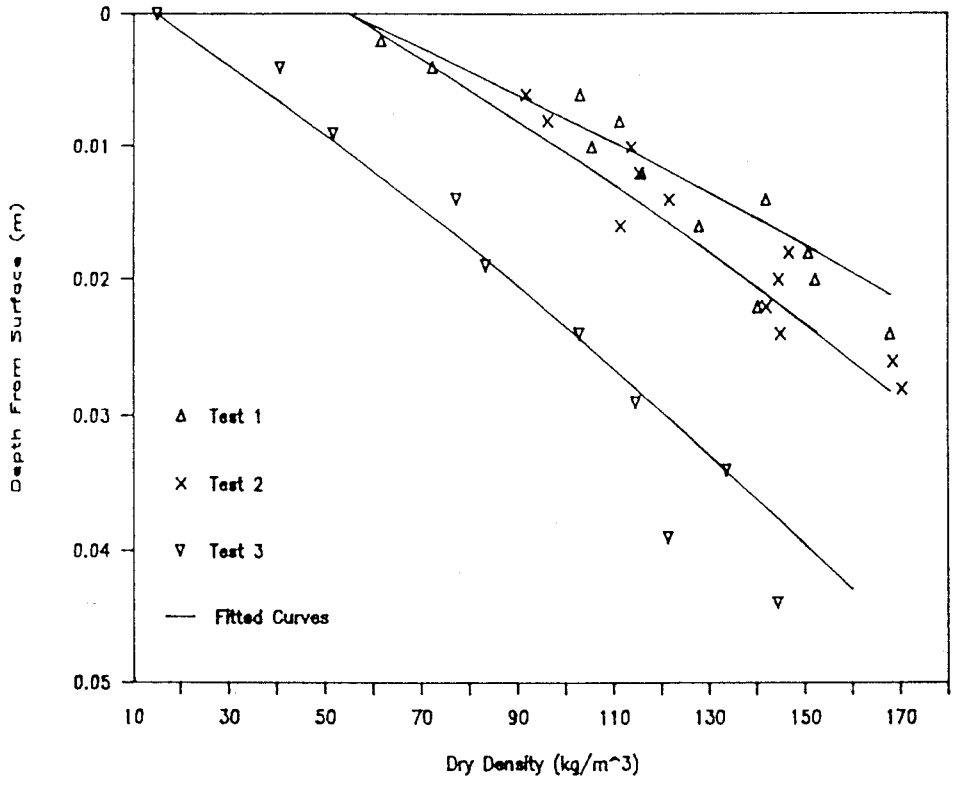

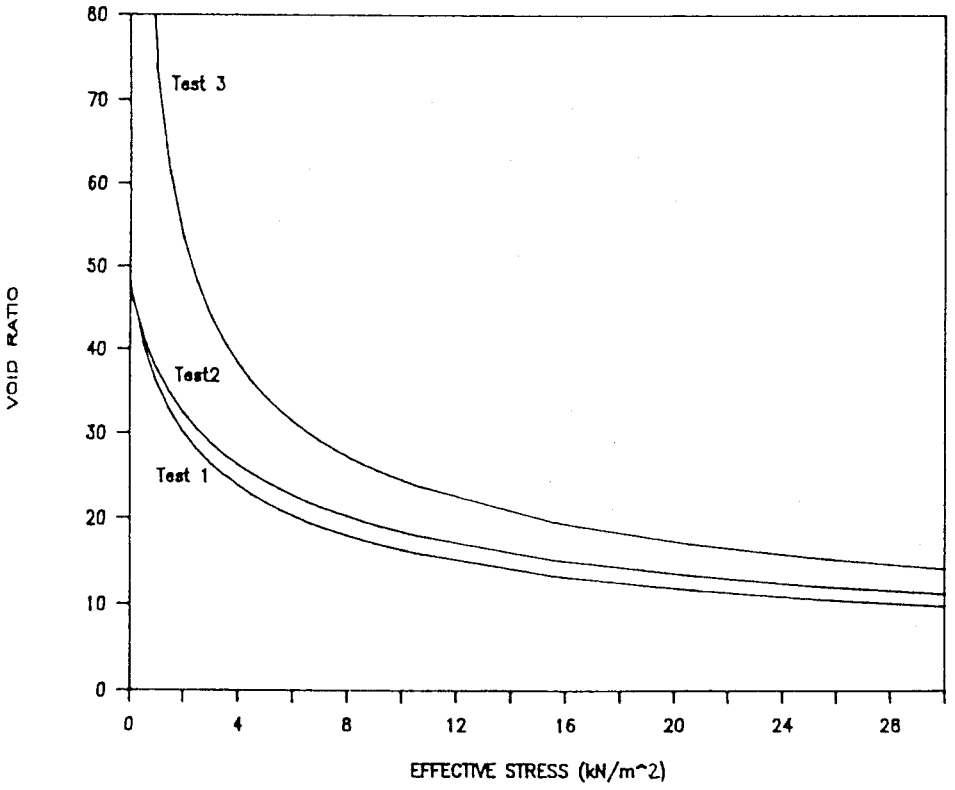

Fig 31 Consolidation Tests 1, 2 and 3 Final density against depth profiles and effective stress against voids ratio

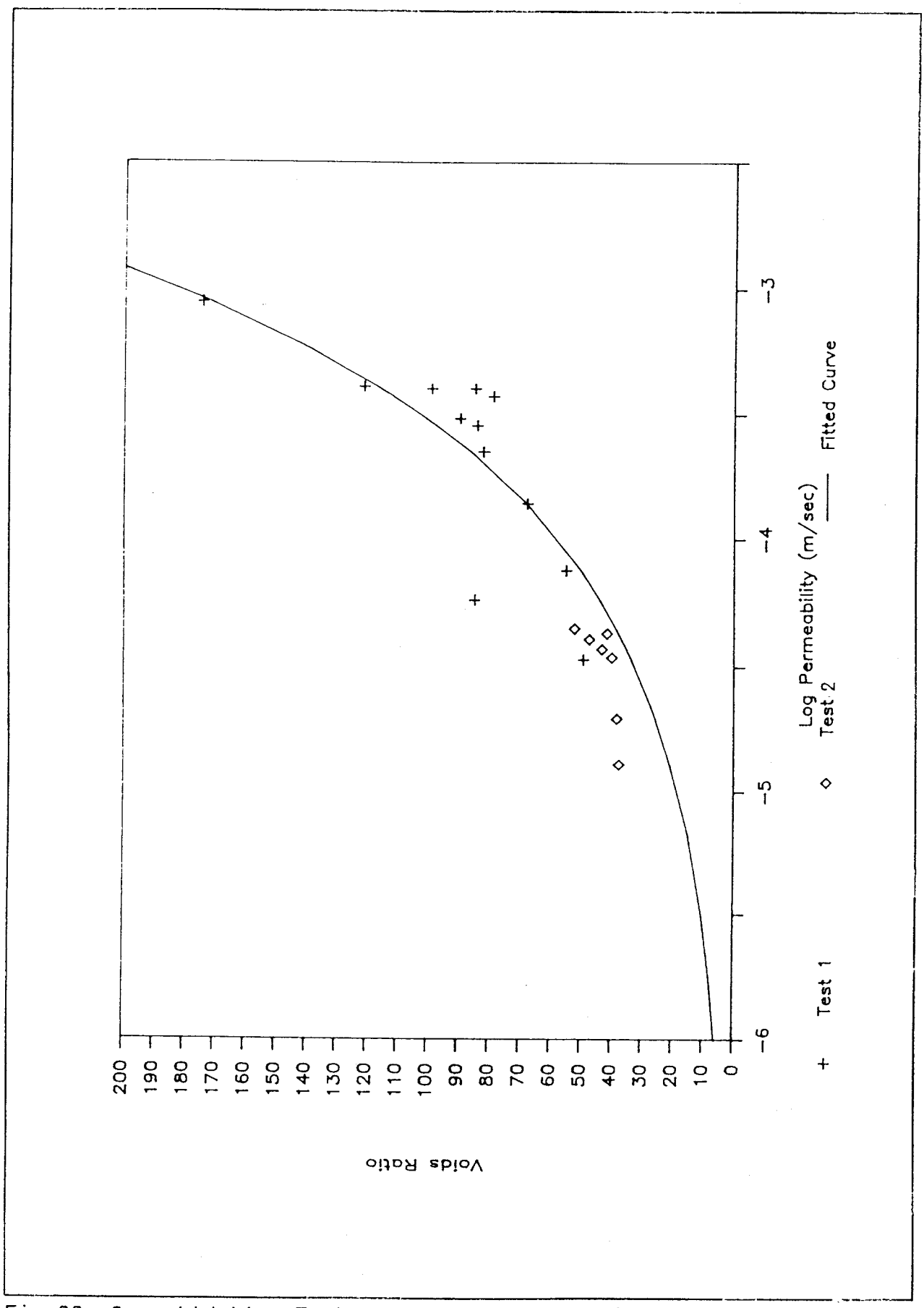

Fig 32 Consolidation Tests 1 and 2 Permeability against voids ratio

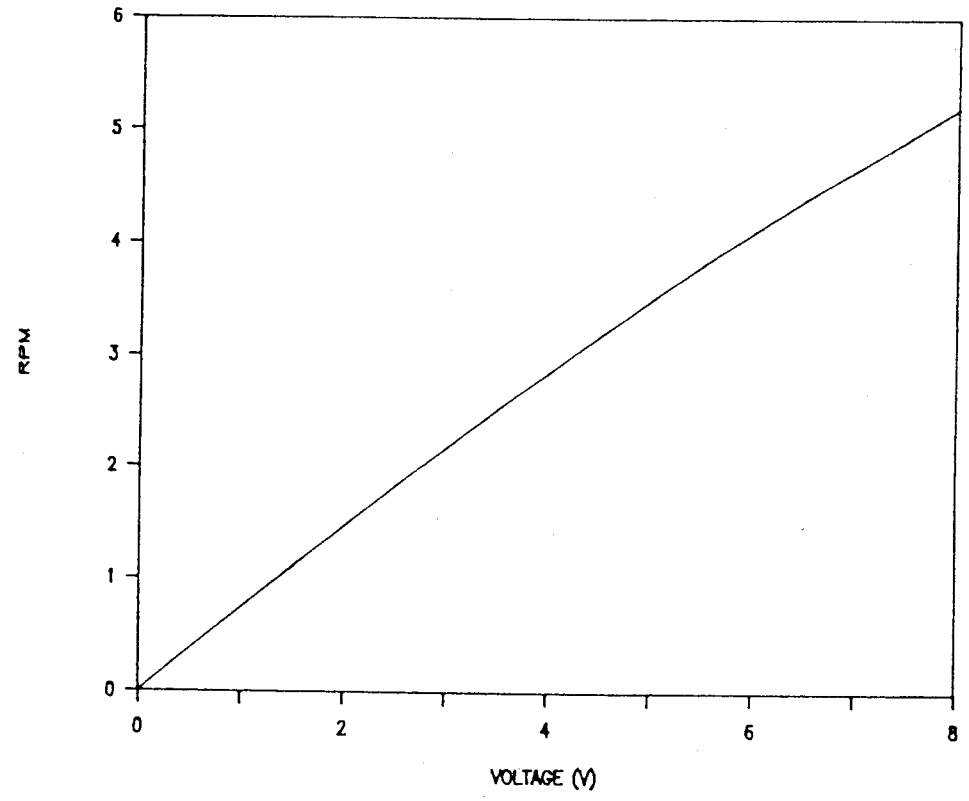

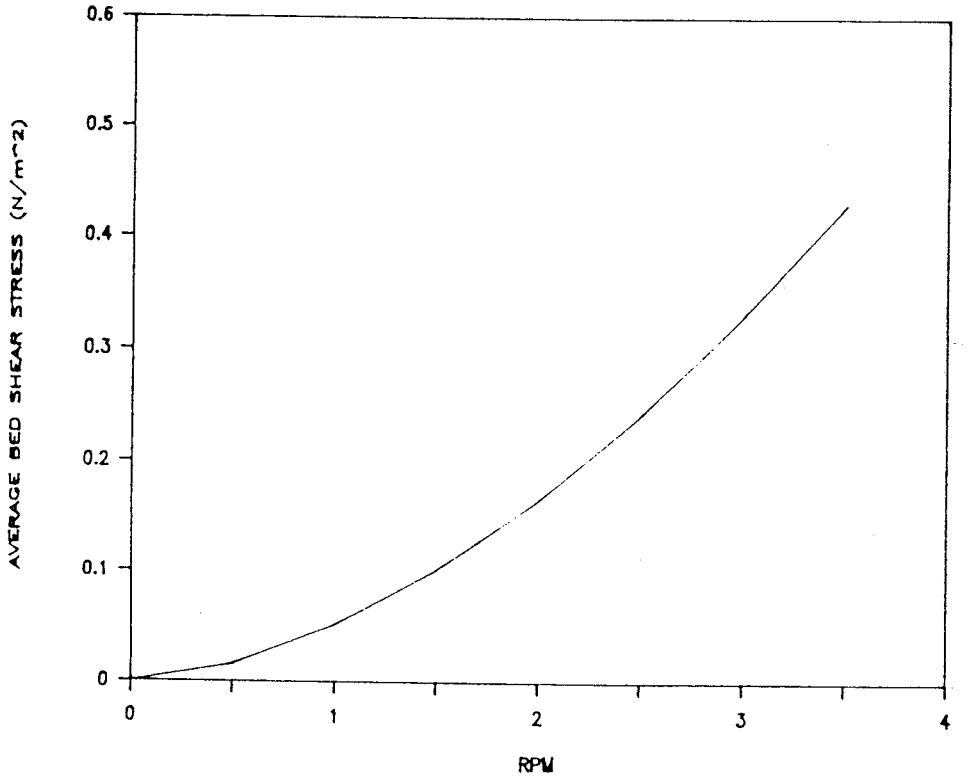

Fig 33 Carousel calibrations Voltage against rpm; rpm against average bed shear stress

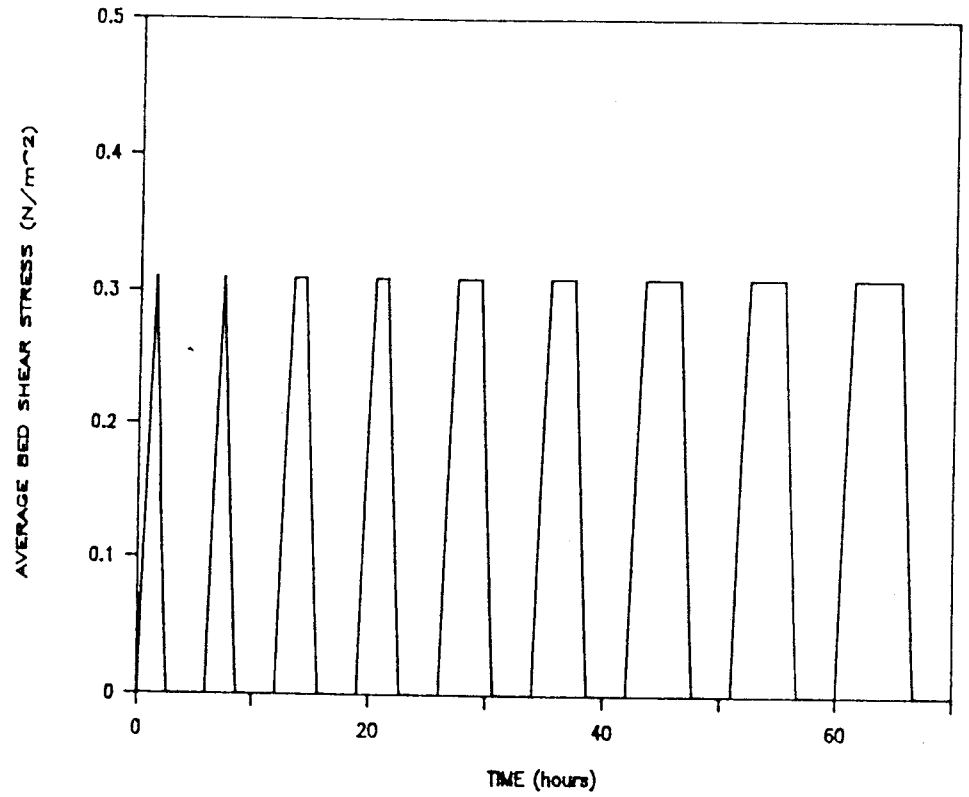

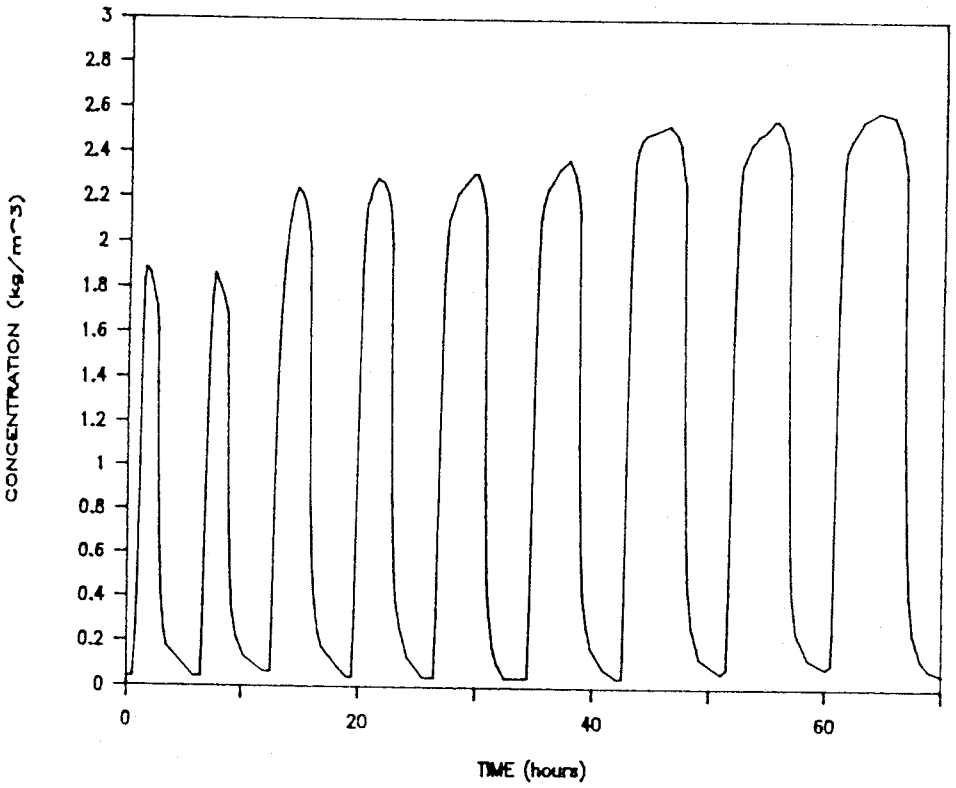

Fig 34 Tidal cycles Test A Average bed shear stress and suspended solids concentration against time

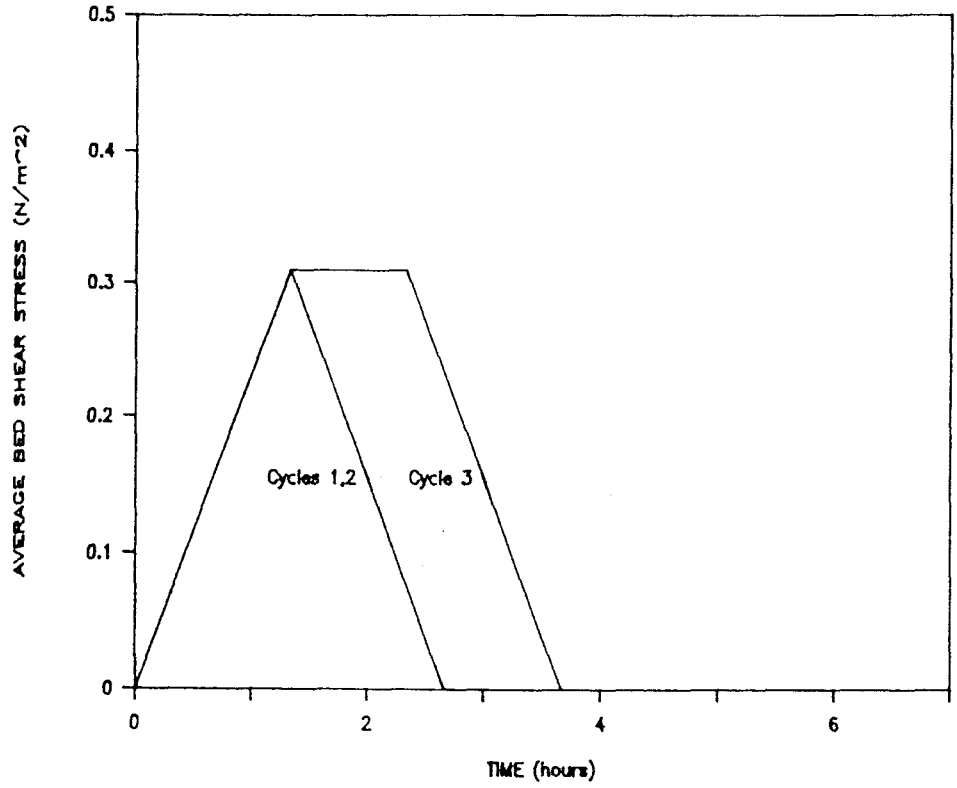

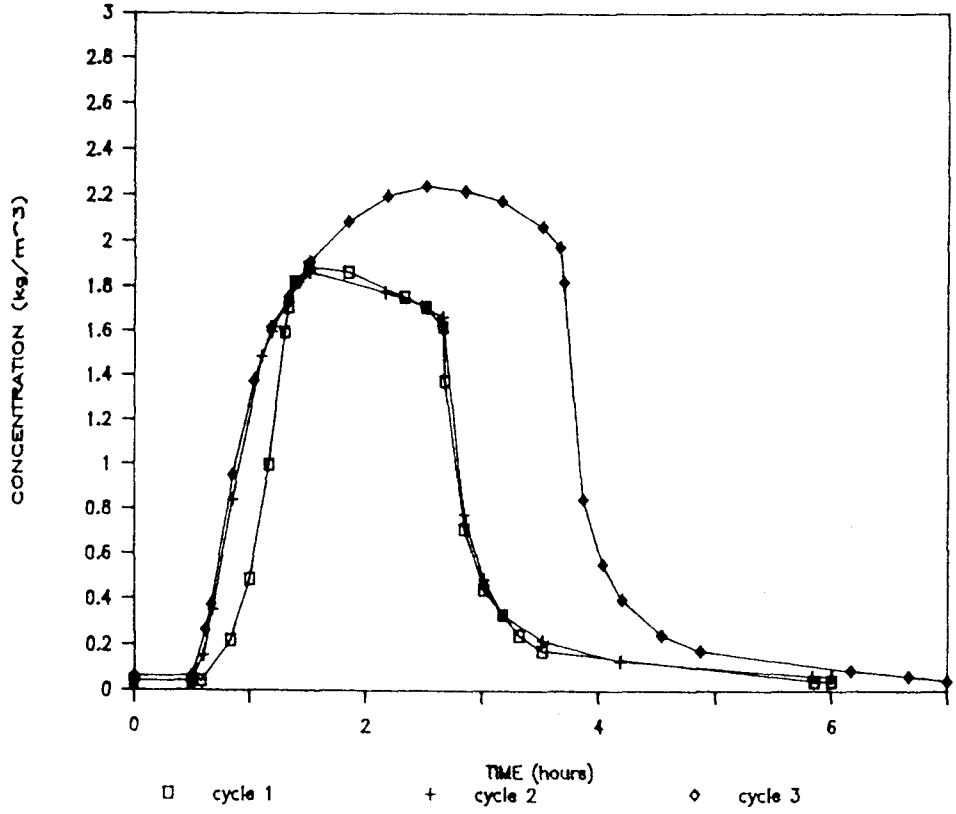

Fig 35 Tidal cycles Test A Cycles 1, 2 and 3 suspended solids concentration against time

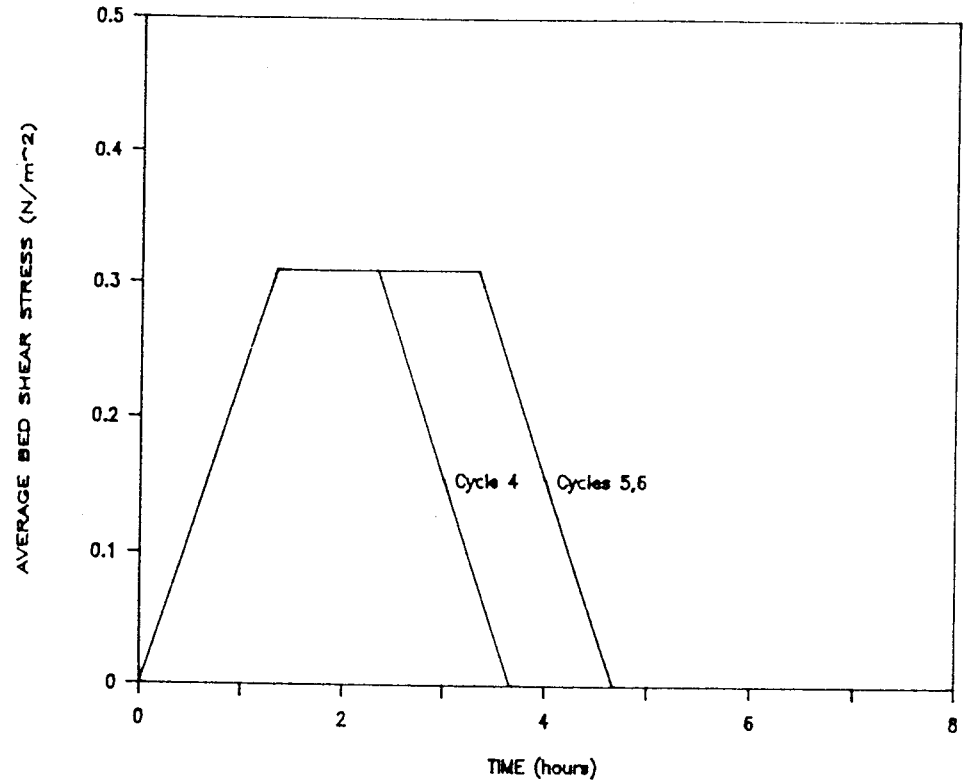

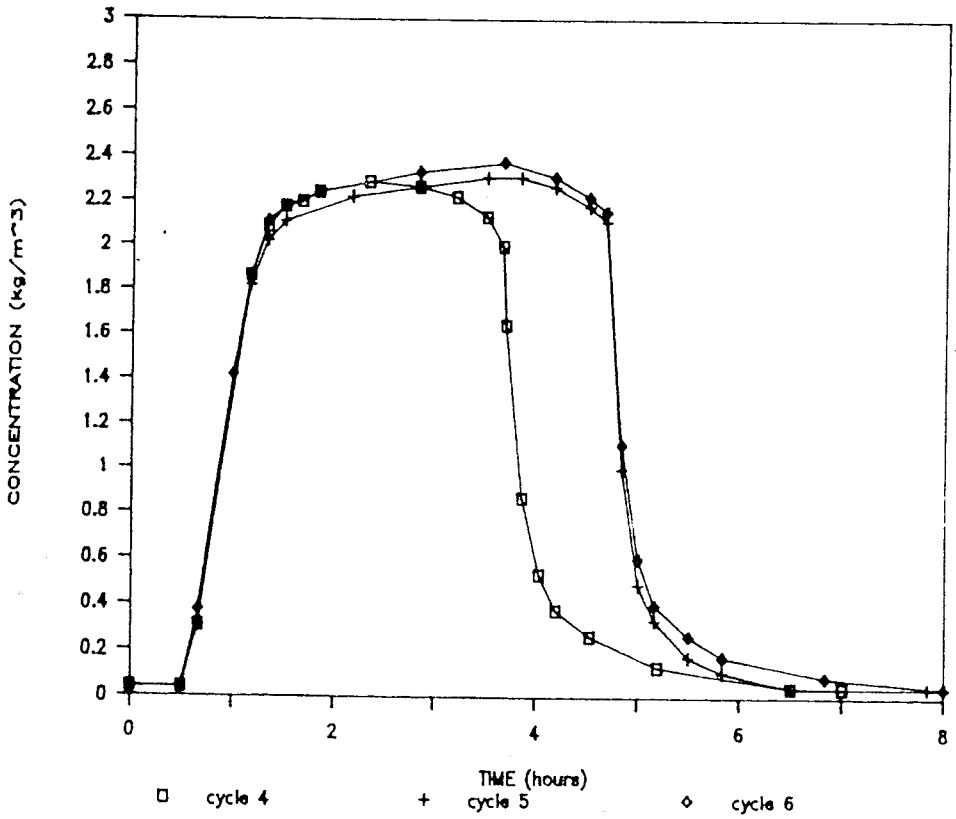

Fig 36 Tidal cycles Test A Cycles 4, 5 and 6 suspended solids

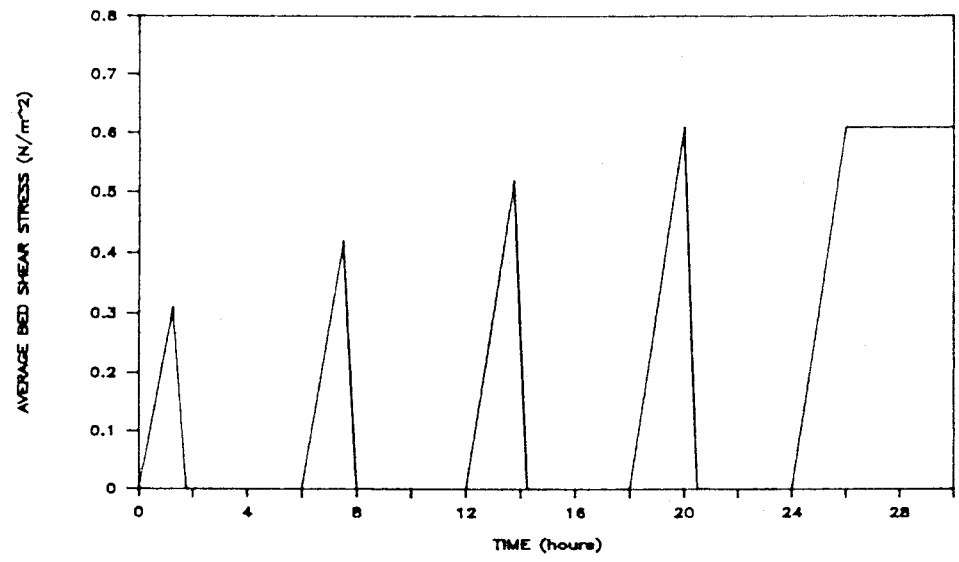

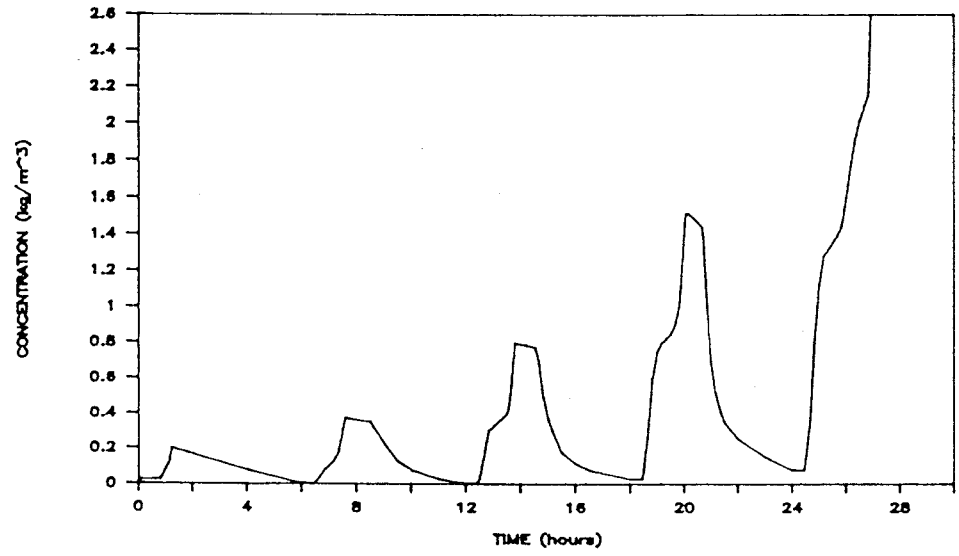

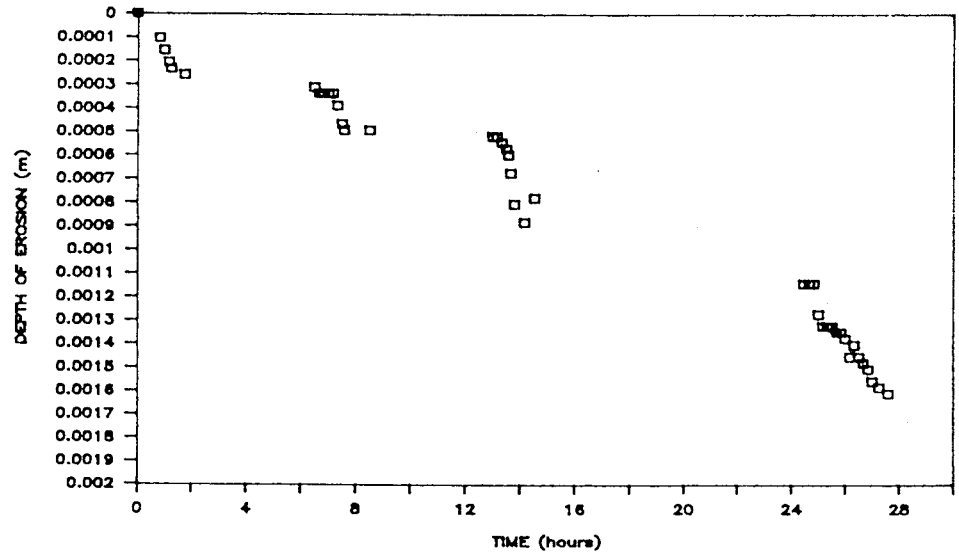

Fig 37 Tidal cycles Test B Average bed shear stress, suspended solids concentration and depth of erosion against time

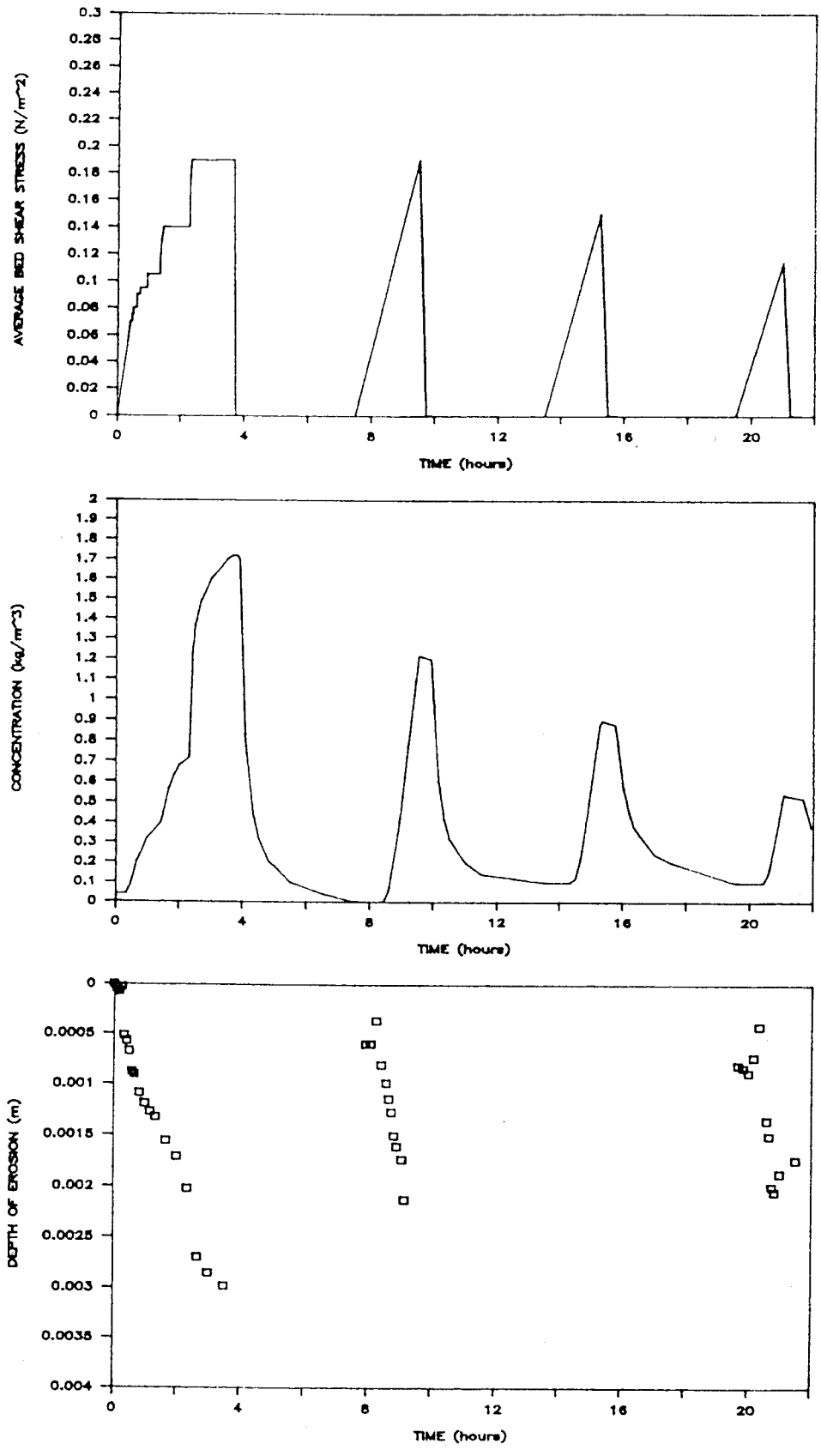

Fig 38 Tidal cycles Test C Average bed shear stress, suspended solids concentration and depth of erosion against time

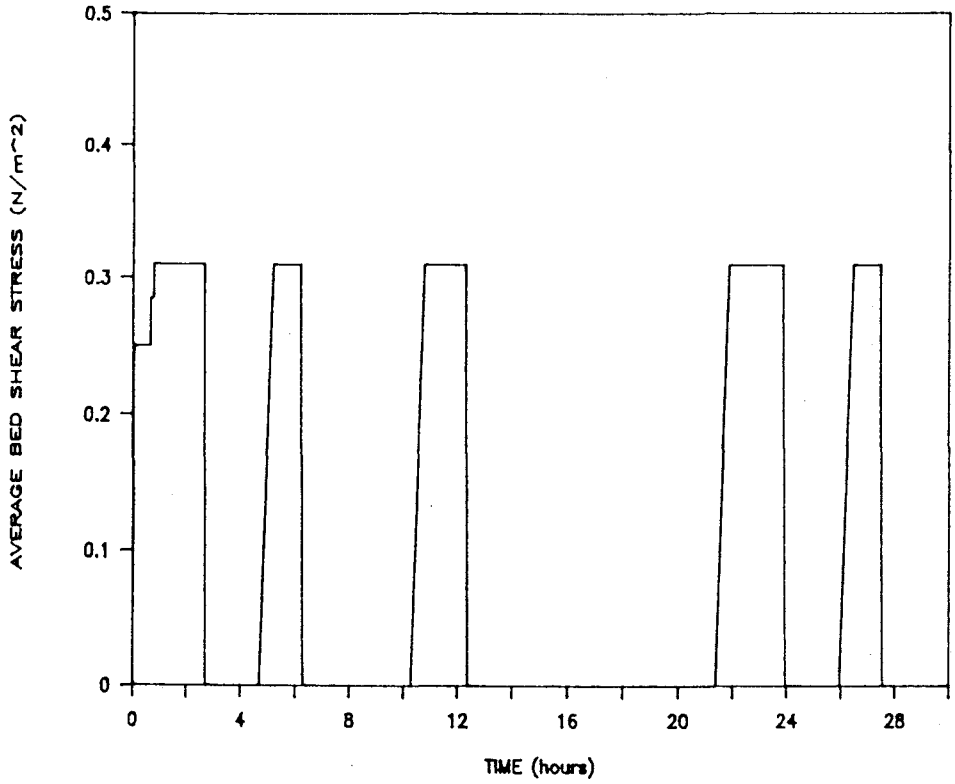

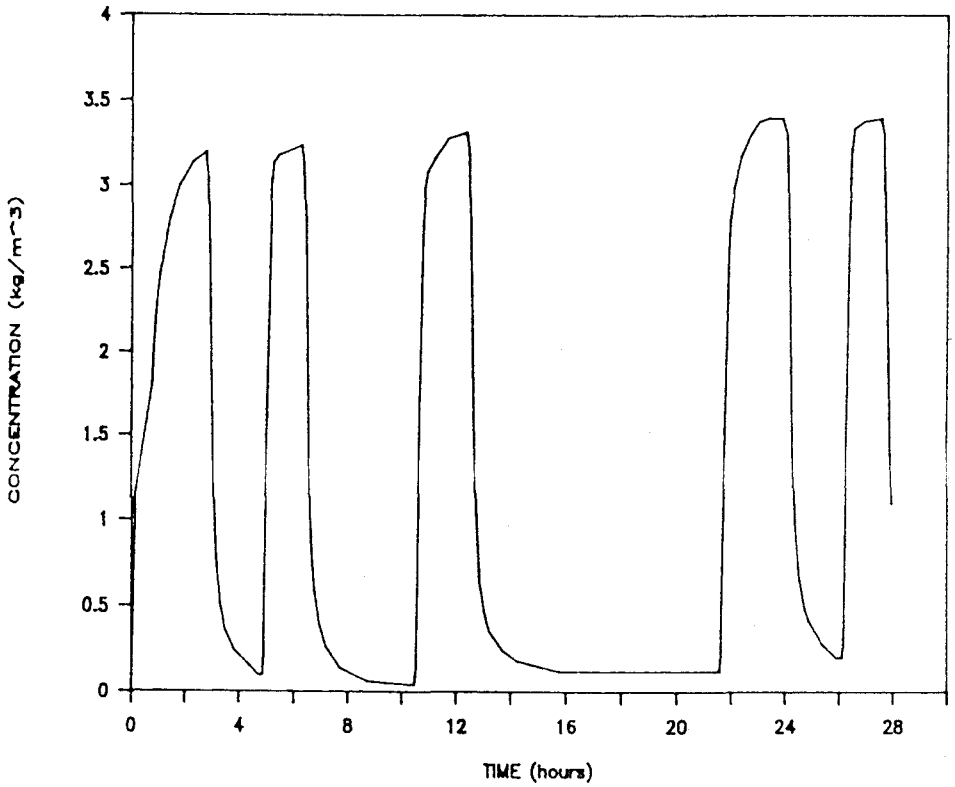

Fig 39 Tidal cycles Test D Average bed shear stress and suspended solids concentration against time

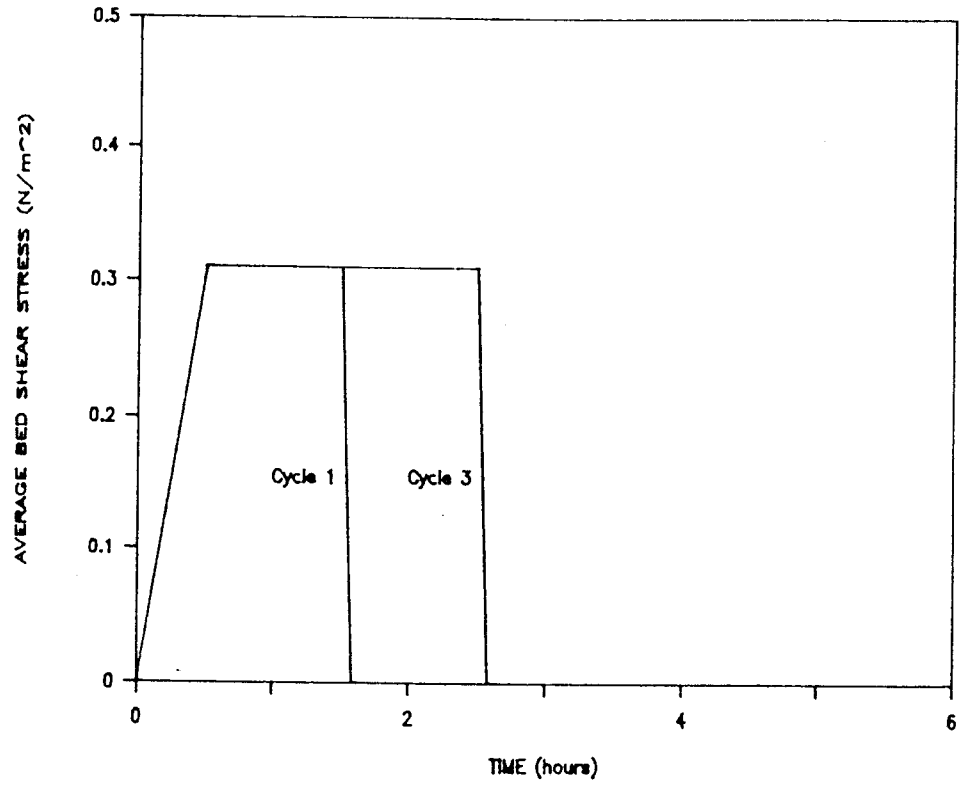

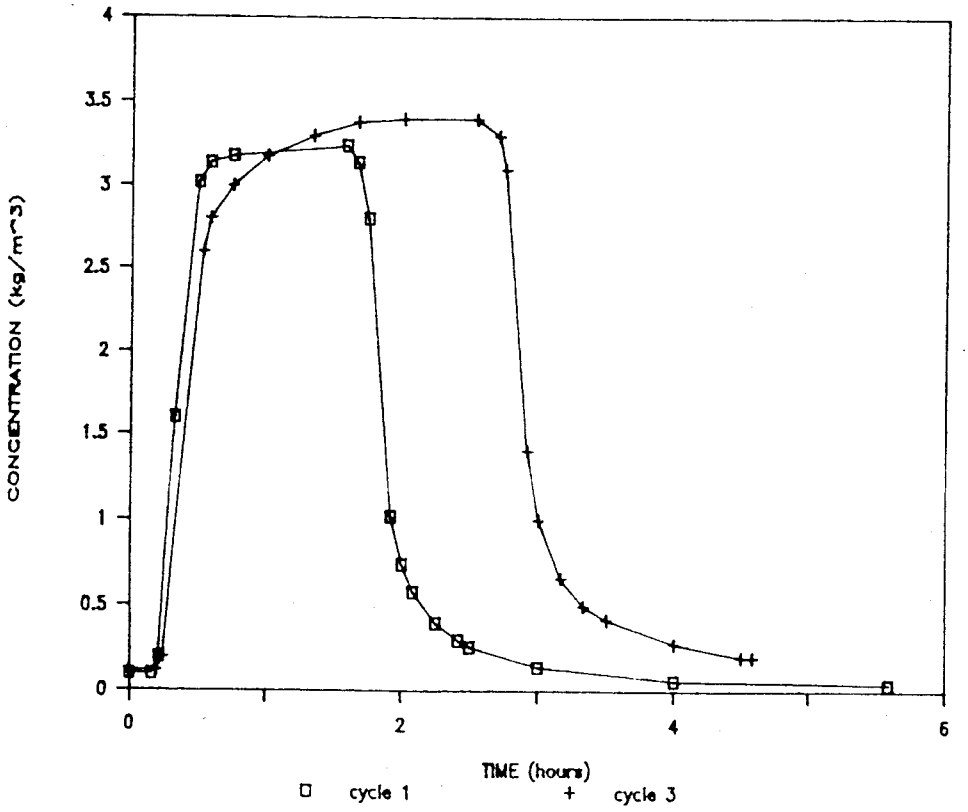

Fig 40 Tidal cycles Test D Cycles 1 and 3 Average bed shear stress and suspended solids concentration against time

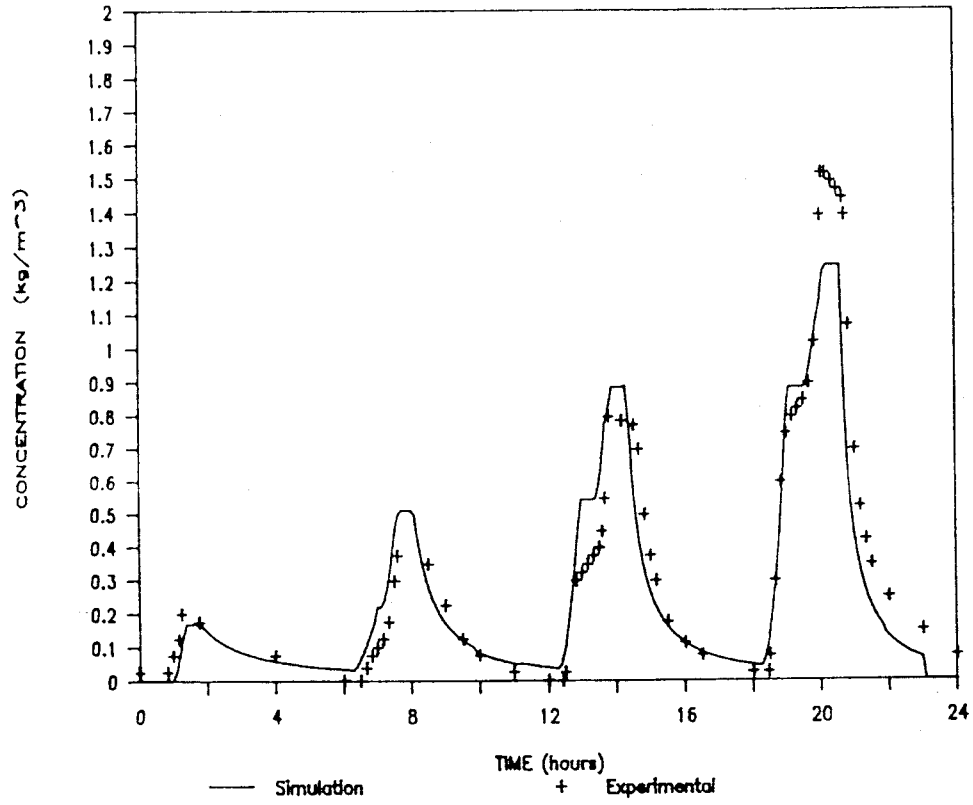

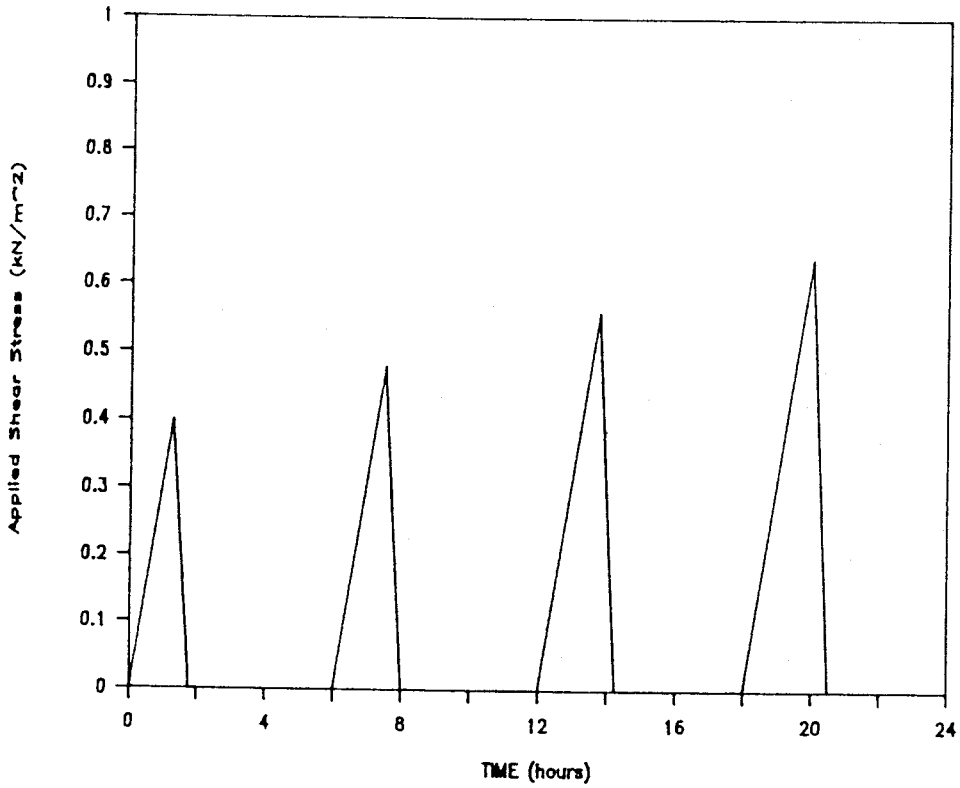

Fig 41 Model simulation Test B Suspended solids concentration and average bed shear stress against time

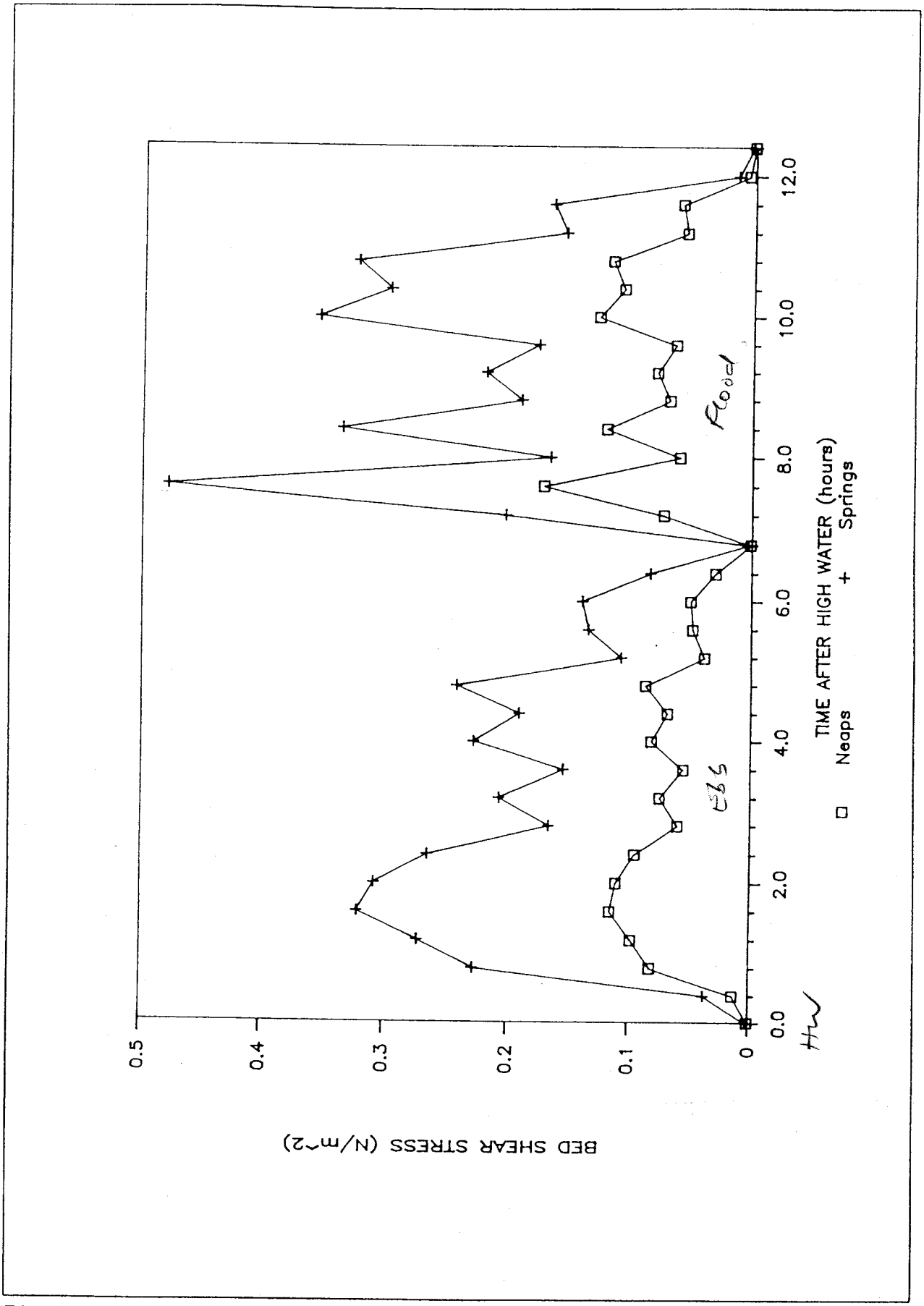

Fig 42 Cardiff docks entrance channel Springs and neaps bed shear stress against time

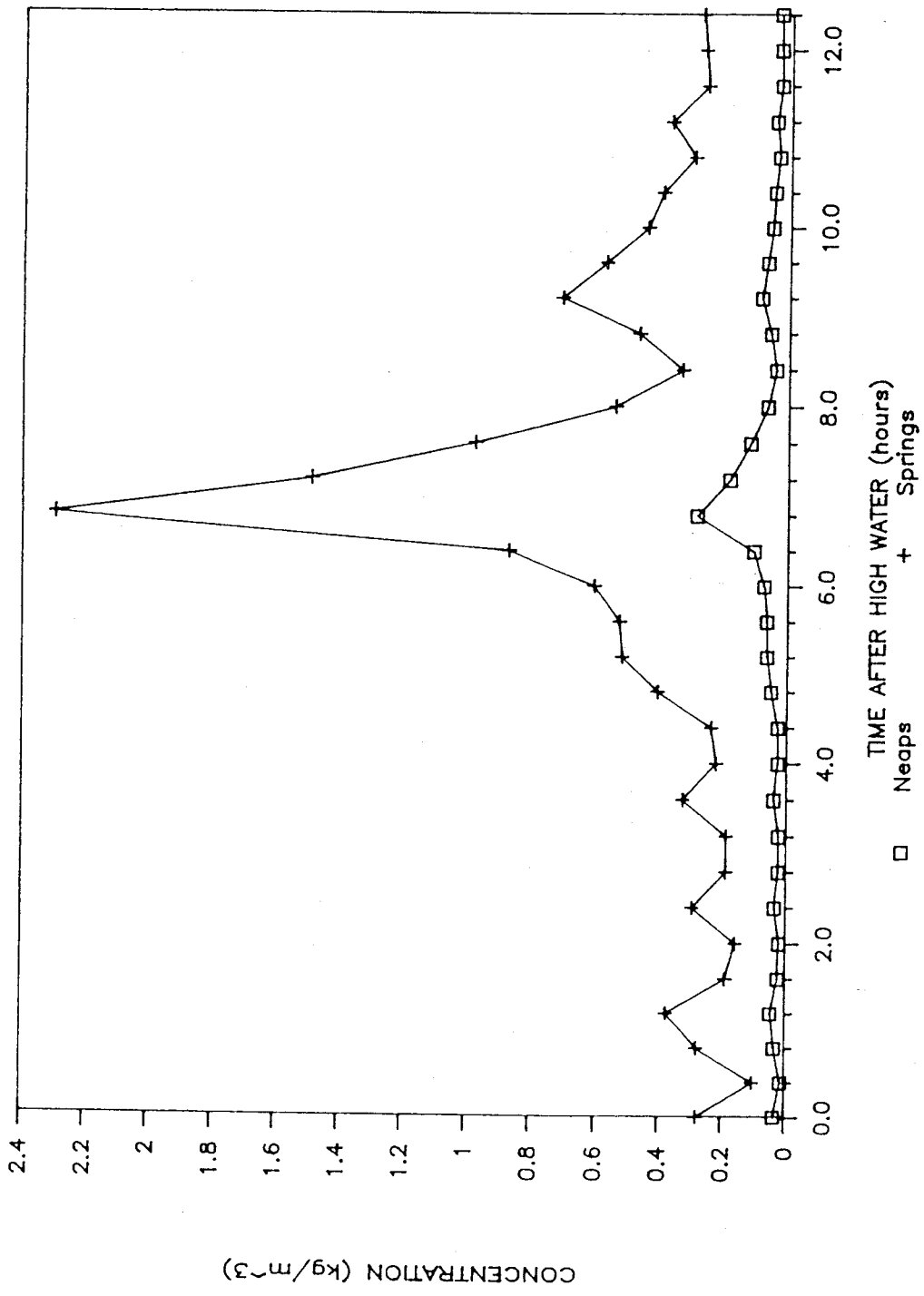

ig 43 Cardiff Docks entrance channel Springs and neaps near-bed concentration of suspended solids against time

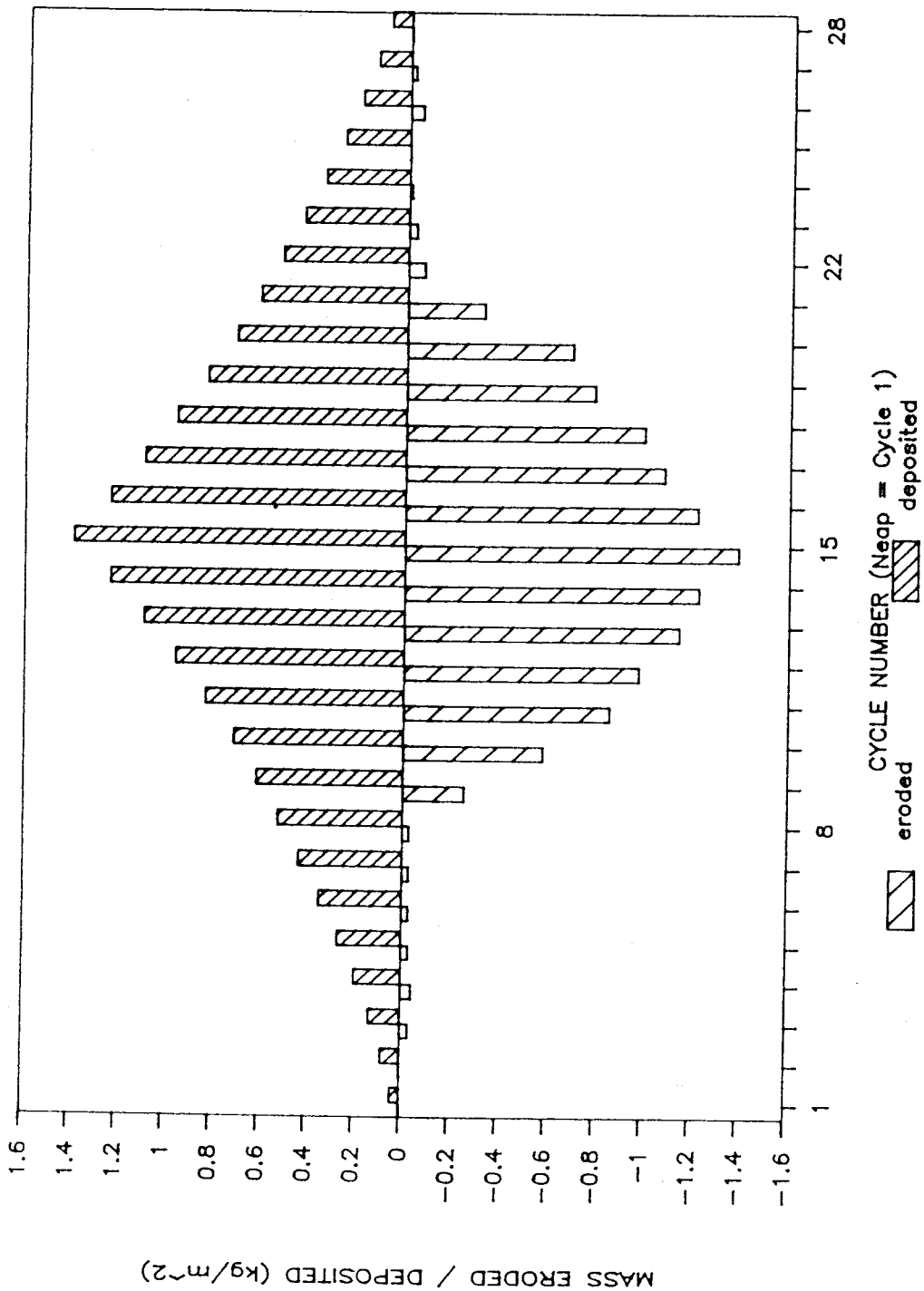

Fig 44 Cardiff Docks entrance channel Mass deposited and eroded per tide during spring-neap cycle

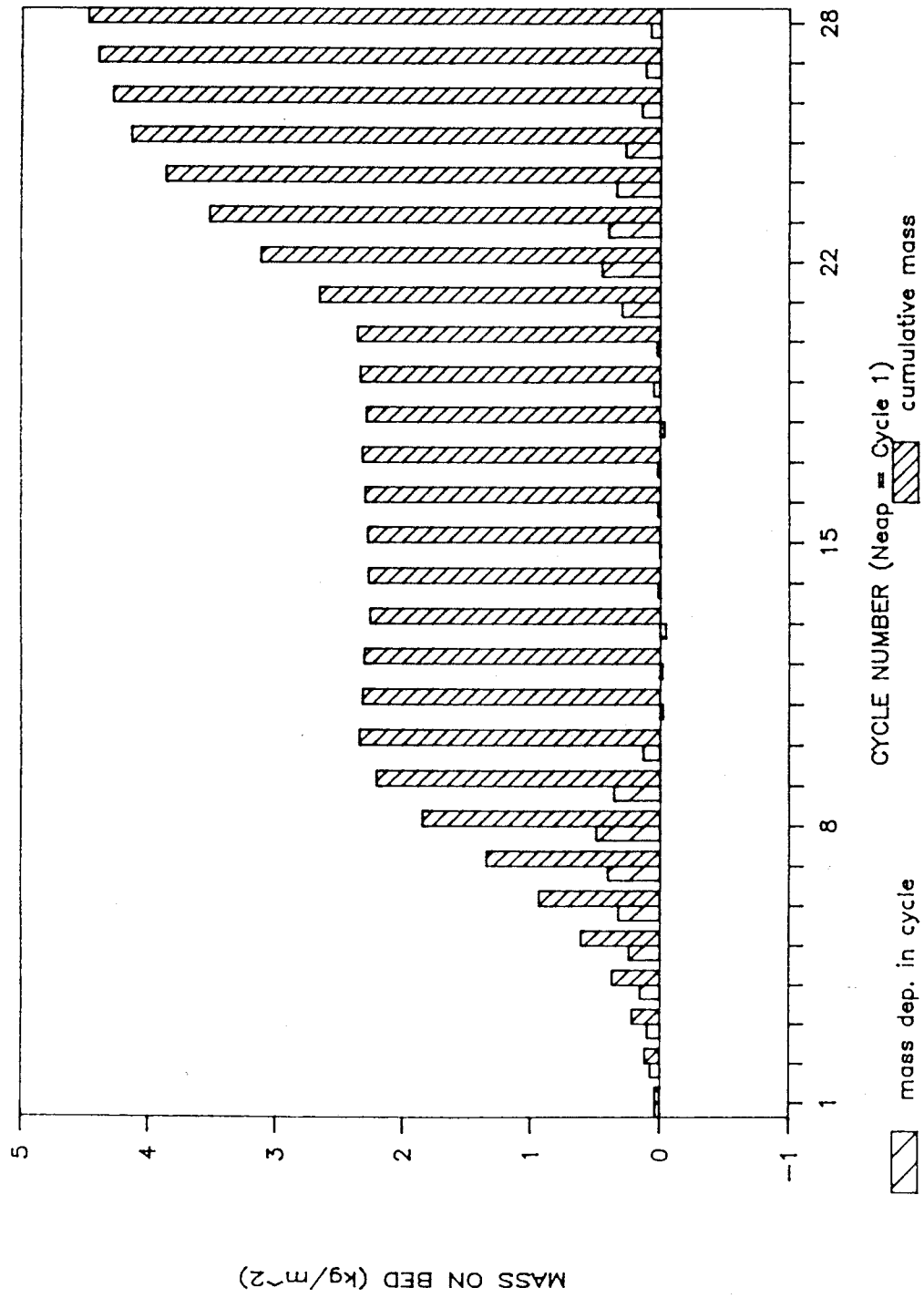

Fig 45 Cardiff Docks entrance channel Cumulative mass on bed during spring-neap cycle

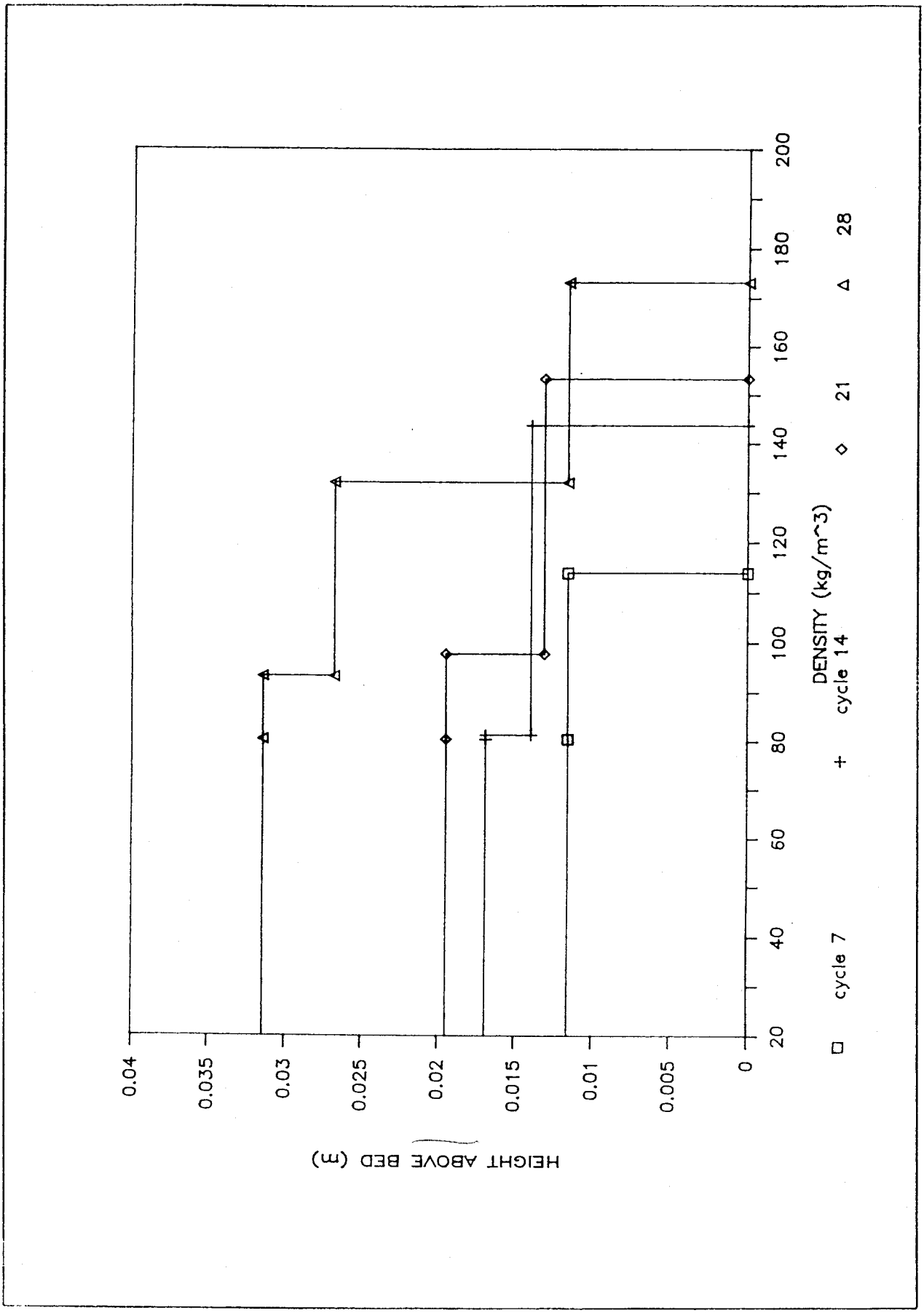

Fig 46 Cardiff Docks entrance channel Density against depth of bed during spring-neap cycle